

AD-A077 629 RENSSELAER POLYTECHNIC INST TROY NY DEPT OF CIVIL EN--ETC F/G 8/11
STUDY OF GROUND MOTIONS AT SOIL SITES DURING TWO CALIFORNIA EARTHQUAKES (U)
OCT 79 R DOBRY , S SINGH , W E BOND DACW37-78-M-0140

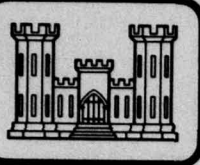
UNCLASSIFIED

WES/BL-79-22

NL

| DF 2
AD
AD-077629
SPE





LEVEL ✓

12
B.S.



MISCELLANEOUS PAPER GL-79-22

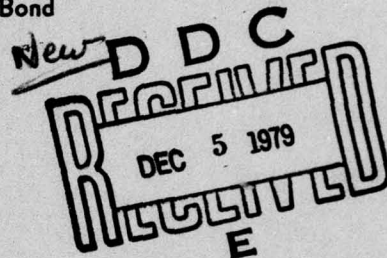
ADA077629

STUDY OF GROUND MOTIONS AT SOIL SITES DURING TWO CALIFORNIA EARTHQUAKES

by

Ricardo Dobry, Sohan Singh, William E. Bond

Department of Civil Engineering
Rensselaer Polytechnic Institute
Troy, New York 12181



October 1979

Final Report

Approved For Public Release; Distribution Unlimited

411 492



Prepared for Office, Chief of Engineers, U. S. Army
Washington, D. C. 20314

Under Purchase Order No. DACW37-78-M-0140
Work Unit No. 4A161102AT22

new

Monitored by Geotechnical Laboratory
U. S. Army Engineer Waterways Experiment Station
P. O. Box 631, Vicksburg, Miss. 39180

DDC FILE COPY
DDC

79 12 4 127

**Destroy this report when no longer needed. Do not return
it to the originator.**

**The findings in this report are not to be construed as an official
Department of the Army position unless so designated
by other authorized documents.**

Unclassified

SECURITY CLASSIFICATION OF THIS PAGE (When Data Entered)

REPORT DOCUMENTATION PAGE		READ INSTRUCTIONS BEFORE COMPLETING FORM
1. REPORT NUMBER Miscellaneous Paper GL-79-22	2. GOVT ACCESSION NO.	3. RECIPIENT'S CATALOG NUMBER
4. TITLE (and Subtitle) STUDY OF GROUND MOTIONS AT SOIL SITES DURING TWO CALIFORNIA EARTHQUAKES.	5. TYPE OF REPORT & PERIOD COVERED Final report.	
6. AUTHOR(s) Ricardo/Dobry, Sohan/Singh William E./Bond	7. CONTRACT OR GRANT NUMBER(s) Purchase Order No. DACA37-78-M-0140	
8. PERFORMING ORGANIZATION NAME AND ADDRESS Department of Civil Engineering Rensselaer Polytechnic Institute Troy, N. Y. 12181	9. PROGRAM ELEMENT, PROJECT, TASK AREA & WORK UNIT NUMBERS Work Unit 4A161102AT22	
10. CONTROLLING OFFICE NAME AND ADDRESS Office, Chief of Engineers, U. S. Army Washington, D. C. 20314	11. REPORT DATE October 1979	
12. NUMBER OF PAGES 111	13. SECURITY CLASS. (of this report) Unclassified	
14. MONITORING AGENCY NAME & ADDRESS (if different from Controlling Office) U. S. Army Engineer Waterways Experiment Station Geotechnical Laboratory P. O. Box 631, Vicksburg, Miss. 39180	15a. DECLASSIFICATION/DOWNGRADING SCHEDULE	
16. DISTRIBUTION STATEMENT (of this Report) Approved for public release; distribution unlimited.	17. DISTRIBUTION STATEMENT (of the abstract entered in Block 20, if different from Report) DACW37-78-M-0140	
18. SUPPLEMENTARY NOTES		
19. KEY WORDS (Continue on reverse side if necessary and identify by block number) Accelerograms Ground motion Earthquakes		
20. ABSTRACT (Continue on reverse side if necessary and identify by block number) Nine strong motion accelerograms recorded at rock and soil stations during two California earthquakes are analyzed using recently developed processing techniques. These techniques study the characteristics of the records in the time domain, including graphs of the buildup of energy of the horizontal acceleration with time, the variation with time of the RMS horizontal acceleration, and the variation with time of the angle between the principal axis of the ground acceleration and the vertical axis.		
(Continued)		

DD FORM 1 JAN 73 1473 EDITION OF 1 NOV 65 IS OBSOLETE

Unclassified

SECURITY CLASSIFICATION OF THIS PAGE (When Data Entered)

411 492

LB

Unclassified

SECURITY CLASSIFICATION OF THIS PAGE(When Data Entered)

20. ABSTRACT (Continued).

The examination of these graphs allowed the determination of the times, t_1 and t_2 , corresponding to the beginning and end of the strong part of each record. During this strong part, $\phi \approx 90^\circ$, which suggests that the motions at both rock and soil sites are caused mainly by SH-waves. The comparisons of the graphs showed that the wave arrivals are generally consistent between stations during the strong part but that some soil accelerograms have additional significant motions after t_2 . The consistency of wave arrivals during the strong part was especially good for the 1971 San Fernando records in the Pasadena Area. There, the strongest wave arrival occurred at all four stations considered, approximately 3 seconds after the first S-wave arrival.

Several one-dimensional site response simulations were performed at some of the soil stations studied, using the equivalent linear approach. The results showed that the simulated soil accelerations essentially preserve the time domain features of the input rock motion. One consequence of this was that the simulations predicted reasonably well the characteristics of soil motions in the strong part, but did not predict the additional soil motions after t_2 .

T sub 2 (c)

Unclassified

SECURITY CLASSIFICATION OF THIS PAGE(When Data Entered)

PREFACE

This report was prepared for the Office, Chief of Engineers (OCE), U. S. Army, under Purchase Order No. ~~DACA37-78-M-0140~~, as a task under Work Unit No. 4A161102AT22, titled "Site Effects on Characteristics of Earthquake Ground Motion." This work unit was monitored for OCE by Mr. Gus Muller.

This study was monitored by Dr. A. G. Franklin of the Earthquake Engineering and Geophysics Division (EE&GD), Geotechnical Laboratory (GL), U. S. Army Engineer Waterways Experiment Station (WES). General supervision was provided by Dr. P. F. Hadala, Chief, EE&GD, and Mr. J. P. Sale, Chief, GL.

The authors, Messrs. R. Dobry, S. Singh, and W. E. Bond, wish to acknowledge Professor Michael O'Rourke, who made useful suggestions during the study and also reviewed the final manuscript of this report.

The Directors of the WES during the period of this work and preparation of the report were COL J. L. Cannon, CE, and COL N. P. Conover, CE. Technical Director was Mr. F. R. Brown.

Accession For	
NTIS	GRA&I
DDC TAB	<input checked="" type="checkbox"/>
Unannounced	<input type="checkbox"/>
Justification	
By _____	
Distribution/	
Availability Codes	
Dist	Avail and/or special
P	

TABLE OF CONTENTS

	<u>Page</u>
PREFACE	i
1. INTRODUCTION	1
2. METHODS FOR ANALYZING ACCELEROGrams	4
2.1 Energy Buildup and Level of Shaking	6
2.2 Direction of Ground Motion	18
2.3 Frequency Content of the Motion	20
3. GROUND MOTIONS IN THE PASADENA AREA	
(San Fernando Earthquake, February 9, 1971)	22
3.1 Recorded Motions	23
3.2 Site Response Simulations	38
4. GROUND MOTIONS IN THE SAN FRANCISCO BAY AREA	
(San Francisco Earthquake, March 22, 1957)	51
4.1 Recorded Motions	53
4.2 Site Response Simulations	64
5. SUMMARY AND CONCLUSIONS	80
5.1 Summary	80
5.2 Conclusions	84
REFERENCES	86
APPENDIX 1: VARIATION OF ANGLE $\phi_3(t)$ WITH TIME	91
APPENDIX 2: VARIATION OF PREDOMINANT FREQUENCY $f(t)$ WITH TIME . . .	101

1. INTRODUCTION

This report presents the results of studies on recorded ground accelerations for selected rock and soil sites located close to the generating fault during two California earthquakes. The two earthquakes are:

- San Fernando earthquake of February 9, 1971 ($M_L = 6.3$)
- San Francisco earthquake of March 22, 1957 ($M_L = 5.3$)

where the values of local magnitude, M_L are those given by Kanamori and Jennings (1978).

The development of modern earthquake engineering has included a significant number of studies of recorded strong motion accelerograms. Many of these studies have focused on the characteristics of the response spectrum and on the value of the peak acceleration. Studies of the time domain characteristics of recorded ground motions, such as their duration and the sequence of the acceleration pulses have been relatively scarce. However, more recently, these time characteristics are receiving increased attention, in recognition of their importance to engineering problems such as nonlinear response and liquefaction potential of soil deposits, permanent displacements of earth slopes, and the damage and collapse potential of yielding structures. Examples of time domain studies published in the last few years are Bolt (1973), Seed et. al. (1975a), Trifunac and Brady (1975), Franklin and Chang (1977), Vanmarcke and Lai (1977) and Dobry et. al. (1977, 1978, 1978a).

The present study focuses on these time domain characteristics, and uses recently developed analytical procedures for processing accelerograms in the time domain. A summary of the main features of the methods used in this study is presented in Section 2 of this report. The time domain procedures mentioned above have already proven quite useful for uncovering hidden features of recorded accelerograms, and also for understanding the relation between

these features and relevant seismological parameters (Dobry et. al., 1978, Bond, 1979). Most of the work done to date has focused on earthquake records obtained at rock sites and hilly areas, which very often appear to be simpler than records obtained at nearby soil sites and valley areas. Some results of this previous work are also reproduced and discussed in Section 2.

A main objective of the present study is to develop a better understanding of the time domain characteristics of accelerograms obtained at soil sites, as compared with the characteristics of records at neighboring rock sites. A second objective is to evaluate the one dimensional amplification technique currently being used to predict soil motions. Therefore, two criteria were used to select the earthquake records for analysis: a) several ground motion accelerograms should be available which were recorded in the same general area during an earthquake, and at least one of the records must correspond to a rock site, and b) for some of the soil accelerograms, there should be enough information available on local soil conditions so that analytical site response simulations could be performed. The records selected for this study fulfill both criteria.

Section 3 presents the results for one rock and three soil accelerograms recorded in the Pasadena area during the San Fernando earthquake. Section 4 presents similar results for one rock and four soil accelerograms during the San Francisco earthquake. All nine accelerograms were processed using the time domain techniques described in Section 2, and the results compared to study the possible influence of geologic and site conditions. In addition, site response analyses were performed at some of the soil sites using as input the neighboring rock records. These analyses used the widely utilized shear beam, equivalent linear analysis technique (Program SHAKE, see Schnabel et. al., 1972). Finally, the simulated soil motions computed in the response

analyses were processed and compared with the recorded motions using the same time domain techniques mentioned above. The results of these site response studies are also presented in Sections 3 and 4.

All records used in the present study are corrected accelerograms which were obtained from California Institute of Technology, and which are described in Volume II of the series, Strong Motion Earthquake Accelerograms (Hudson et. al., 1971).

2. METHODS FOR ANALYZING ACCELEROGRAMS

The recent interest in the time domain characteristics of strong ground motion accelerograms has created the need for new methods of analysis. This need will no doubt increase even further as more records become available from future earthquakes. Therefore, a significant effort has already been spent at Rensselaer Polytechnic Institute (R.P.I.) in developing these new procedures. A detailed discussion of these methods and of their application to rock accelerograms is outside the scope of this report, and can be found elsewhere (Bond, 1979). A summary description of basic concepts and procedures, needed for this report, follows.

A strong ground motion accelerogram usually consists of the three components of the particle ground acceleration, $a_x(t)$, $a_y(t)$, $a_z(t)$, where a_x and a_y are orthogonal horizontal components and a_z is the vertical component. The time t is the same for the three components and is measured from the moment the instrument is triggered. The triggering time is not known on an absolute time scale and it usually varies between stations. Typical horizontal components $a_x(t)$ and $a_y(t)$ for the San Fernando earthquake are presented in Fig. 1.

The procedure used for the time domain analysis of the accelerogram is to study several graphs showing the variation with time of the main characteristics of the record. These characteristics are: i) the level of shaking or energy buildup of the motion, ii) the direction of the motion, and iii) the frequency content of the motion.

Graphs of these time domain characteristics are shown in Figures 1 and 3 through 7. These will be discussed in more detail subsequently. The basic concepts used in developing these graphs are those proposed originally by Arias (1969), Husid (1973) and Penzien and Watabe (1975) and later extended

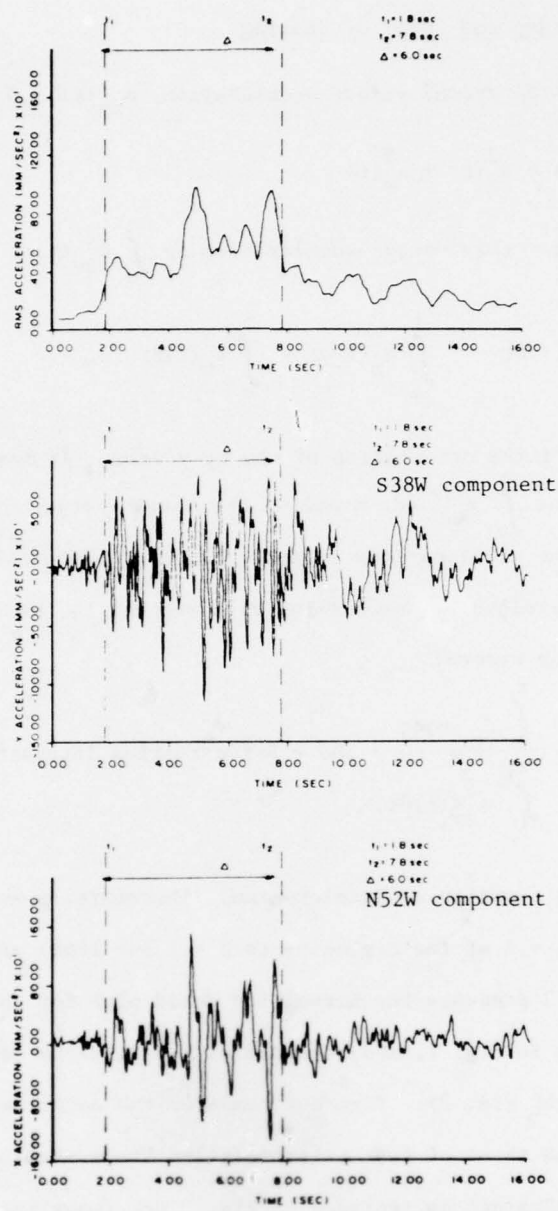


Figure 1 - HORIZONTAL (a_x and a_y) ACCELERATION COMPONENTS, AND VARIATION OF RMS FOR THE VECTOR ACCELERATION, a_{xy} WITH TIME, 445 FIGUEROA STREET
(Bond, 1979)

by Dobry et. al. (1978a) and Bond (1979).

2.1 Energy Buildup and Level of Shaking

The horizontal ground vector acceleration, $a_{xy}(t) \geq 0$ is defined as:

$$a_{xy}^2(t) = a_x^2(t) + a_y^2(t) \quad (1)$$

The Husid plot for this vector acceleration is $\int_0^t a_{xy}^2(t)dt$ versus t , where

$$\int_0^t a_{xy}^2(t)dt = \int_0^t a_x^2(t)dt + \int_0^t a_y^2(t)dt \quad (2)$$

is independent of the orientation of the x, y axes. It has been demonstrated (Arias, 1969) that $\int_0^t a_{xy}^2(t)dt$ measures the total energy buildup with time associated with the accelerations in the horizontal plane. The normalized Husid plot is $h(t)$, obtained by normalizing with respect to the value of the energy at the end of the record:

$$h(t) = \frac{\int_0^t a_{xy}^2(t)dt}{\int_0^{t_f} a_{xy}^2(t)dt} * 100 = \text{Percent Arias Intensity} \quad (3)$$

where t_f = total duration of accelerogram. Therefore, a normalized Husid plot goes from $h = 0$ at the beginning to $h = 1$ (or 100%) at the end of the record. Figure 3 presents the normalized Husid plot for the acceleration components shown in Fig. 1, and recorded at 445 Figueroa Street (Station C054 in the map of Fig. 2). Figure 6 compares the normalized Husid plots for Figueroa with those of four sites labelled "rock stations" in Fig. 2. (The names of all stations included in Fig. 2 are shown in Table 1.) These five stations are all located in the hilly area between San Fernando Valley and Los Angeles Basin, with the ground conditions consisting of either

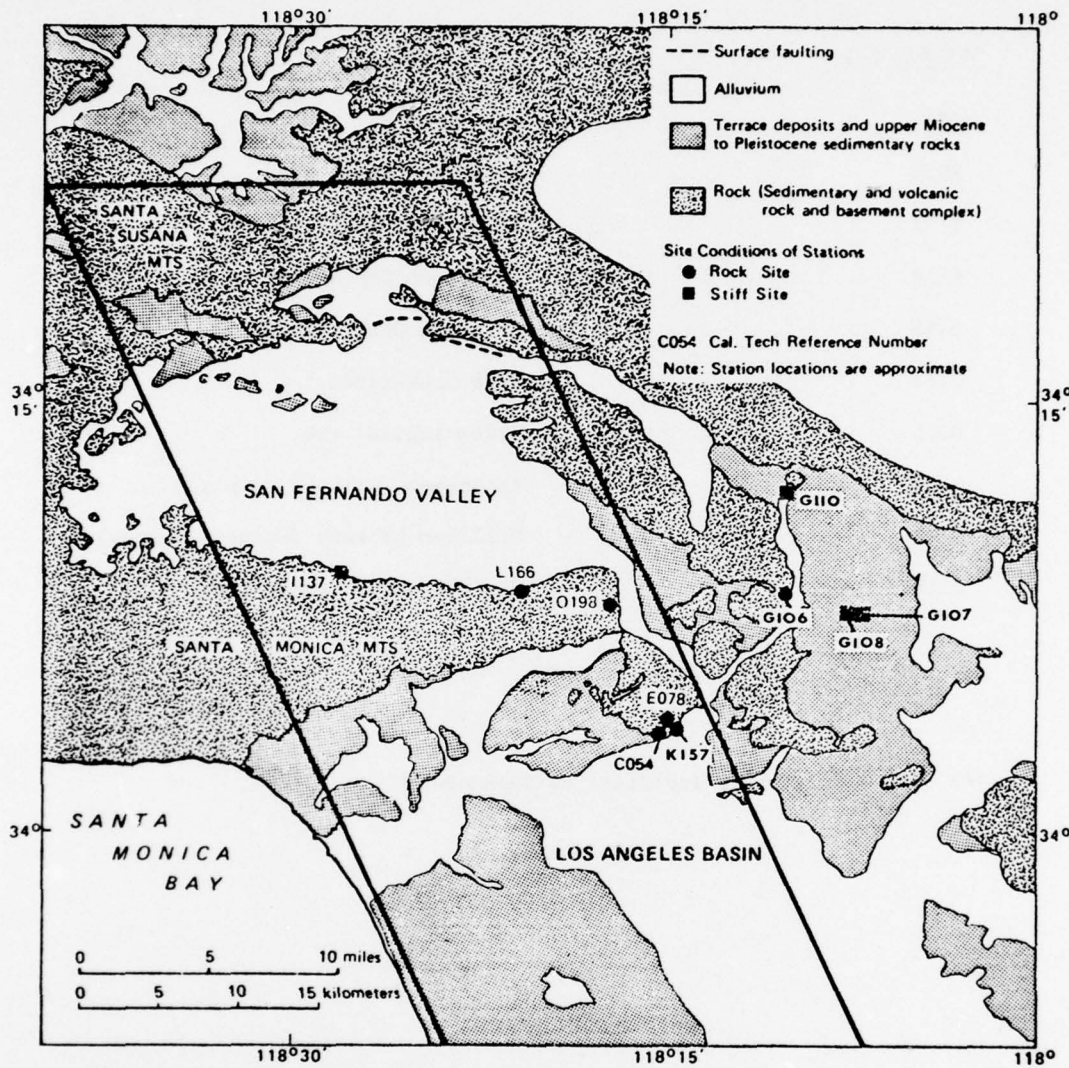


Figure 2 - LOCATION MAP OF GROUND RECORDING ACCELEROMETERS, SAN FERNANDO EARTHQUAKE, FEB. 9, 1971

Table 1

Accelerograph Stations and Numbers used in Map of Fig. 1

San Fernando Earthquake

<u>CIT No. (*)</u>	<u>Station</u>
C054	445 Figueroa
E078	Water and Power Bldg.
I137	15910 Ventura Blvd.
K157	420 South Grand Ave.
O198	Griffith Observatory
L166	3838 Lankershim
G106	Seismological Lab.
G107	Athenaeum (Caltech Campus)
G108	Millikan Library (Caltech Campus)
G110	Jet Propulsion Laboratory

(*) CIT = California Institute of Technology

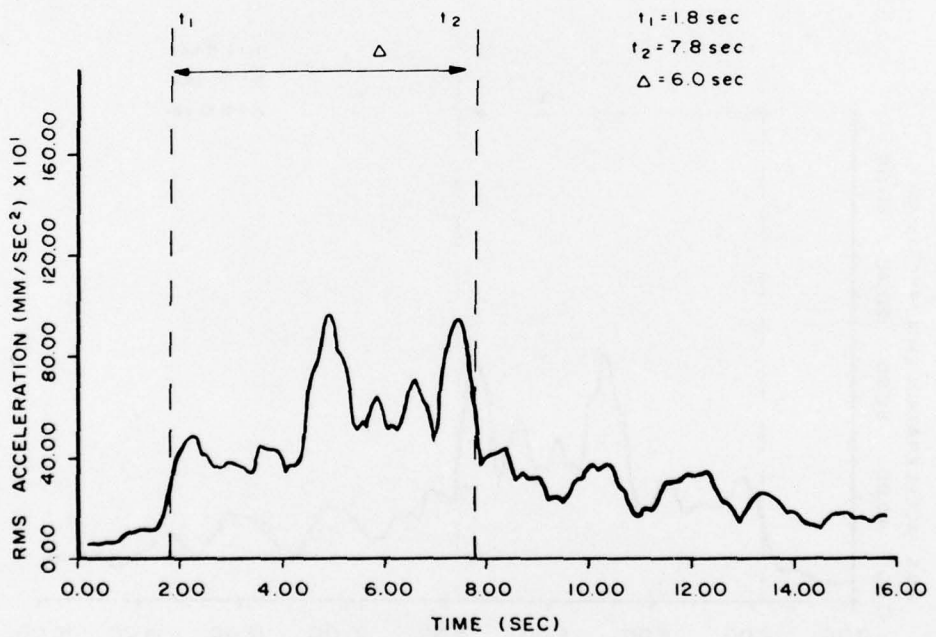
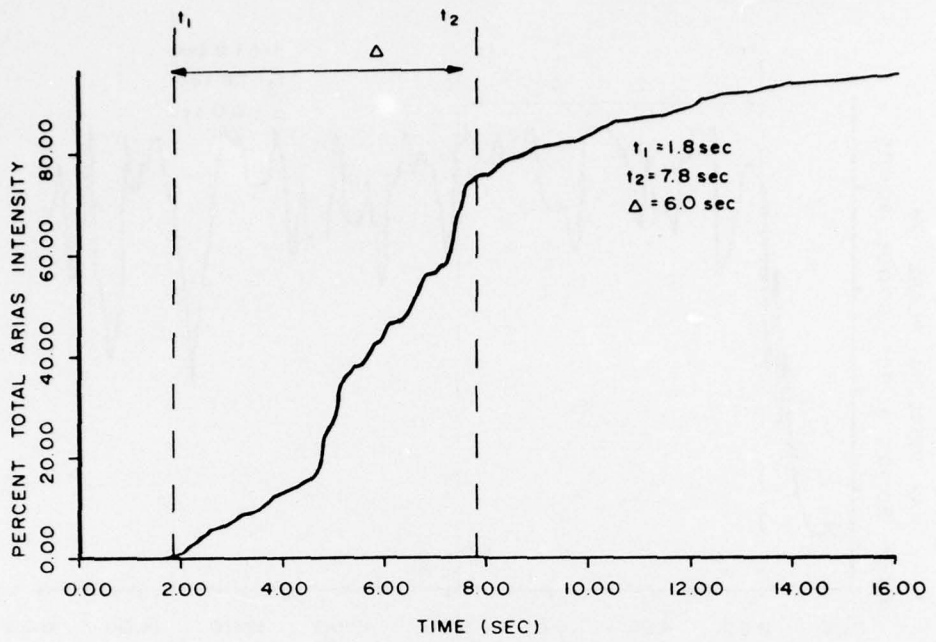


Figure 3 - NORMALIZED HUSID PLOT AND VARIATION OF RMS WITH TIME FOR
RECORDED GROUND ACCELERATIONS, 445 FIGUEROA STREET
(Bond, 1979)

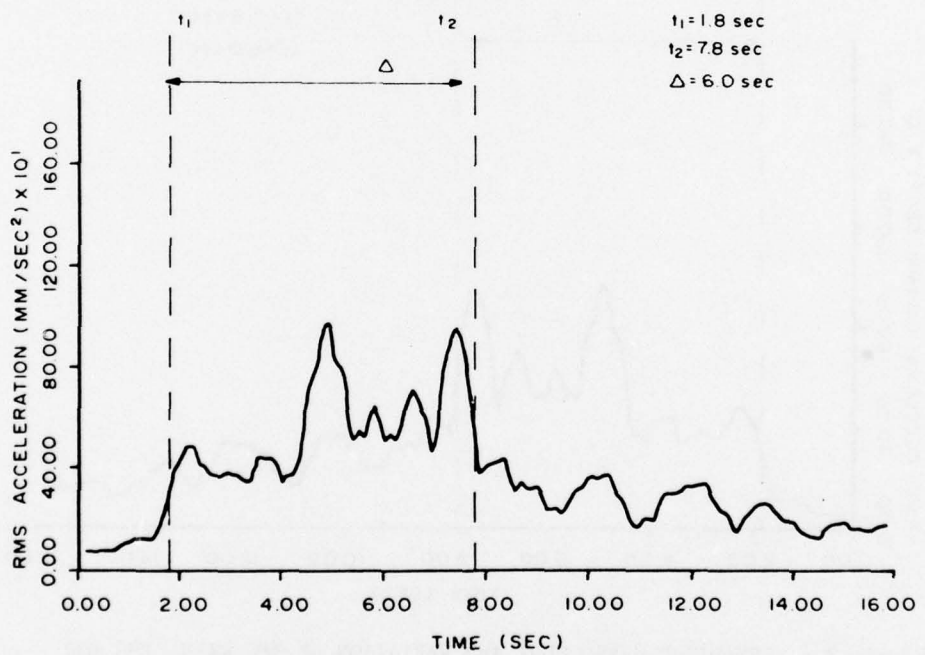
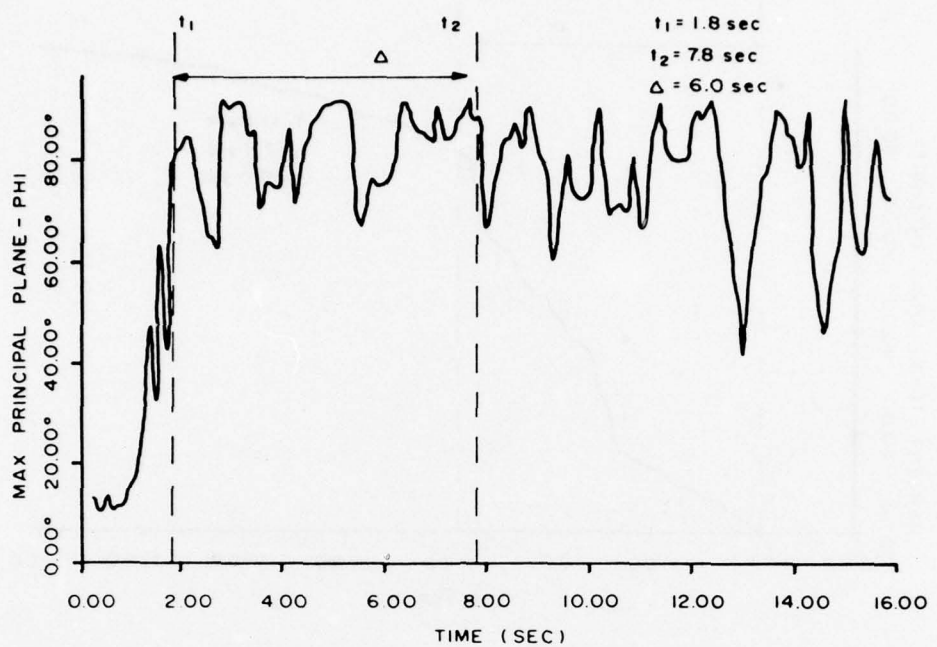


Figure 4 - VARIATION OF RMS AND ϕ_1 FOR RECORDED GROUND ACCELERATIONS,
445 FIGUEROA STREET (Bond, 1979)

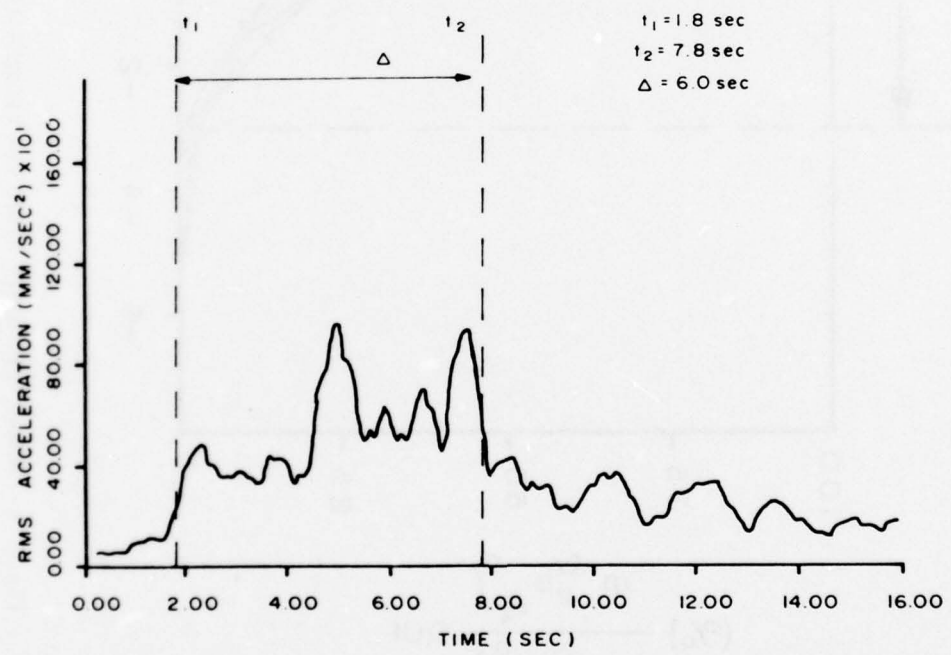
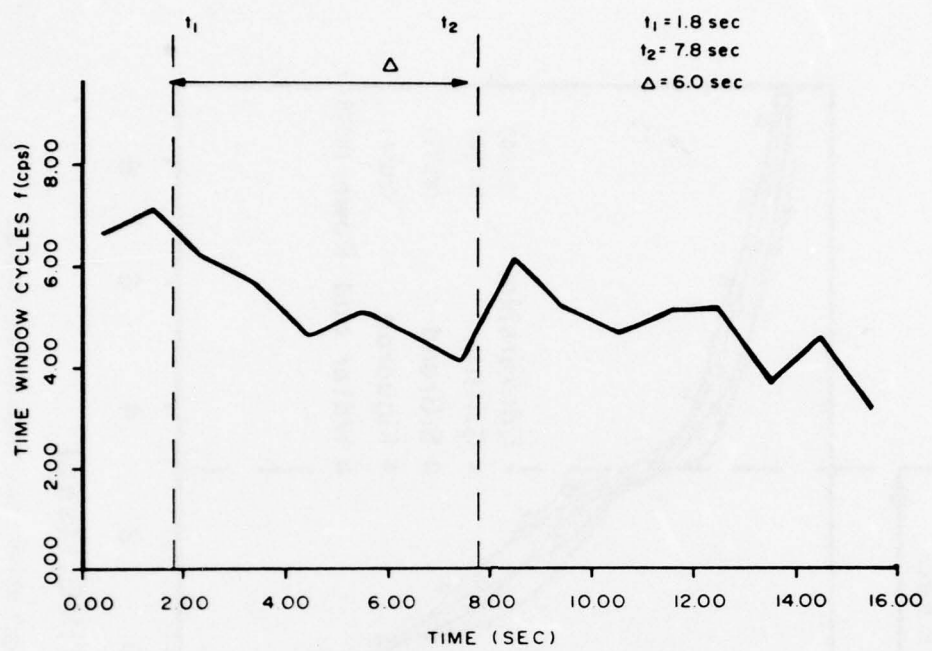


Figure 5 - VARIATION OF RMS AND PREDOMINANT FREQUENCY, f WITH TIME,
FOR GROUND ACCELERATIONS RECORDED AT 445 FIGUEROA STREET

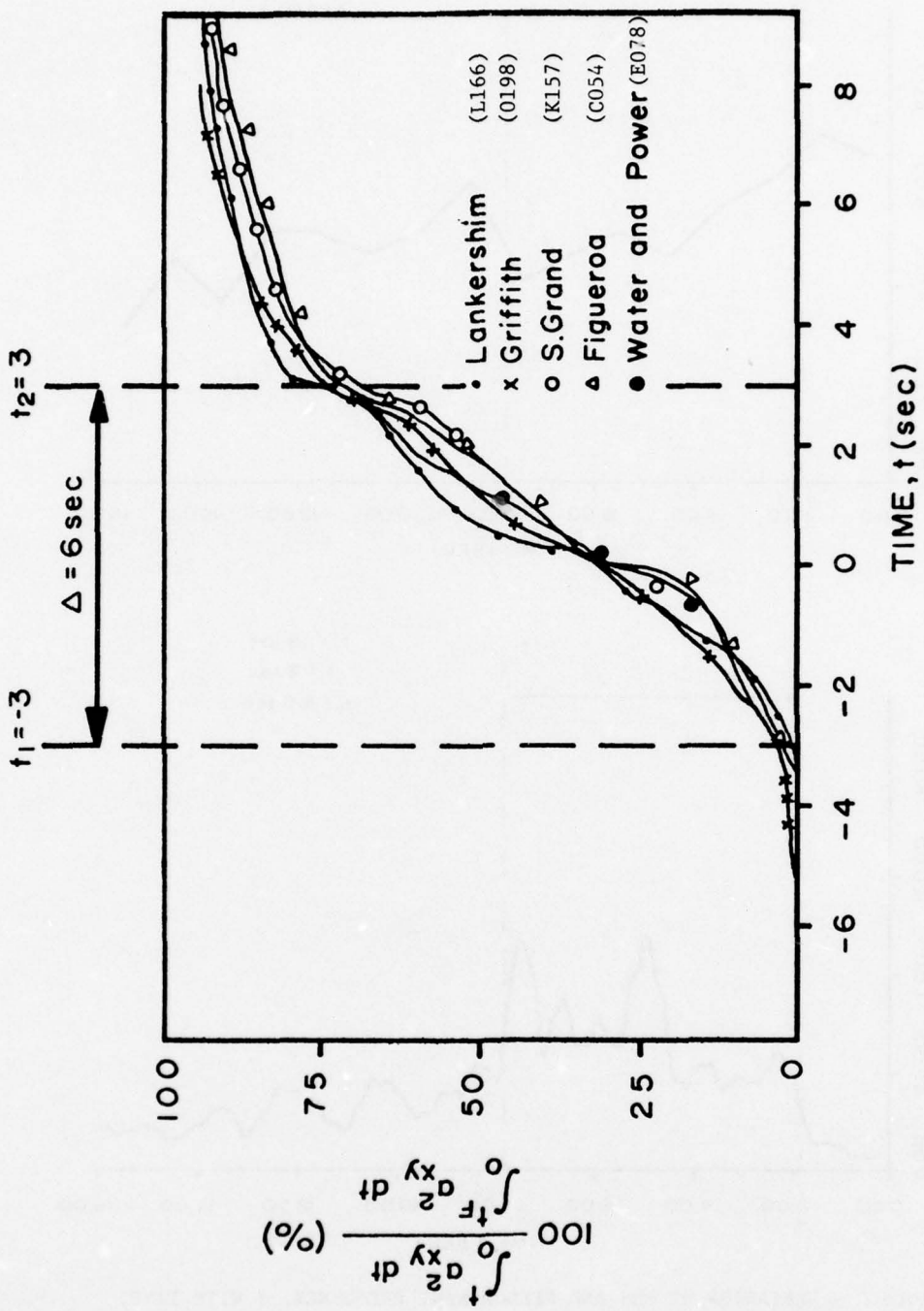


Figure 6 - NORMALIZED HUSID PLOTS FOR RECORDS AT "ROCK" SITES, SAN FERNANDO EARTHQUAKE
 (Bond, 1979)

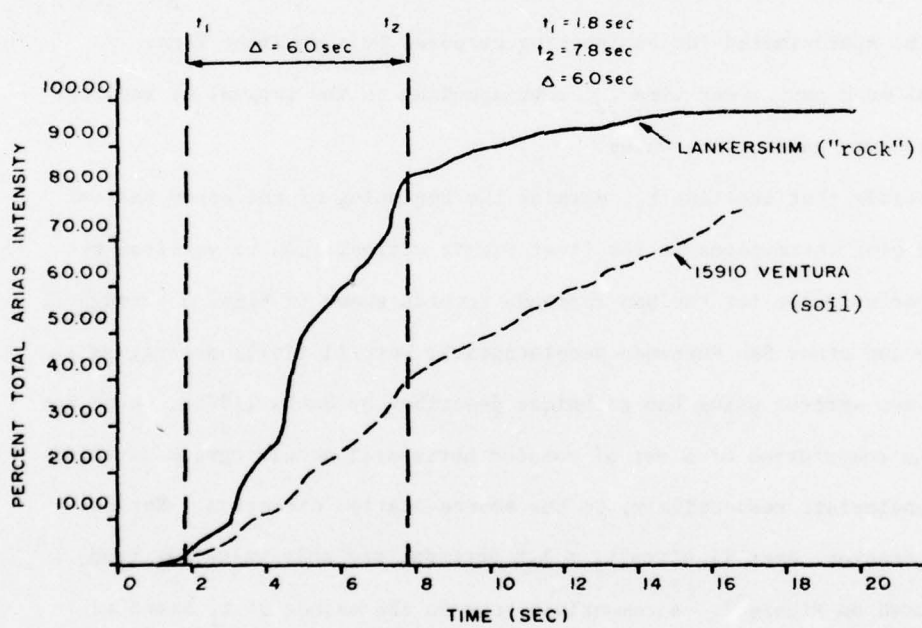
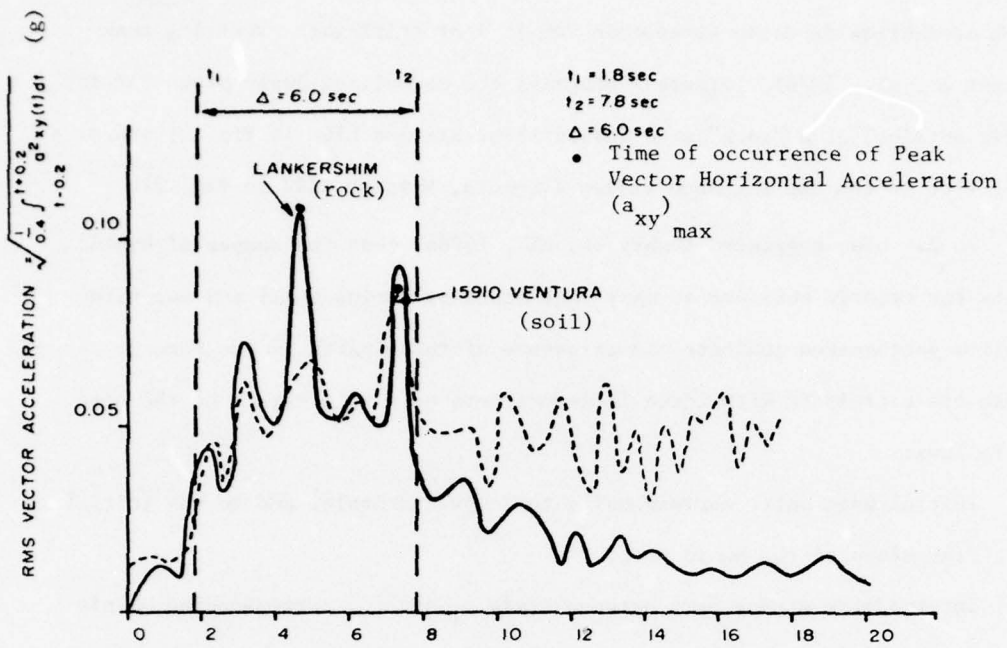


Figure 7 - NORMALIZED HUSID PLOTS AND VARIATION OF RMS WITH TIME FOR ACCELERATIONS RECORDED AT "ROCK" AND SOIL SITES (time scale, t_1 and t_2 values are from Lankershim) (Bond, 1979)

rock or shallow deposits (less than 200 ft.) of stiff soil overlying rock (Grant et. al., 1978). Figure 7 compares the normalized Husid plots for records obtained at a "rock" site (Lankershim, Station L166 in Fig. 2) and at a soil site in the San Fernando Valley (Ventura, Station I137 in Fig. 2).

It has been suggested (Dobry et. al., 1978a) that the shapes of Husid plots for records obtained at many rock stations during small and moderate shallow earthquakes indicate the existence of three parts in the record. These are correlated with three different sets of wave arrivals to the site, as follows:

- 1) Initial weak part, corresponding to P-wave arrivals, and to the initial flat slope of the Husid plot.
- 2) Intermediate strong part between times t_1 and t_2 , corresponding mainly to the arrival of S-waves following a direct path between earthquake source and recording station. This strong part corresponds to the line with a steep slope of the Husid plot, it has a duration $\Delta = t_2 - t_1$ and can be approximated for engineering purposes by a straight line.
- 3) Final weak part after time t_2 , corresponding to the arrival of indirect body waves and surface waves.

The hypothesis that the time t_1 , marking the beginning of the steep part of the Husid plot corresponds to the first S-wave arrival, can be verified by independent evidence for the San Fernando records shown in Figs. 3 through 7. For these and other San Fernando accelerograms, Berrill (1975) determined the first S-wave arrival using the technique described by Hanks (1975), which requires the computation of a set of rotated horizontal accelerograms parallel and perpendicular, respectively, to the source-station direction. For the Figueroa station, Berrill gives $t_1 = 1.8$ seconds, and this value has been superimposed on Figure 3. A comparison between the values of t_1 based on

the shape of the Husid plot, and those given independently by Berrill, is presented in Table 2 for several records. Good agreement exists between the two methods. All of this confirms that the beginning of the strong, steep part in the Husid plot can be used for a visual estimate of the time of first S-wave arrival, for both rock and soil records.

The duration of direct S-wave arrivals, (strong part) has been estimated to be $\Delta \approx 6$ seconds for the San Fernando earthquake records considered, and the corresponding end time of the strong part, $t_2 = t_1 + 6$ has also been included in Figs. 1, 3 and 6. It should be noticed that t_2 generally coincides in these figures with the time at which the Husid curves become flatter. Furthermore, the similarity between all curves in Fig. 6 shows that the energy buildup with time was quite consistent for ground motions over the hilly area South and SE of the San Fernando Valley.

In addition to the Husid plot, a second graph is also used to study the variation of the level of shaking with time. This is the RMS(t) (Root-Mean-Square) horizontal vector acceleration, computed for a moving time window of width δ (seconds). RMS(t) is defined as:

$$\text{RMS}(t) = \left(\frac{1}{\delta} \int_{t-0.5\delta}^{t+0.5\delta} a_{xy}^2(t) dt \right)^{1/2} \quad (4)$$

RMS(t) is also independent of the orientation of the horizontal components x and y. The value of RMS(t) is closely related to the slope of the Husid plot at the same time t. Therefore, it should be expected that the values of RMS(t) are larger during the strong part of the record than for $t < t_1$ or $t > t_2$. This is illustrated by the plot of RMS(t) versus t presented in Fig. 3 for the Figueroa records computed using $\delta = 0.5$ seconds. Figure 3 shows the correspondence between the RMS(t) and the Husid plot for the same station. The RMS(t)

Table 2

Comparison Between t_1 Values for Ground Accelerograms

San Fernando Earthquake

Station	t_1 (seconds)	
	From Husid Plot (used in Fig. 6)	From first S-wave arrival, Berrill (1975)
Lankershim	1.62	1.80
Griffith	3.22	3.50
Water and Power	1.50	1.30
445 Figueroa	2.00	1.80
420 South Grand	2.80	----
15910 Ventura	4.80	4.90

graph has proven extremely useful to study the sequence of the main acceleration pulses, and also to understand them in terms of wave arrivals to the station.

Dobry et. al. (1979) and Bond (1979) have demonstrated that the particular shape of $\text{RMS}(t)$ for $t_1 < t < t_2$ illustrated by Fig. 3 is essentially the same for rock and soil stations covering a large area South and SE of the generating fault during the San Fernando earthquake; these include all stations plotted in Figs. 6 and 7. What this says is that the peaks of the $\text{RMS}(t)$ graph do not occur at random but correspond to definite wave arrivals, which are the same for different stations. These wave arrivals should be correlated with the source mechanism and the propagation characteristics of the seismic waves between the source and the station. Furthermore, the horizontal peak accelerations of the records occur much more often at the peaks of the $\text{RMS}(t)$ graph than at the valleys of the same graph. This is illustrated by Fig. 7, which compares the Husid and $\text{RMS}(t)$ graphs between a "rock" and soil station (Stations L166 and I137 in Fig. 1). The normalized Husid plots in Fig. 7 are very different, and indicate a significant longer duration of motion at the soil site. The reason for this becomes clear by a comparison of the $\text{RMS}(t)$ graphs in the same figure. For $t_1 < t < t_2$, the two $\text{RMS}(t)$ curves are very similar, and have the same sequence and locations of peaks and valleys, indicating the same wave arrivals at both stations^(*). However, for $t > t_2$, the "rock" Lankershim record essentially ends, with $\text{RMS}(t)$ dropping below 0.05 g. On the other hand, for $t > t_2$ the soil record has $\text{RMS}(t)$ values larger than 0.05 g for an additional 10 seconds. These motions after the

(*) The two main wave arrivals occur at about $t_1 + 3$ and $t_1 + 5$ as indicated by the major peaks in $\text{RMS}(t)$ in both Figs. 3 and 7. The peak accelerations of the horizontal components and of the vector accelerations, a_{xy} also occur at about these times (also see Dobry et. al., 1979).

end of the strong part in the soil record can be explained by surface waves trapped in the alluvium of the San Fernando Valley, which did not propagate into the rock of the hills south of the valley due to the high impedance ratio between rock and alluvium.

Throughout the rest of this report, normalized Husid plots and RMS(t) graphs are shown for all nine records considered. For the RMS(t) calculations, a value $\delta = 0.5$ sec. was generally used.

2.2 Direction of Ground Motion

It is possible to define a "ground acceleration tensor", $[G(t)]$ at a given station for a particular earthquake:

$$[G(t)] = \begin{pmatrix} g_{xx} & g_{xy} & g_{xz} \\ g_{yx} & g_{yy} & g_{yz} \\ g_{zx} & g_{zy} & g_{zz} \end{pmatrix} \quad (5)$$

where $g_{ij} = g_{ij}(t) = \int_{t-0.5\delta}^{t+0.5\delta} a_i(t) a_j(t) dt$. Therefore, the diagonal terms

of the matrix have the form:

$$g_{xx}(t) = \int_{t-0.5\delta}^{t+0.5\delta} a_x^2(t) dt$$

while the off-diagonal terms have the form:

$$g_{xy}(t) = g_{yx}(t) = \int_{t-0.5\delta}^{t+0.5\delta} a_x(t) a_y(t) dt$$

As before, x , y are horizontal axes and z denotes the vertical axis.

The symmetric tensor $[G(t)]$ varies with time, and it is also a function of the window width, δ . Arias (1969) and Penzien and Watabe (1975) have shown that $[G(t)]$ is indeed a tensor, as its components for any new set of orthogonal axes x' , y' , z' can be computed by using the rules of tensor transformation.

It is possible to compute the principal directions of this acceleration tensor using standard procedures. Of special interest is the angle, ϕ_1 between the major principal direction (major principal plane) and the vertical axis. Some results by Kubo and Penzien (1976) using a very large value of $\delta = 5$ seconds suggested that ϕ_1 is close to 0 for $t < t_1$ and that it switches to $\phi_1 \approx 90^\circ$ for $t > t_1$. This means that the acceleration is predominantly vertical (P-wave) for $t < t_1$ and predominantly horizontal (SH-wave) for $t > t_1$. That this is indeed the case, and the fact that the $\phi_1(t)$ graph calculated with a much narrower window, $\delta = 0.5$ sec. can be very helpful in determining t_1 and for analyzing ground accelerograms, is shown conclusively by Bond (1979). This is illustrated by the plot of ϕ_1 versus t for the Figueroa record in Fig. 4. Figure 4 compares the $\phi_1(t)$ and $RMS(t)$ graphs for the same record, and clearly demonstrates that these two plots supplement each other. Of particular interest is the jump in both graphs at $t_1 \approx 1.8$ seconds.

In this report, $\phi_1(t)$ graphs were systematically plotted for $\delta = 0.5$ seconds and are discussed throughout the text. The corresponding $\phi_3(t)$ graphs, which give the angle between the minor principal direction (minor principal plane) and the vertical axis, were also obtained and are included in Appendix 1. The angle $\phi_2(t)$, and the azimuth angles with respect to the North of the three principal directions, $\theta_1(t)$, $\theta_2(t)$ and $\theta_3(t)$ can also be computed and plotted versus t . In general, ϕ_1 is the most important of all these angles. The use

of graphs for some of the other angles in the analysis and interpretation of accelerograms is discussed by Bond (1979).

2.3 Frequency Content of the Motion

The graphs discussed in Sections 2.1 and 2.2 are very useful for time-domain analysis of accelerograms. They depict in a simple way the variation with time of level of shaking and energy buildup of the record, and of the direction of the ground accelerations. Furthermore, these graphs are independent of the orientation of the horizontal components of the instrument, which eliminates the need to consider this additional variable. It would be desirable to have a similar simple graph for the predominant frequency of the ground acceleration, $f(t)$ (cps), which could provide information on changes in the frequency content associated with different parts of the record or with specific wave arrivals. It would also be convenient that this graph be independent of the orientation of the instrument.

There are several definitions of predominant frequency of the motion (i.e., Crandall and Mark, 1963; Clough and Penzien, 1975). Also, different techniques have been developed for characterizing and plotting the time variation of the frequency content of the motion, which are mostly based on the use of multi-filtering procedures (Liu, 1970 and 1971; Trifunac, 1971; Perez, 1973; Saragoni and Hart, 1973; Kameda, 1975; Joannon et. al., 1977). These and other definitions and techniques are presently being studied at RPI, with the purpose of developing the desired graph of predominant frequency versus time.

For the purpose of this report, a crude technique was used to estimate $f(t)$. This consisted of counting the number of peaks, N , of the vector horizontal acceleration squared, $a_{xy}^2(t) = a_x^2(t) + a_y^2(t)$, between the times $t - 0.5\delta_f$ and $t + 0.5\delta_f$, and defining $f(t)$ by Eq. 6:

$$f(t) = \frac{N}{2\delta_f} \quad (6)$$

The graph of $f(t)$ versus t for the Figueroa record is presented in Fig. 5, for the time window $\delta_f = 1$ sec. Figure 5 also reproduces the corresponding graph of $RMS(t)$. The values of $f(t)$ in Fig. 5 during the strong part are between 4 and 6 cps. A similar value for the average $f(t)$ in the range $t_1 < t < t_2$ was found for San Fernando records by Dobry et. al. (1979) using a more refined computational method.

Graphs of $f(t)$ using Eq. (6) and $\delta_f = 1$ second were obtained for all records considered in this study, and are included in Appendix 2.

3. GROUND MOTIONS IN THE PASADENA AREA

(San Fernando Earthquake, February 9, 1971)

The San Fernando, California earthquake of February 9, 1971 was a thrust fault event occurring along the San Fernando Fault. The fault ruptured along an estimated 15-23 km length, and it broke to the ground surface at the North end of the San Fernando Valley as shown in Fig. 2. Estimates for the total duration of the fault rupture vary between 6 and 9 seconds (Dobry et. al., 1978a). Values of local magnitude, M_L = 6.3 and surface wave magnitude, M_S = 6.6 have been reported by Kanamori and Jennings (1978).

The earthquake occurred near Los Angeles, in an area densely instrumented for strong-motion measurements. Many useful ground motion accelerograms were obtained, which have been and still are being studied by many workers (i.e., Bolt, 1973, Boore and Zoback, 1974; Bouchon and Aki, 1977; Hanks, 1975, 1976; Crouse, 1973; Berrill, 1975; Seed et. al., 1974, 1975). Time domain and duration studies performed by the authors on San Fernando accelerograms are reported by Dobry et. al. (1977, 1978a, 1979) and Bond (1979). Basic information on various aspects of this earthquake can be found in the Report on San Fernando, California Earthquake of Feb. 9, 1971, 3 vol. (Murphy, 1973).

Four ground accelerograms recorded in the Pasadena area were selected for this study. These correspond to the following stations in Figs. 2 and 8.

Fig. 2

G106

G110

G107

G108

Fig. 8

SL

JPL

ATH

ML

CIT* Seismological Laboratory (rock station)

Jet Propulsion Laboratory (soil station)

CIT* Athenaeum (soil station)

CIT* Millikan Library (soil station)

* CIT = California Institute of Technology

Detailed descriptions and discussions of these accelerograms, of their response spectra and of additional seismoscope ground records from the same area have been published by Hudson (1972), Jennings (1973) and Berrill (1975). Additional information on site conditions at some of the stations including measured shear-wave velocities of the subsoil are available in Eguchi et. al. (1976), and more recently in Shannon and Wilson (1978).

Figure 8 is a map of the Pasadena area, originally published by Gutenberg (1957), and including the locations of strong-motion accelerographs and seismoscopes which recorded during the San Fernando earthquake. The four accelerograph stations are SL, ATH, ML and JPL. Additional information on the four stations is provided in Table 3.

3.1 Recorded Motions

The accelerograms at stations SL, JPL, ATH and ML were studied using the time domain techniques described in Section 2. As indicated by Hudson (1972), and illustrated by the maps in Figs. 2 and 8, the distances between the stations and the earthquake source is such that distance attenuation effects should be a minor factor in explaining differences between ground motions at the four sites.

Table 4 summarizes the values of the recorded peak accelerations and their times of occurrence for the NS and EW components. All values of peak acceleration are in the range 0.1 - 0.2 g, and they do not show any clear influence of site conditions. The peak accelerations at ML are about twice than those at ATH, although the two instruments were within 1,000 feet of each other and on essentially the same soil conditions. Berrill (1975) suggested that the stronger motions at ML may have been caused by standing waves formed in the soil between the basement of the ML building and those of adjacent buildings. If that is the case, the ATH record would be more representative

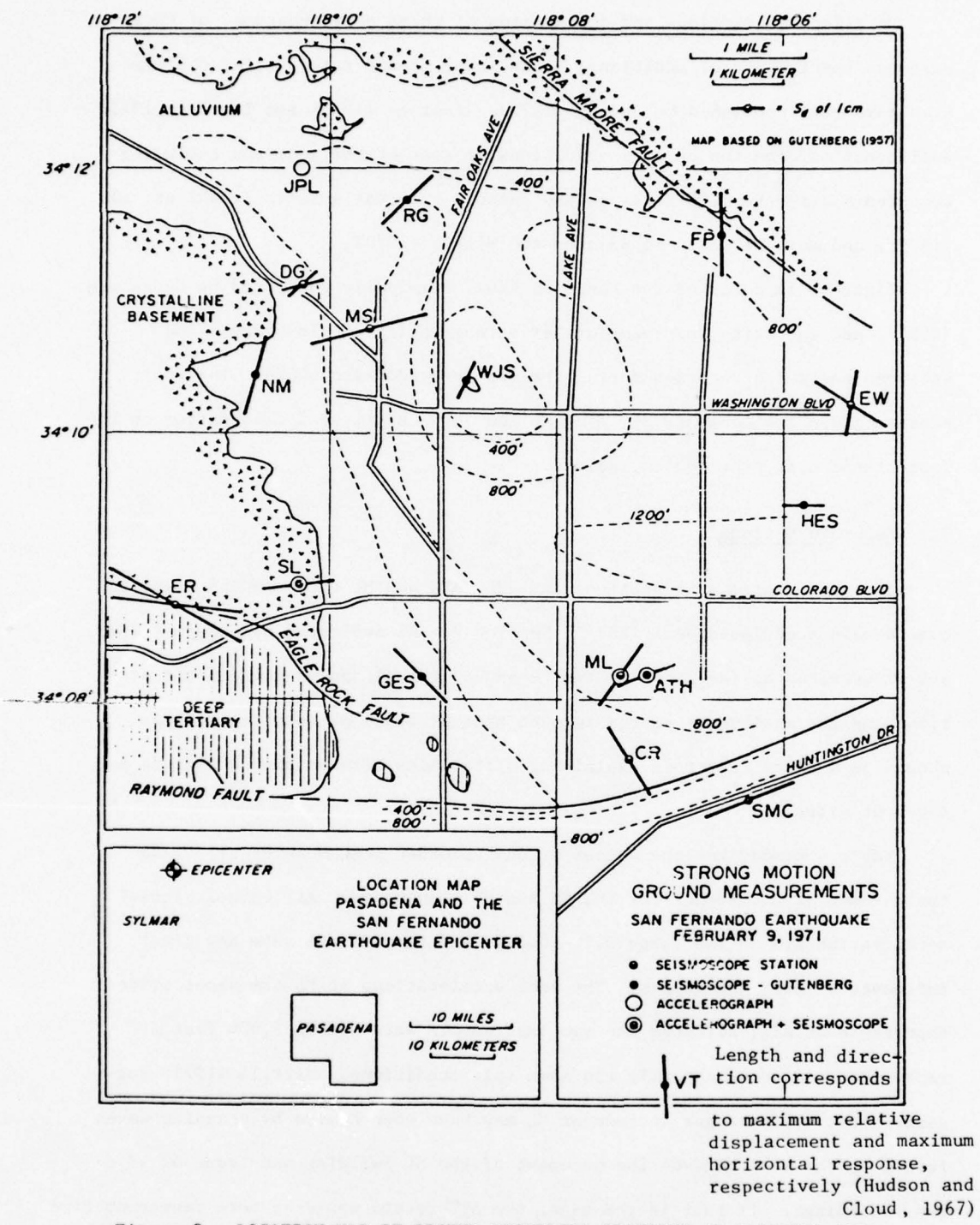


Figure 8 - LOCATION MAP OF GROUND RECORDING STATIONS AT PASADENA AREA
(Hudson 1972)

Table 3

Instrument and Site Characteristics
Pasadena Area, San Fernando Earthquake
(From Hudson, 1972)

Station Name	Seismological Laboratory	Jet Propulsion Laboratory	Millikan Library
Symbol for Fig. 8	SL	JPL	ML
Caltech No. for Fig. 1	G106	G110	G107
Accelerograph Type	RFT-250	RFT-250	SMA-1
Location	Basement of 2-story Building	Basement of 9-story Steel Frame Building	Basement of 2 1/2-story RC Building
Site Conditions	Granite Crystalline Rock	400 ft. Alluvium	900 ft. Alluvium 900 ft. Alluvium

Table 4

Recorded Peak Horizontal Accelerations
 Pasadena Area, San Fernando Earthquake

Station Name	Seismological Lab. (SL)		Jet Propulsion Lab. (JPL)	Athenaeum (ATH)	Millikan Library (ML)	Reference
Peak Horizontal Acceleration	NS	0.09 g	0.14 g (*)	0.10 g	0.20 g	---
	EW	0.19	0.21 (*)	0.11	0.19	---
Time of Peak Horizontal Acceleration, t_p	NS	5.14 sec.	5.16 sec. (*)	7.66 sec.	7.12 sec.	Hudson et. al. (1972)
	EW	5.78	5.10 (*)	7.90	7.24	
Time of First S-Wave Arrival, t_1			1.8 sec.	5.0 sec.	4.5 sec.	Berrill (1975)
	NS	2.24 sec.				
$t_p - t_1$	NS	2.24 sec.	3.36 sec. (*)	2.66 sec.	2.62 sec.	---
	EW	2.88	3.30 (*)	2.90	2.74	

(*) For JPL Station, the S08W component of the instrument was taken as NS, and the S82E component as EW.
 For SL, ATH and ML Stations, the components of the instruments were oriented in NS and EW directions.

of free field accelerations than the ML record.

Another interesting fact in Table 4 is the consistency of the times of occurrence of the peak accelerations. For seven out of the eight horizontal components, the times ($t_p - t_1$) are clustered around the narrow range 2.6 - 3.4 seconds, and for one component, $(t_p - t_1) = 2.2$ seconds. This is consistent with the discussion of Figs. 3 and 7 in Section 2, and suggests that the wave arrival at $t \approx t_1 + 3$ seconds was more prominent in the Pasadena area than the second arrival at $t \approx t_1 + 5$ sec.

The results of the time domain analyses of the accelerograms recorded at the four stations are presented in Figs. 9 through 18. These include normalized Husid plots, and RMS(t) and $\phi_1(t)$ graphs. (The $\phi_3(t)$ and f(t) graphs are included in Appendices 1 and 2.) In all these figures, the estimated values of t_1 from Berrill (1975) and of $t_2 = t_1 + 6$ have also been superposed. Figure 19 includes the acceleration response spectra for the SL (rock) and ATH (soil) stations.

Figures 9 and 10 include the normalized Husid plots for the four stations. For all four plots, the locations of t_1 given by Berrill are consistent with the shape of the curves. The comparison in Fig. 9 indicates a rate of energy buildup almost identical for SL and JPL, with $h(t_2) \approx 85$ to 90%. Figure 10 indicates a rate of energy buildup very similar for the two nearby ATH and ML soil stations, with $h(t_2) = 70$ to 75%. The comparison with the SL plot in Fig. 10 also suggests that some additional wave reflections occurred after t_2 in the soil area represented by ATH and ML which were not present on rock at SL. This is similar (although not as prominent) to the wave reflections in the San Fernando Valley soil stations illustrated by Fig. 7. It also becomes apparent if the Trifunac and Brady (1975) duration D for the four records are compared. (D is defined as the time needed to buildup the ordinates in the Husid plot from 5% to 95%.) The values of D are:

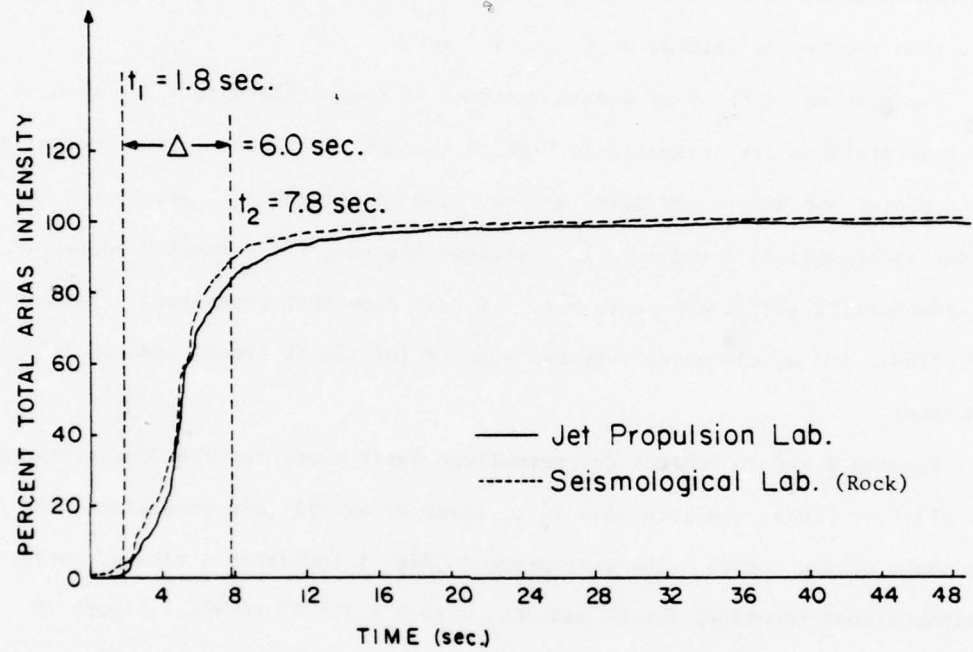


Figure 9 - NORMALIZED HUSID PLOTS OF RECORDED HORIZONTAL ACCELERATIONS,
PASADENA AREA
(time scale, t_1 and t_2 values are from Jet Propulsion Lab.)

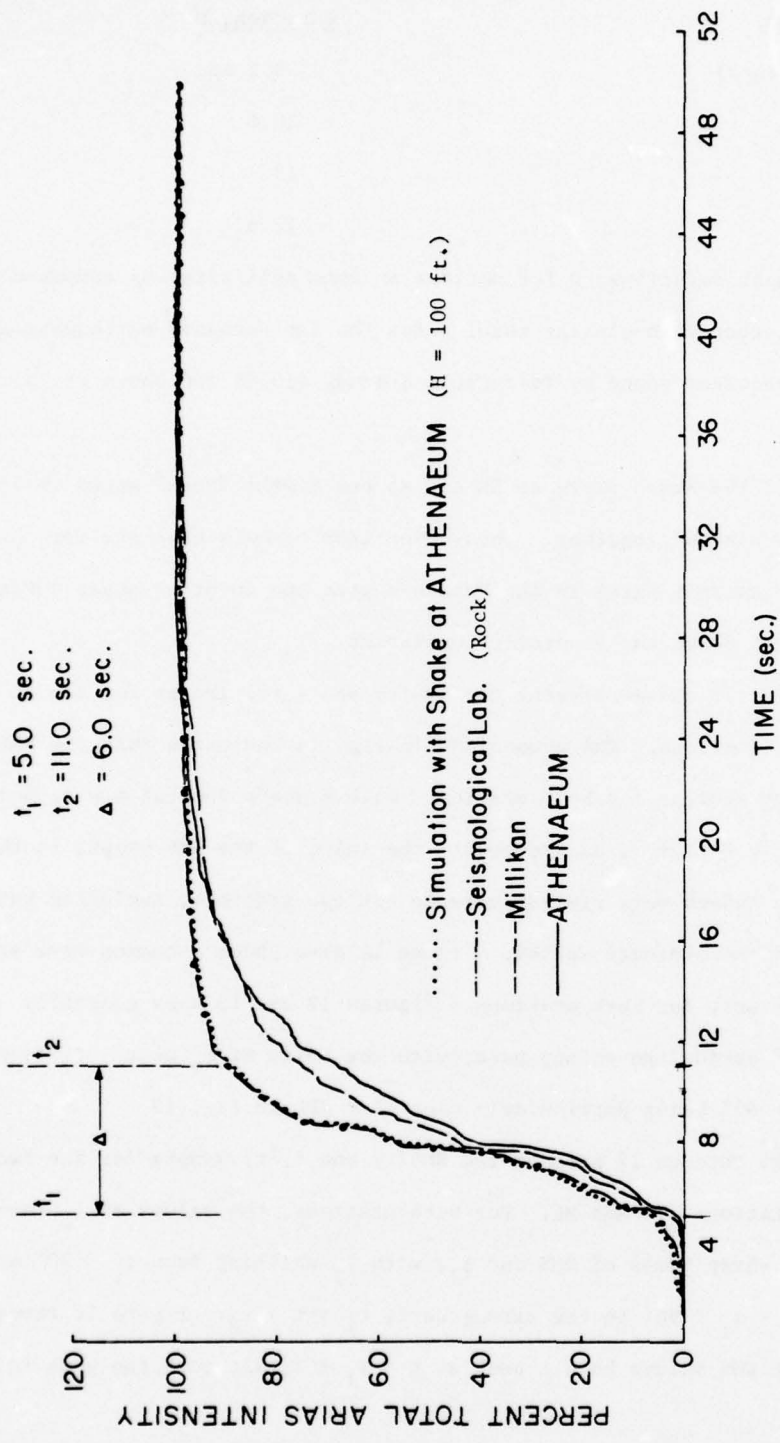


Figure 10 - NORMALIZED HUSID PLOTS OF RECORDED AND SIMULATED HORIZONTAL ACCELERATIONS,
PASADENA AREA (time scale, t_1 and t_2 values are from Atheneum)

<u>Station</u>	<u>Duration, D</u>
SL (rock)	9.1 sec.
JPL	10.6
ATH	13
ML	15.6

These longer durations, D for motions at some soil sites as compared with rock are consistent with similar results for the San Fernando earthquake and for other earthquakes found by Trifunac and Brady (1975) and Dobry et. al. (1977, 1978a).

In Fig. 11 the Husid plots at SL and at one of the "rock" sites included in Fig. 6, are plotted together. This comparison reveals that the rate of energy buildup at rock sites in the Pasadena area and in other areas during the San Fernando quake was generally consistent.

Figures 12, 13 and 14 present the RMS(t) and $\phi_1(t)$ graphs for the SL (rock) and JPL (soil) stations. The comparison in Fig. 14 indicates that the RMS(t) graphs are very similar for both stations, with a sharp jump at $t = t_1$ and a larger peak at $t \approx t_1 + 3$, as expected. The shape of the RMS graphs in the strong part is indeed very similar between the two stations, including both the shapes and the ordinate values. Figure 14 also shows a common wave arrival at $t = t_1 + 30$ sec. for both stations. Figures 12 and 13 show generally $60^\circ < \phi_1 < 90^\circ$ during the strong part, with the shift of ϕ_1 at $t = t_1$ from low values to $\phi_1 > 60^\circ$ being particularly clear for JPL in Fig. 13.

Figures 15 through 17 present the RMS(t) and $\phi_1(t)$ graphs for the two nearby soil stations ATH and ML. For both stations, the values of t_1 coincide well with the sharp jumps of RMS and ϕ_1 , with ϕ_1 shifting from $\phi_1 \leq 20^\circ$ at $t < t_1$ to $60^\circ < \phi_1 < 90^\circ$ in the strong part, $t_1 < t < t_2$. Figure 16 reveals again that the RMS values have a peak at $t \approx t_1 + 3$, although the peak is

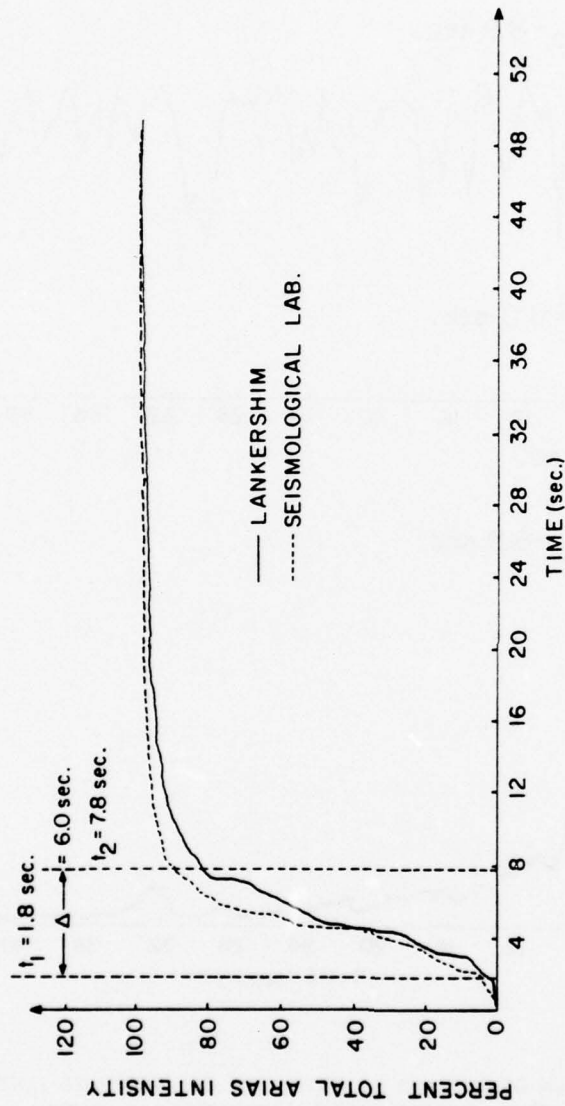


Figure 11 - NORMALIZED HUSID PLOTS OF RECORDED HORIZONTAL ACCELERATIONS
(time scale, t_1 and t_2 values are from Lankershim)

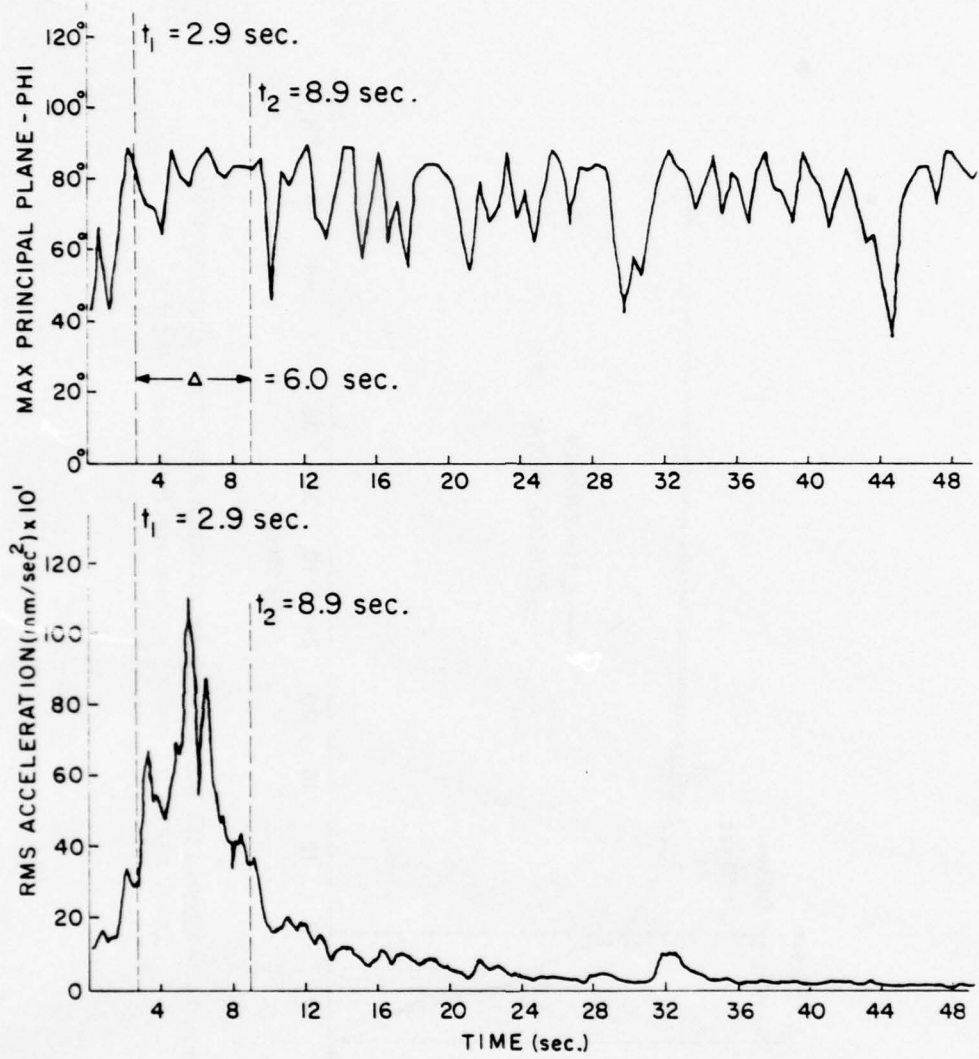


Figure 12 - VARIATION OF RMS AND ϕ_1 WITH TIME FOR RECORDED ACCELERATIONS
AT ROCK SITE, SEISMOLOGICAL LABORATORY, PASADENA.
(0.5 - SEC. WINDOW)

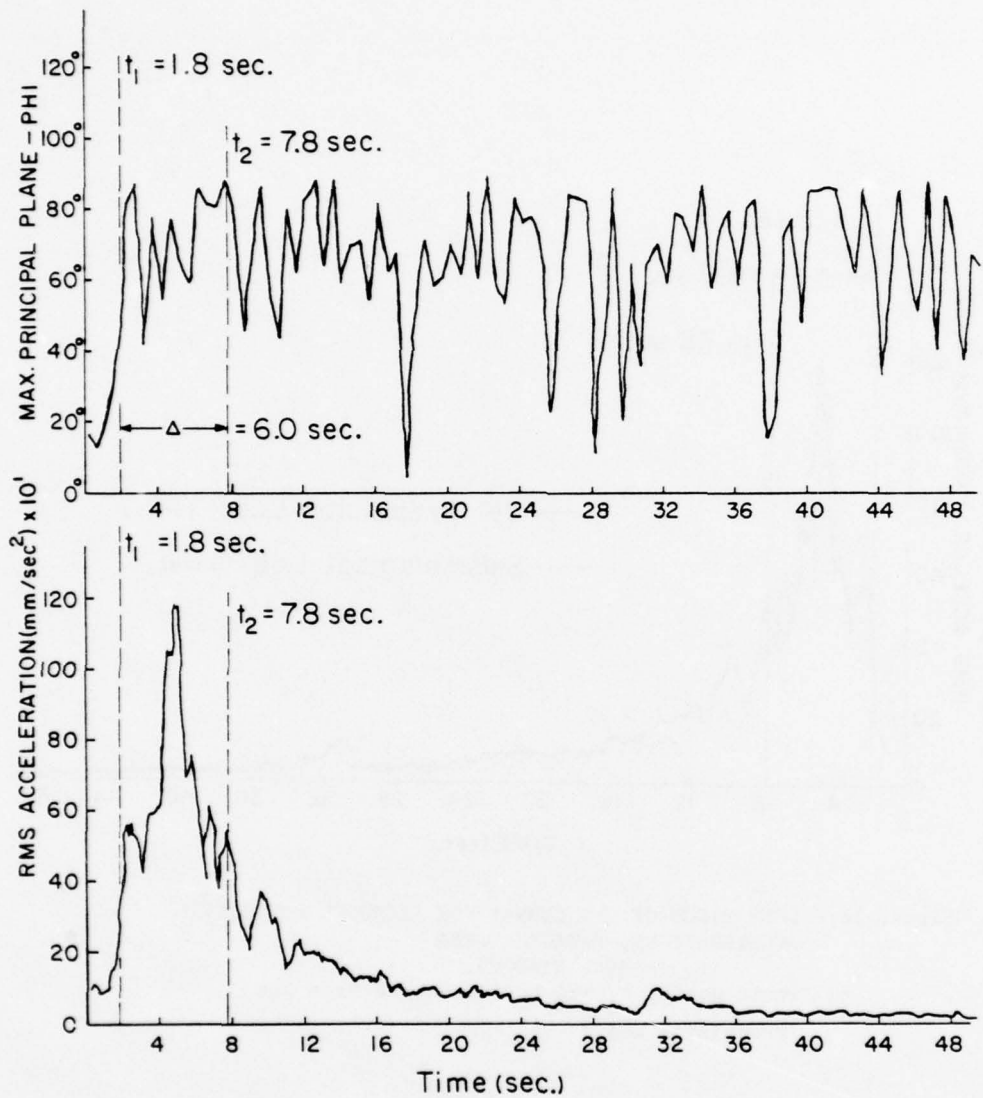


Figure 13 - VARIATION OF RMS AND ϕ_1 WITH TIME FOR RECORDED ACCELERATIONS,
JET PROPULSION LABORATORY, PASADENA
(0.5 - SEC. WINDOW)

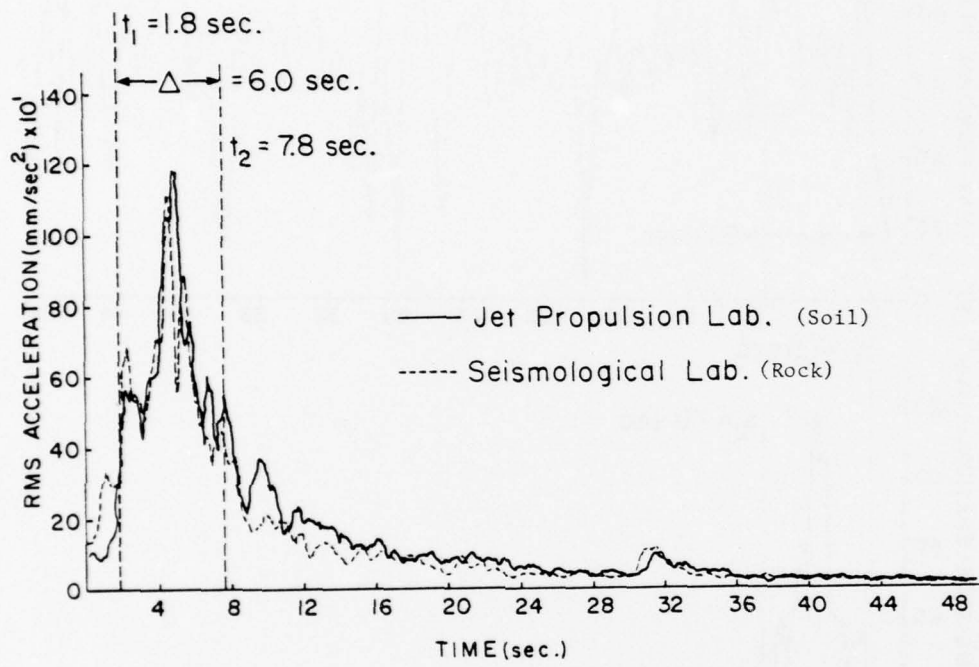


Figure 14 - COMPARISON OF RMS CURVES FOR RECORDED HORIZONTAL ACCELERATIONS, PASADENA AREA
 (0.5 - SEC. WINDOW)
 (time scale, t_1 and t_2 values are from Jet Propulsion Lab.)

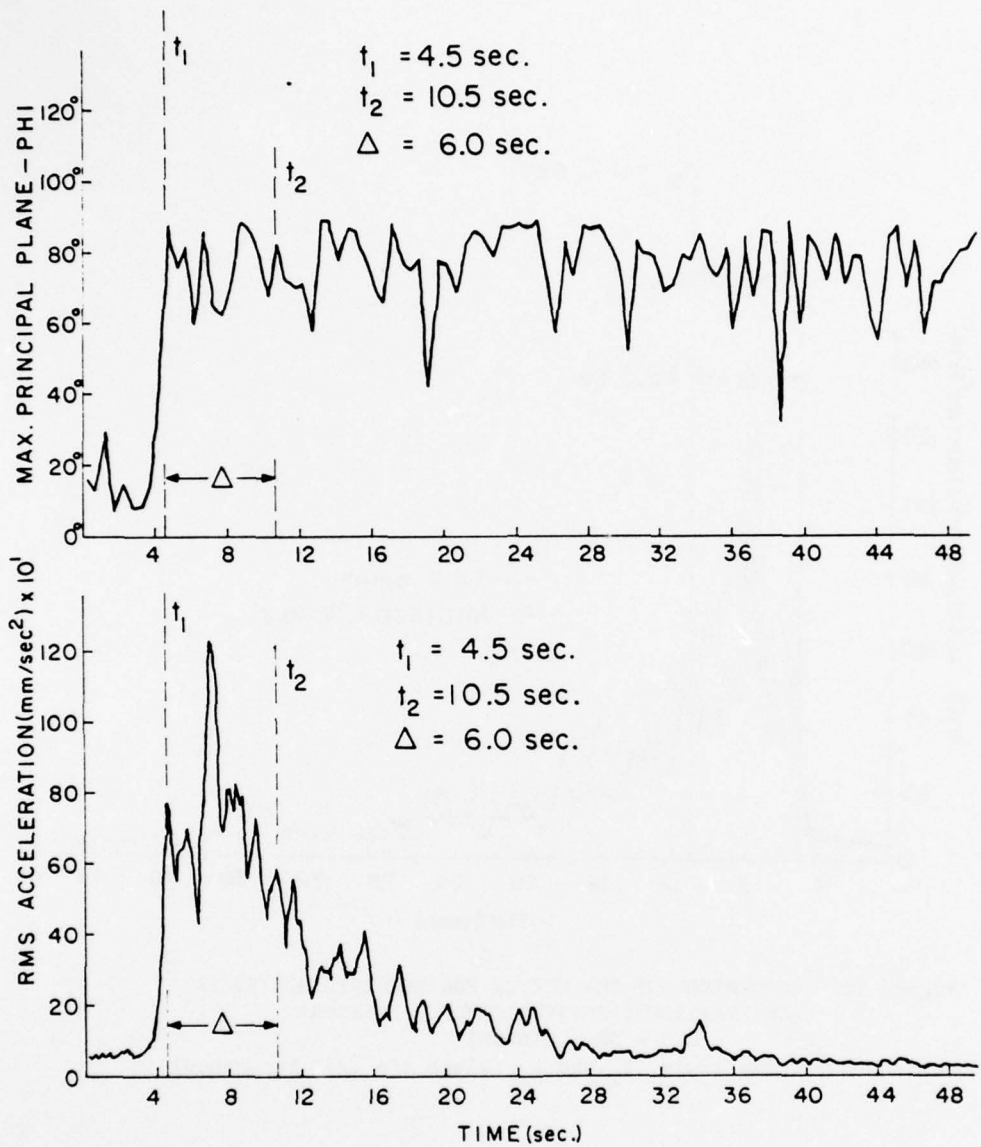


Figure 15 - VARIATION OF RMS AND ϕ_1 WITH TIME FOR RECORDED ACCELERATIONS,
 MILLIKAN LIBRARY, PASADENA
 (0.5 - SEC. WINDOW)

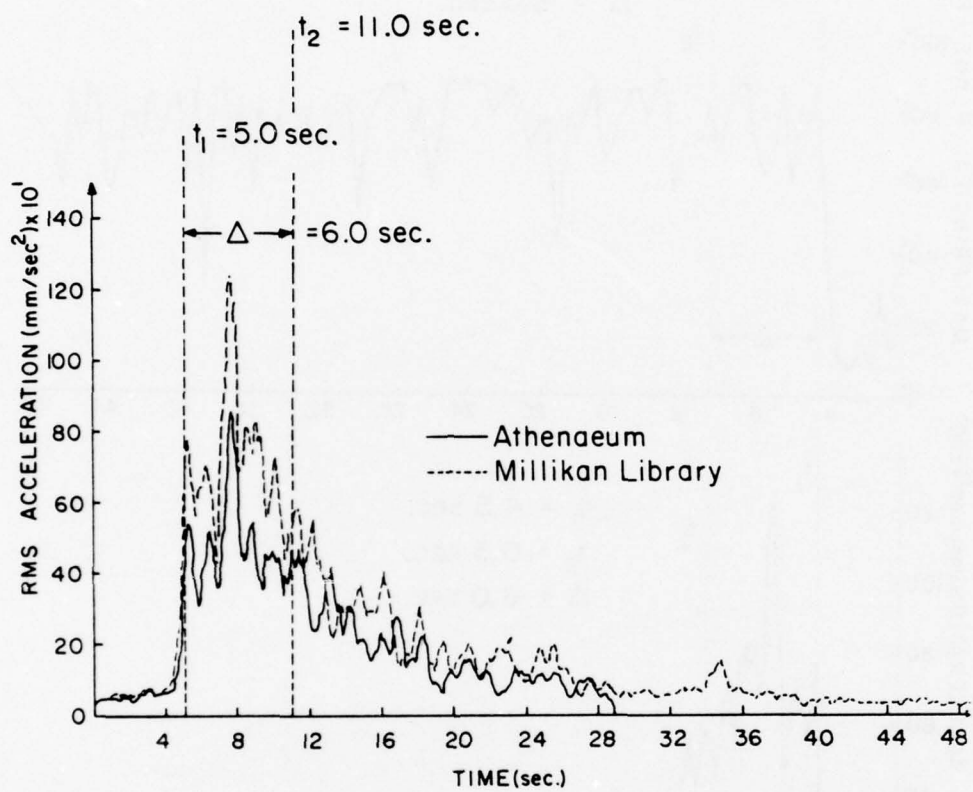


Figure 16 - COMPARISON OF RMS CURVES FOR RECORDED HORIZONTAL ACCELERATIONS, CALTECH CAMPUS, PASADENA
(0.5 - SEC. WINDOW)
(time scale, t_1 and t_2 values are from Athenaeum)

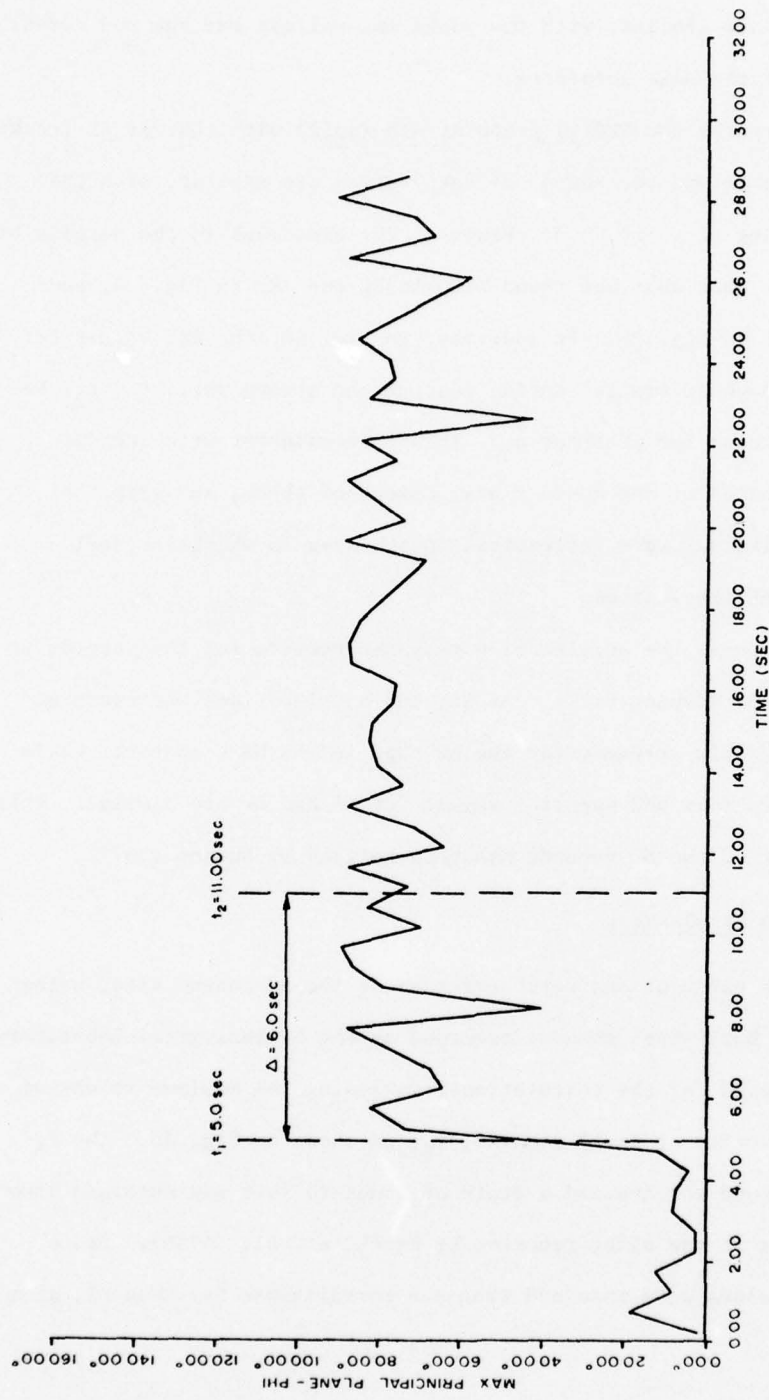


Figure 17 - VARIATION OF ϕ_1 WITH TIME FOR RECORDED ACCELERATIONS, ATHENAEUM, PASADENA
 (0.5 - SEC. WINDOW)

significantly larger for the ML curve, as could be expected from the larger values of the peak accelerations at ML (see Table 4). The shapes of the RMS curves in Fig. 16 are similar, with the peaks and valleys for the two curves being generally at the same locations.

Figure 18 compares the RMS(t) graph at ATH (soil) with that at SL (rock). The general ordinates and the shapes of both curves are similar, with the major peak occurring at $t \approx t_1 + 3$. However, the agreement in the details of the shapes is less than what was found between SL and JPL in Fig. 14, and between ATH and ML in Fig. 16. In addition, in Fig. 18, the RMS values for ATH, which were somewhat smaller during most of the strong part, $t < t_2$, become larger than those for SL after t_2 . This is consistent with the differences in the shapes of the Husid plots, discussed above, and with the hypothesis of additional wave reflections in the area in which the soil stations ATH and ML are located.

Figure 19 compares the acceleration response spectra for the records at SL and ATH, for a 5% damping ratio. At SL, the accelerations and spectral values are considerably stronger for the EW than in the NS component, while at ATH the accelerations and spectral values for NS and EW are similar. This directional aspect of the SL records has been noticed by Hudson (1972).

3.2 Site Response Simulations

Site response calculations were performed at the Athenaeum site, using as rock input the horizontal motions recorded at the Seismological Laboratory. The soil profile used for the calculations, including the maximum values of the shear wave velocity at small strains, V_S , is shown in Fig. 20. The V_S values between ground surface and a depth of about 25 feet was obtained from refraction surveys at the site, reported by Eguchi et. al. (1976). Below 25 feet, the V_S values were obtained from the correlations for "Old Alluvium"

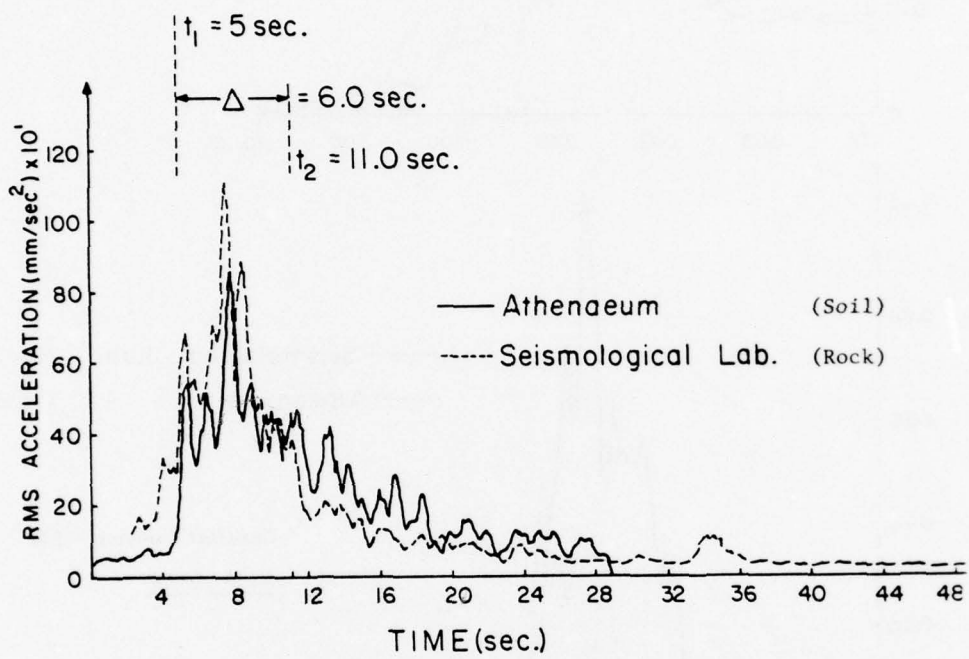


Figure 18 - COMPARISON OF RMS CURVES FOR HORIZONTAL ACCELERATIONS
RECORDED AT ROCK AND SOIL SITES, PASADENA AREA
(0.5 - SEC. WINDOW)
(time scale, t_1 and t_2 values are from Athenaeum)

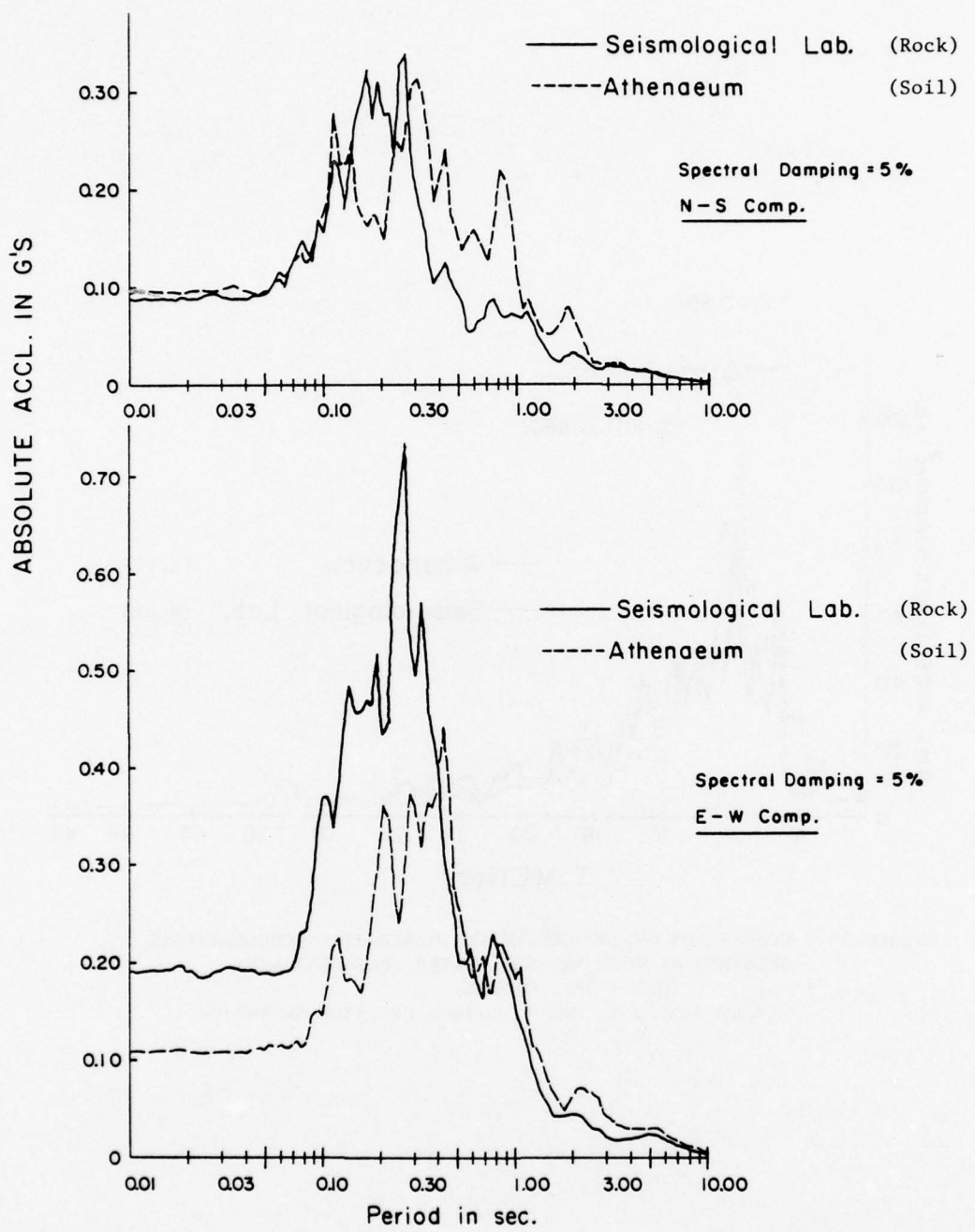
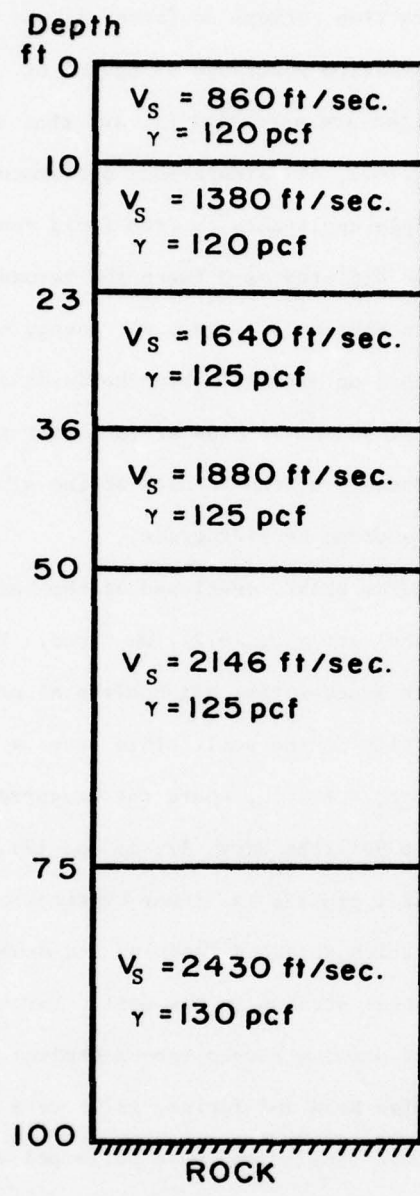


Figure 19 - COMPARISON OF RESPONSE SPECTRA FOR ACCELERATIONS RECORDED AT ROCK AND SOIL SITES, PASADENA AREA



$V_s = 2500 \text{ ft/sec.}$

$\gamma = 135 \text{ pcf}$

Figure 20 - SOIL PROFILE AT ATHENEUM SITE USED FOR SITE RESPONSE SIMULATIONS.

published by Campbell and Duke (1976) for the Los Angeles Area.

Shear wave velocity refraction surveys performed at the Millikan Library site together with other information published by Eguchi et. al. (1976), indicate that the ATH and ML sites are very similar, and that the profile in Fig. 20 is valid also at ML. Therefore, all simulations performed using the profile in Fig. 20 are in principle applicable to free field conditions at both sites. This confirms that the differences between the recorded motions at the two stations, discussed in Section 3.1, were not caused by differences in local site conditions. Based on Berrill's hypothesis discussed in Section 3.1, it is believed that the Athenaeum records are a better representation of the free field motions. Therefore, the results of the simulations were compared with the Athenaeum recorded accelerograms.

For the simulations, Program SHAKE, developed at the University of California at Berkeley (Schnabel et. al., 1972), was used. This code is a one-dimensional program, which assumes that all horizontal ground motions are shear waves travelling vertically in the soil. This seems a reasonable assumption for the strong part, $t_1 < t < t_2$, where the measured values of ϕ_1 at SL, ATH and ML are close to 90° (see Figs. 12, 15 and 17).

SHAKE assumes that the soil profile is linear-hysteretic (viscoelastic) and it iterates until the soil properties selected (modulus and damping) are consistent with the calculated seismic shear strains in the soil. For the simulations, the standard modulus reduction and damping curves versus strains provided in the program for sand soils (see also Seed and Idriss, 1970) were used.

Two series of site response simulations were performed with SHAKE, to evaluate the sensitivity of the results with respect to the selected depth-to-rock. In one of these series, the profile shown in Fig. 20 was used, with a total soil thickness of 100 ft., and a value $V_S = 2,500$ fps for the rock; this V_S is consistent with the near-surface values measured in the rock at

the SL site (Eguchi et. al., 1976). In the second series, only the upper 0-50 ft. of the profile in Fig. 20 was used, with $V_S = 2,000$ fps for the rock. In all calculations, the SL input motions were assumed to act at a rock outcrop.

Table 5 presents a comparison between computed and simulated peak horizontal accelerations and their times of occurrence, $(t_p - t_1)$. The comparison between acceleration values is reasonably close for the NS component, but the simulated values are two to three times larger than the recorded accelerations for the EW component. This is related to the uni-directional character of the input SL accelerograms already mentioned in Section 3.1. On the other hand, the simulated values of $(t_p - t_1)$ are closer to the recorded value in the EW direction.

Figures 21 and 22 present comparisons between the simulated and recorded acceleration response spectra for the NS and EW components, respectively. In the NS direction (Fig. 21) the simulated spectral values are larger than the recorded values for periods up to about 0.30 seconds, while the opposite is true for larger periods. This is similar to the comparison between NS recorded spectra for ATH and SL in the upper part of Fig. 19. In the EW direction (Fig. 22), the simulated spectra is much larger than the recorded spectra for periods up to about 0.3 seconds, while they are similar for periods larger than 0.3 seconds; this is in turn similar to the comparison between recorded ATH and SL spectra in the EW direction shown in the lower part of Fig. 19. In summary, the characteristics of the simulated soil spectra seem to be determined mainly by the characteristics of the corresponding input rock spectra.

Time domain analyses of the simulated soil accelerograms at the ATH Site were also performed. Normalized Husid plots and RMS(t) graphs were developed and compared with the corresponding recorded curves at the site. $\phi_1(t)$ graphs

Table 5

Simulated and Recorded Peak Horizontal Accelerations
Athenaeum Site (ATH), Pasadena, San Fernando Earthquake

Recorded		Simulated (V_S rock = 2,500 fps)	Simulated (V_S rock = 2,000 fps)
Peak Horizontal Acceleration	NS	0.10 g	0.14 g
	EW	0.11	0.29
$t_p - t_1$	NS	2.66 sec.	1.10 sec.
	EW	2.90	2.92

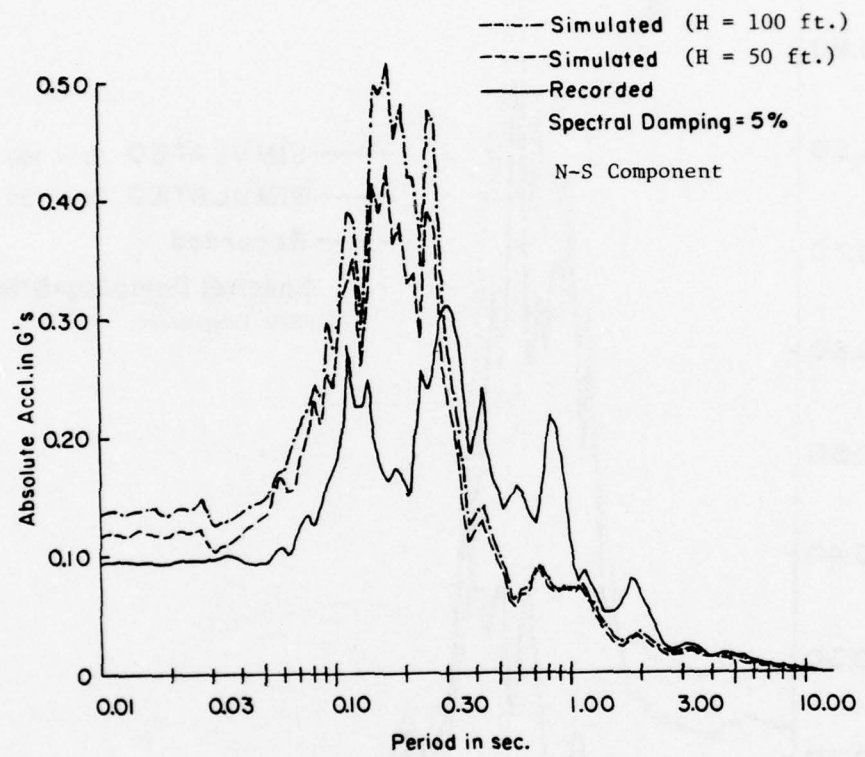


Figure 21 - COMPARISON OF RESPONSE SPECTRA FOR RECORDED AND SIMULATED ACCELERATIONS, ATHENAEUM SITE, NS COMPONENT

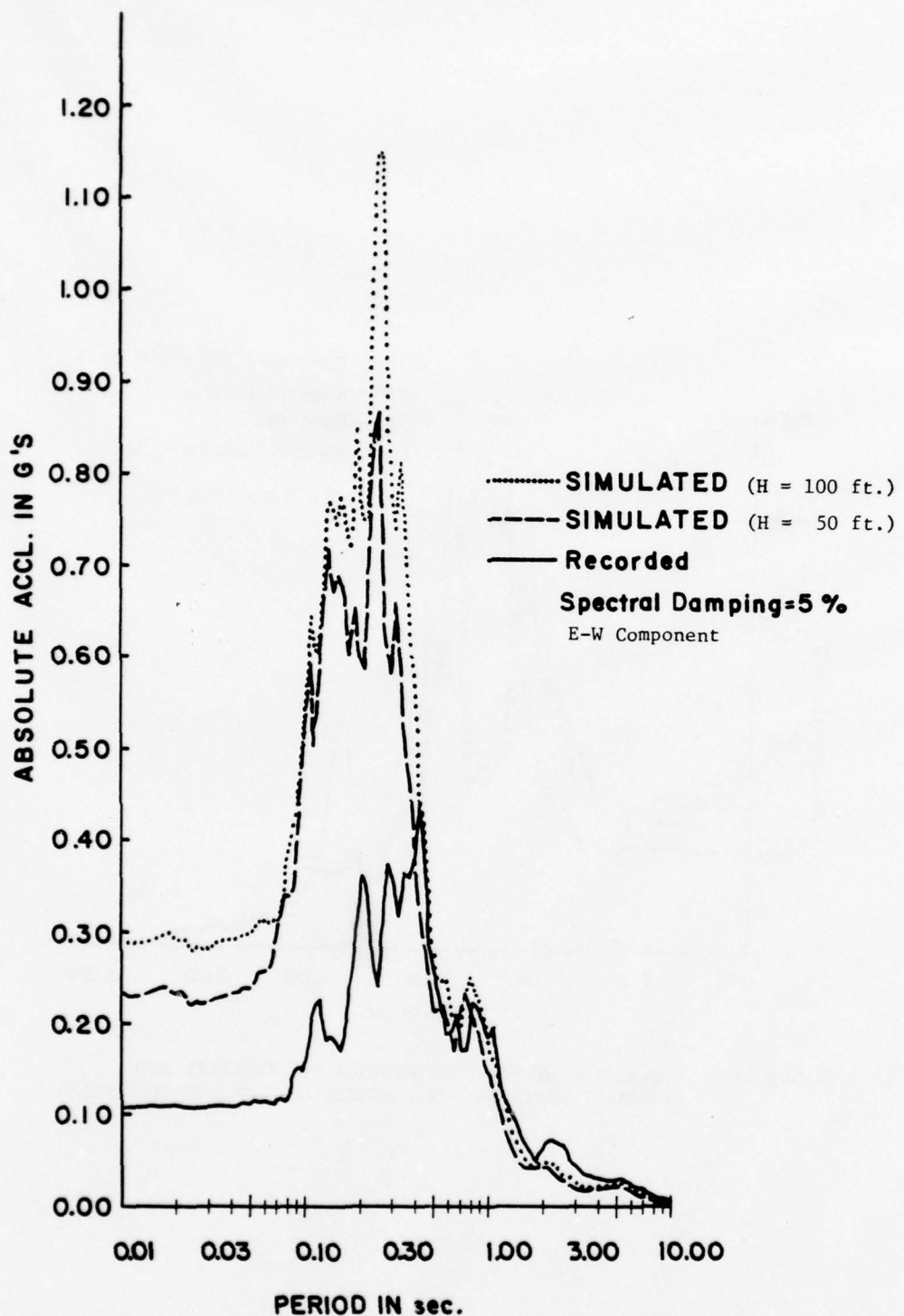


Figure 22 - COMPARISON OF RESPONSE SPECTRA FOR RECORDED AND SIMULATED ACCELERATIONS, ATHENAEUM SITE, EW COMPONENT

could not be obtained as no simulation was performed of the vertical motions at the ATH Site.

The normalized Husid plot for the simulation using $V_S = 2,500$ fps for the rock has been superimposed on Fig. 10. Figure 10 shows that the rate of energy buildup of the simulated soil motions is identical to that of the input (SL) record. Therefore, the increase in duration at the ATH and ML Sites, discussed in Section 3.1, is not predicted by the site response analyses using SHAKE. This is confirmed by a comparison of the 5 to 95% durations D of the motion obtained from the Husid plots in Fig. 10:

<u>Description</u>	<u>Duration, D</u>
SL (rock), recorded	9.1 sec.
ATH (soil), recorded	13
ATH , simulated	9.0
H = 100 ft.	
ATH , simulated	9.0
H = 50 ft.	

The comparisons for the RMS(t) graphs are shown in Figs. 23 and 24.

Figure 23 compares the curve of the simulated ground motions at the Athenaeum site, with the corresponding RMS(t) for the rock input. The curve for the simulation has larger ordinate values, but the shapes of the two curves are very similar, with essentially a total coincidence in the locations of peaks and valleys. The comparison between simulated and recorded RMS curves at Athenaeum is shown in Fig. 24. The shape predicted by the simulations in the strong part is generally similar to that of the recorded curve; in particular, the location of the large recorded peak at $t \approx t_1 + 3$ is predicted by the simulations. However, the details of the shape do not show such good

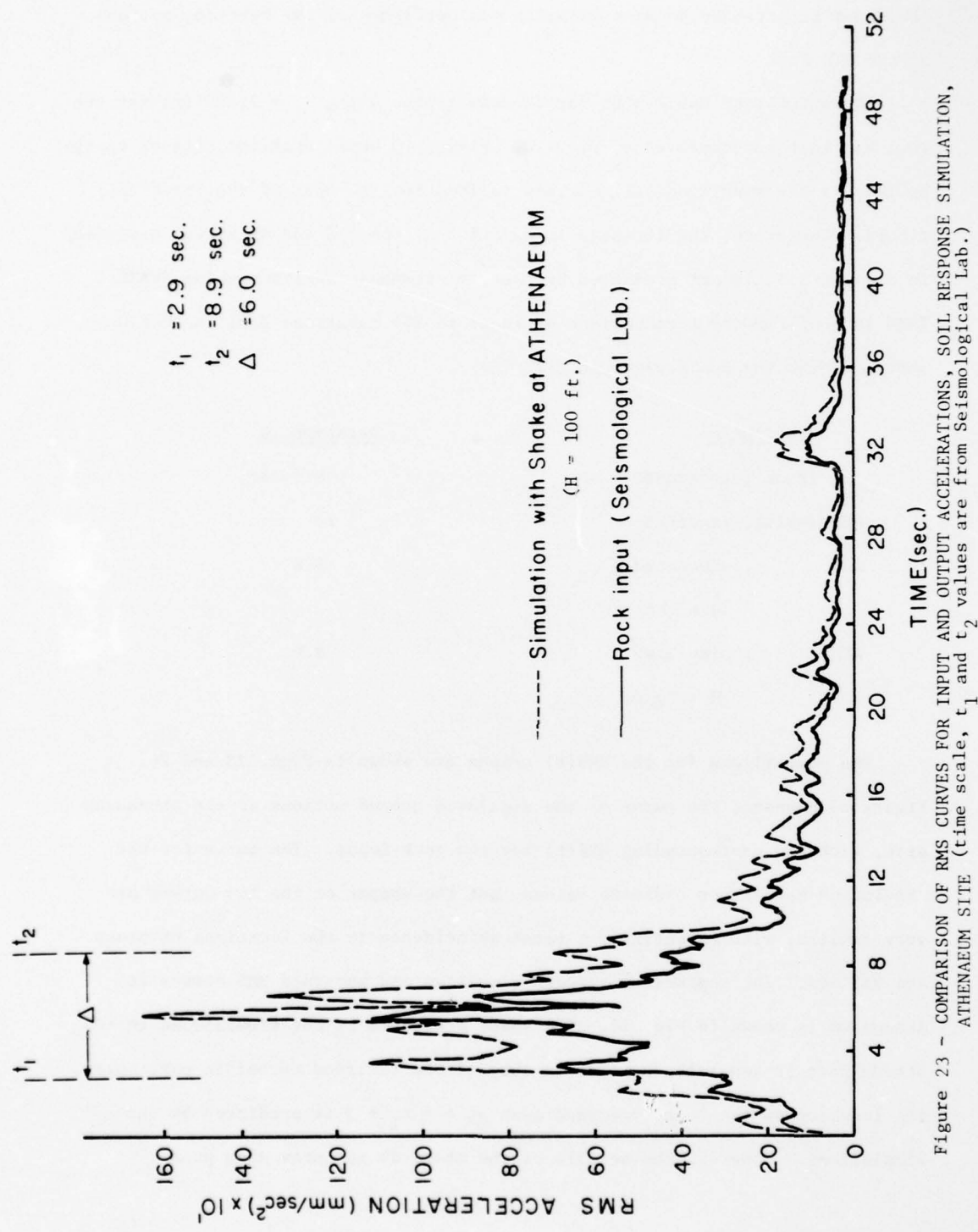


Figure 23 - COMPARISON OF RMS CURVES FOR INPUT AND OUTPUT ACCELERATIONS, SOIL RESPONSE SIMULATION, ATHENAEUM SITE (time scale, t_1 and t_2 values are from Seismological Lab.)

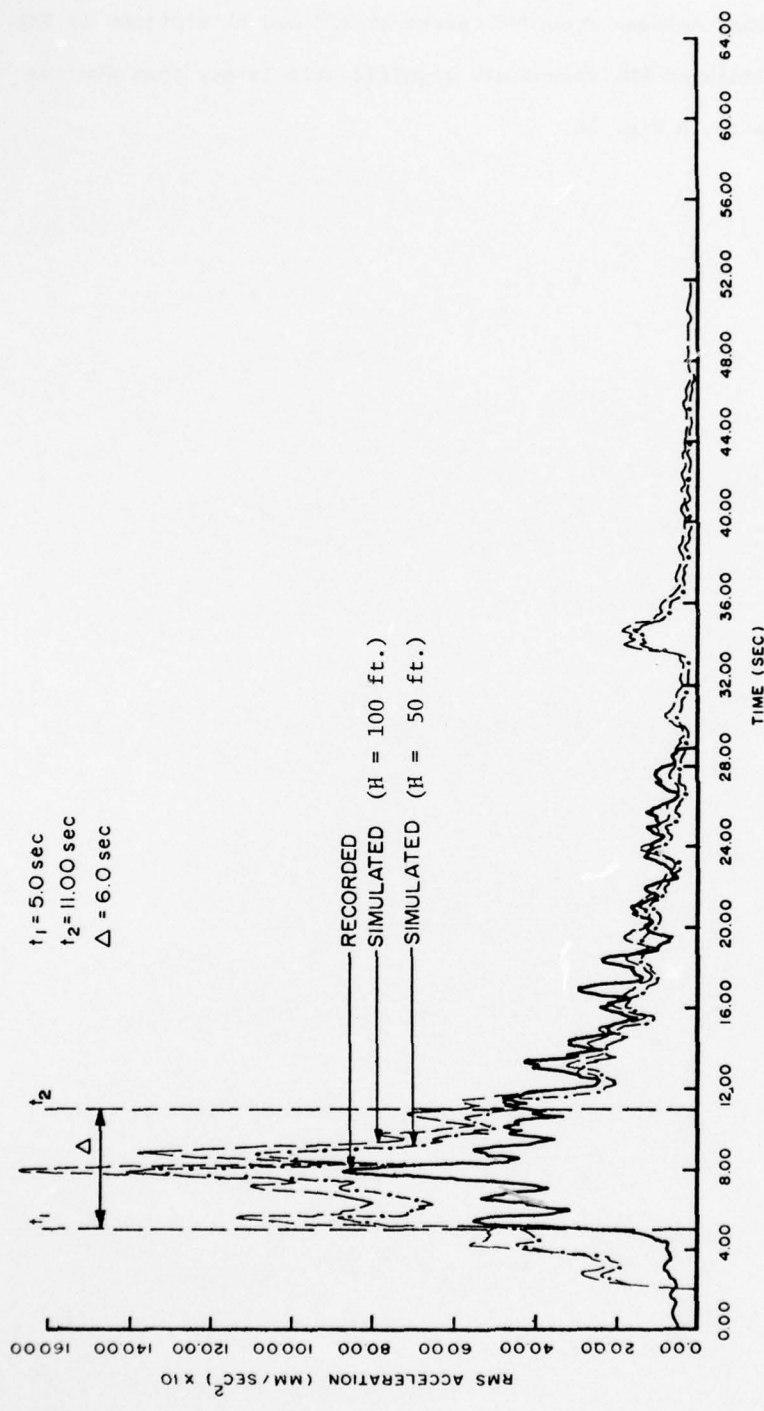


Figure 24 - COMPARISON OF RMS CURVES FOR RECORDED AND SIMULATED HORIZONTAL ACCELERATIONS,
ATHENAEUM SITE, PASADENA

correspondence, and the agreement in the locations of peaks and valleys is not better than that between recorded curves at ATH and SL stations in Fig.

18. Also, the simulated RMS values are significantly larger than the recorded RMS ordinates in Fig. 24.

4. GROUND MOTIONS IN THE SAN FRANCISCO BAY AREA

(San Francisco Earthquake, March 22, 1957)

The San Francisco, California earthquake of March 22, 1957 was a small event, with a local magnitude, $M_L = 5.3$ (Kanamori and Jennings, 1978). However, it occurred along the segment of the San Andreas Fault closer to downtown San Francisco, and some damage to buildings did occur (Steinbrugge et. al., 1959). For an earthquake of this magnitude, it can be estimated that the length of the fault rupture did not exceed a few kilometers and the total duration of the rupture may have been about 2 seconds (Dobry et. al., 1978a).

Ground motions during the earthquake were recorded by strong motion accelerographs at five stations located in San Francisco and Oakland. Studies of this earthquake and of the recorded ground accelerograms include Hudson and Housner (1958), Oakeshott (1959), Idriss and Seed (1968), Dobry et. al. (1978a) and Singh et. al. (1979). These studies have included computation of response spectrum, instrumental intensity and duration, as well as analyses and discussions of the influence of local site conditions. The papers by Idriss and Seed and Singh et. al. include information on site conditions and soil properties at the stations.

Figure 25 is a map showing the five stations and the estimated rupture zone along the San Andreas Fault. One of the instruments was located on rock in Golden Gate Park, while three of the stations were soil sites in downtown San Francisco. The soil profile for these downtown sites consists of sand and clay deposits ranging in thickness from 140 to 285 feet. One of these (Southern Pacific Building), is a clay site, and has been classified as a "soft to medium" site from the viewpoint of the influence of local conditions on earthquake ground motions (Seed et. al., 1974, 1975). The fifth instrument was located across the San Francisco Bay, in Oakland, on 1,000 feet of soil,

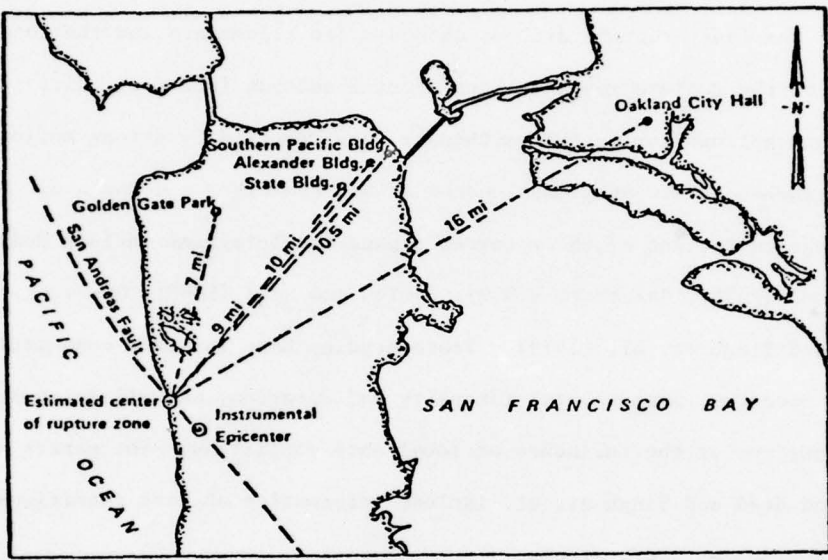


Figure 25 - LOCATION MAP OF GROUND RECORDING ACCELEROMETERS,
SAN FRANCISCO EARTHQUAKE, MARCH 22, 1957
(Idriss and Seed, 1968)

with the upper 100 feet consisting mainly of dense sands. Some additional information on the five stations is provided in Table 6.

4.1 Recorded Motions

Table 7 summarizes the values of the recorded peak accelerations and of their times of occurrence for all horizontal components at the five stations. The peak accelerations range from about 0.10 g at Golden Gate Park to 0.02-0.04 g at Oakland City Hall. Table 7 also includes the estimated times, t_1 of the first S-wave arrival.

The results of the time domain analyses of the accelerograms recorded at the five stations are presented in Figs. 26 through 32. These include normalized Husid plots as well as graphs of RMS(t) and $\phi_1(t)$. The $\phi_3(t)$ and f(t) graphs are included in Appendices 1 and 2. Figure 33 includes a comparison between recorded acceleration response spectra at the rock site and at the soft Southern Pacific Bldg. site.

Figures 26 and 27 present the normalized Husid plots for the five stations. The three curves for soil sites in the downtown area in Fig. 27 indicate an aftershock at about 30 seconds. This aftershock could also be clearly identified in the original accelerograms recorded at Golden Gate Park (not included here), but was not present in the more distant Oakland records. The shapes of the Husid plots indicate significantly longer duration for the motion at the soil sites than at the Golden Gate Park rock site. Of special interest is the much longer duration at the soft Southern Pacific Building site. This longer duration is due to long period motions which occurred in the soil after the end of the strong part of the record. These long period motions have a period of about 1 second and they have been attributed to either soil-structure interaction affects (Hudson and Housner, 1958) or one-dimensional amplification of vertically propagating shear waves

Table 6

Characteristics of Accelerograph Ground Stations

1957 San Francisco Earthquake

Station Name	Golden Gate Park	State Building	Alexander Building	Southern Pacific Bldg.	Oakland City Hall
Caltech No.	A015	A016	A014	A013	A017
Distance to Center of Fault Rupture (see Fig. 25)	7 miles	9 miles	10 miles	10.5 miles	16 miles
Location (from USGS, 1977)	Ground level; free field	Basement of 7-story, Steel Frame Bldg.	Basement of 15-story, Steel Frame Bldg.	Basement of 12-story, Steel Frame Bldg.	Basement of 15-story, Steel Frame Bldg.
Site Conditions (from Idriss and Seed, 1968)	Rock	200 ft. of sand on rock	140 ft. of sand on rock	285 ft. of soil (mostly clay) on rock	1,000 ft. of soil on rock. Upper 100 feet are dense sands

Table 7

Characteristics of Recorded Horizontal Accelerations

1957 San Francisco Earthquake

Station Name	Golden Gate Park	State Building	Alexander Building	Southern Pacific Bldg.	Oakland City Hall
Peak Horizontal Acceleration	N10E: 0.08 g S80E: 0.11	S09E: 0.09 g S81W: 0.06	N09W: 0.04 g N31E: 0.05	N45E: 0.05 g N45W: 0.05	N26E: 0.04 g S64E: 0.02
Time of Peak Horizontal Acceleration, t_p	N10E: 1.34 sec. S80E: 1.44	S09E: 1.80 sec. S81W: 2.12	N09W: 2.68 sec. N81E: 2.04	N45E: 1.76 sec. N45W: 1.76	N26E: 0.48 sec. S64E: 1.25
Estimated time of First S-wave Arrival, t_1	0.95 sec.	0.30 sec.	1.30 sec.	0.65 sec.	0.30 sec.
$t_p - t_1$	N10E: 0.39 sec. S80E: 0.49	S09E: 1.50 sec. S81W: 1.82	N09W: 1.38 sec. N81E: 0.74	N45E: 1.11 sec. N45W: 1.11	N26E: 0.18 sec. S64E: 0.96

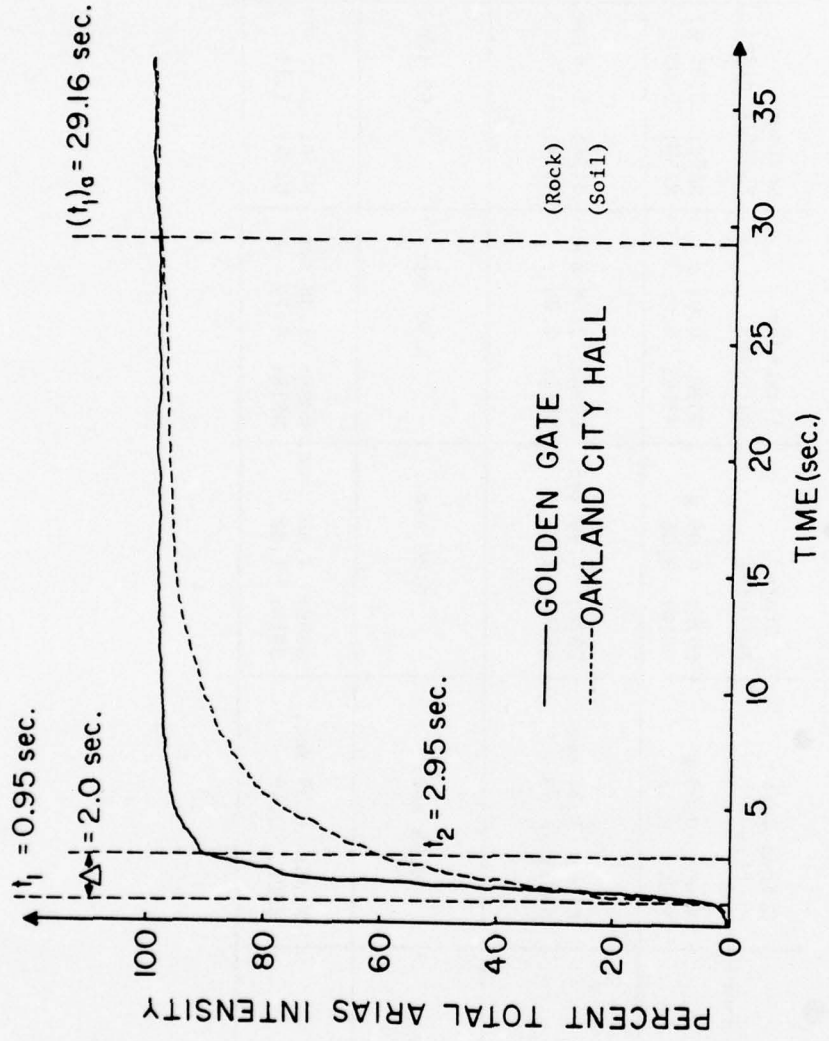


Figure 26 - NORMALIZED HUSID PLOTS OF RECORDED HORIZONTAL ACCELERATIONS,
ROCK AND SOIL SITES, SAN FRANCISCO BAY AREA
(time scale, t_1 , t_1' , t_2 and $(t_1)_a$ values are from Golden Gate)

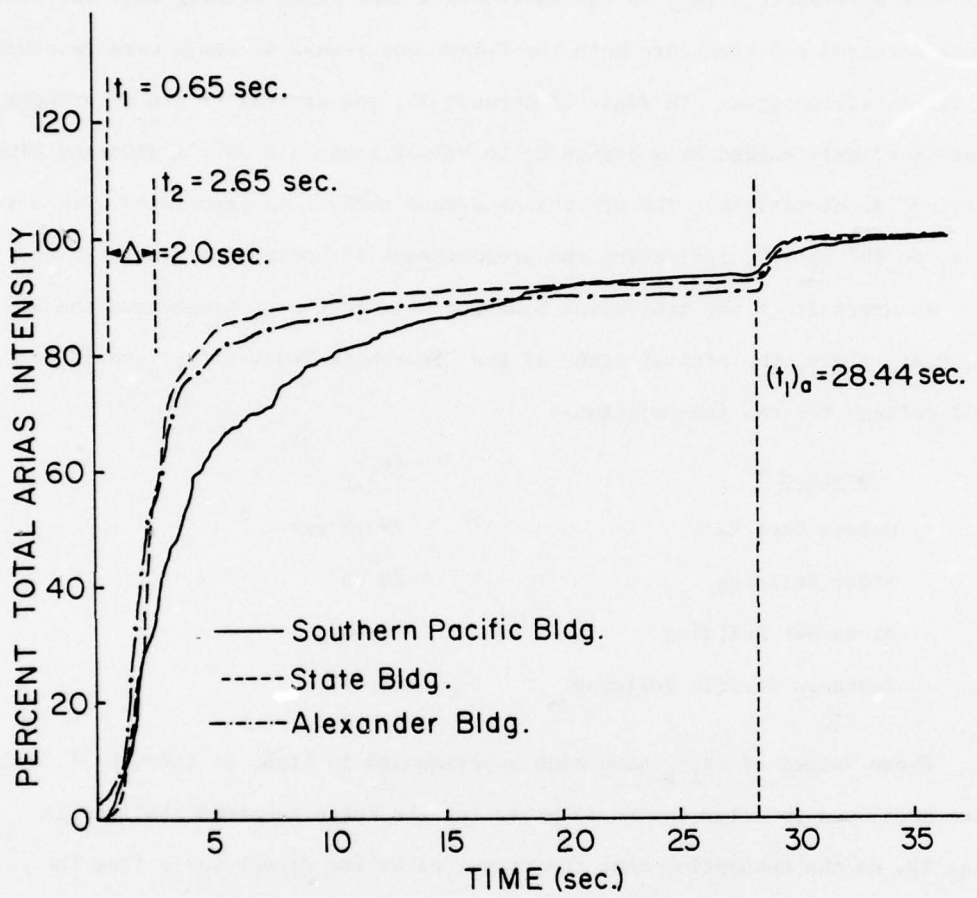


Figure 27 - NORMALIZED HUSID PLOTS OF RECORDED HORIZONTAL ACCELERATIONS, SOIL SITES, SAN FRANCISCO DOWNTOWN AREA (time scale, t_1 , t_2 and $(t_1)_a$ values are from Southern Pacific Bldg.)

(Dobry et. al., 1978a; Singh et. al., 1979).

Figures 28 through 32 present graphs of RMS(t) and $\phi_1(t)$ for the five stations. The presence of the aftershock can be noted in all these figures except in the more distant Oakland City Hall, Fig. 32. It is of interest to discuss the aftershock first, as the instruments were still running when the aftershock occurred and therefore both the P-wave and S-wave arrivals were recorded by the accelerographs. In Figs. 28 through 31, the arrival of the aftershock P-wave is clearly marked by a dip in ϕ_1 to values less than 20° , indicating almost vertical accelerations. The aftershock S-wave arrival is associated with a return of ϕ_1 to 80° to 90° , indicating the predominance of horizontal accelerations.

As a result of the consistent behavior between the ϕ_1 graphs and the RMS and Husid plots, the arrival times of the aftershock S-wave, $(t_1)_a$ could be well defined for the four stations:

<u>Station</u>	<u>$(t_1)_a$</u>
Golden Gate Park	29.16 sec.
State Building	28.06
Alexander Building	29.00
Southern Pacific Building	28.44

These values of $(t_1)_a$ have been superimposed in Figs. 26 through 31, and have been used to align the Husid plots for the three downtown stations in Fig. 27, on the assumption that the travel paths for direct waves from the fault were essentially the same for the main shock and the aftershock.

The times corresponding to the first S-wave arrival for the main event, t_1 , were then estimated from a study of Figs. 26 through 32. The shapes of the Husid plots, and of the RMS(t) and $\phi_1(t)$ graphs were considered for this purpose, together with the values of $(t_1)_a$ for the aftershock determined above.

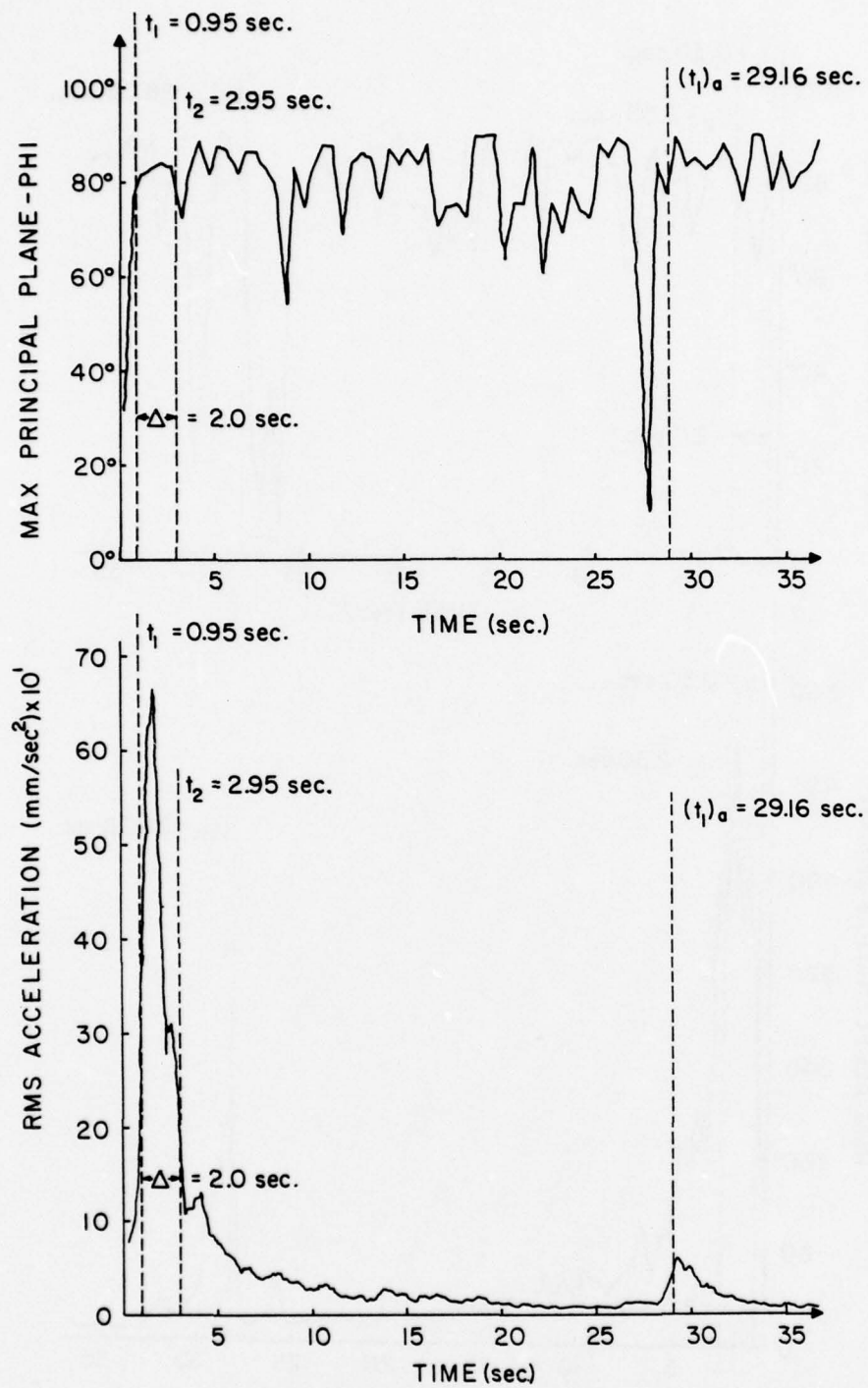


Figure 28 - VARIATION OF RMS AND ϕ_1 WITH TIME FOR ACCELERATIONS RECORDED AT ROCK SITE, GOLDEN GATE PARK, SAN FRANCISCO
(0.5 - SEC. WINDOW)

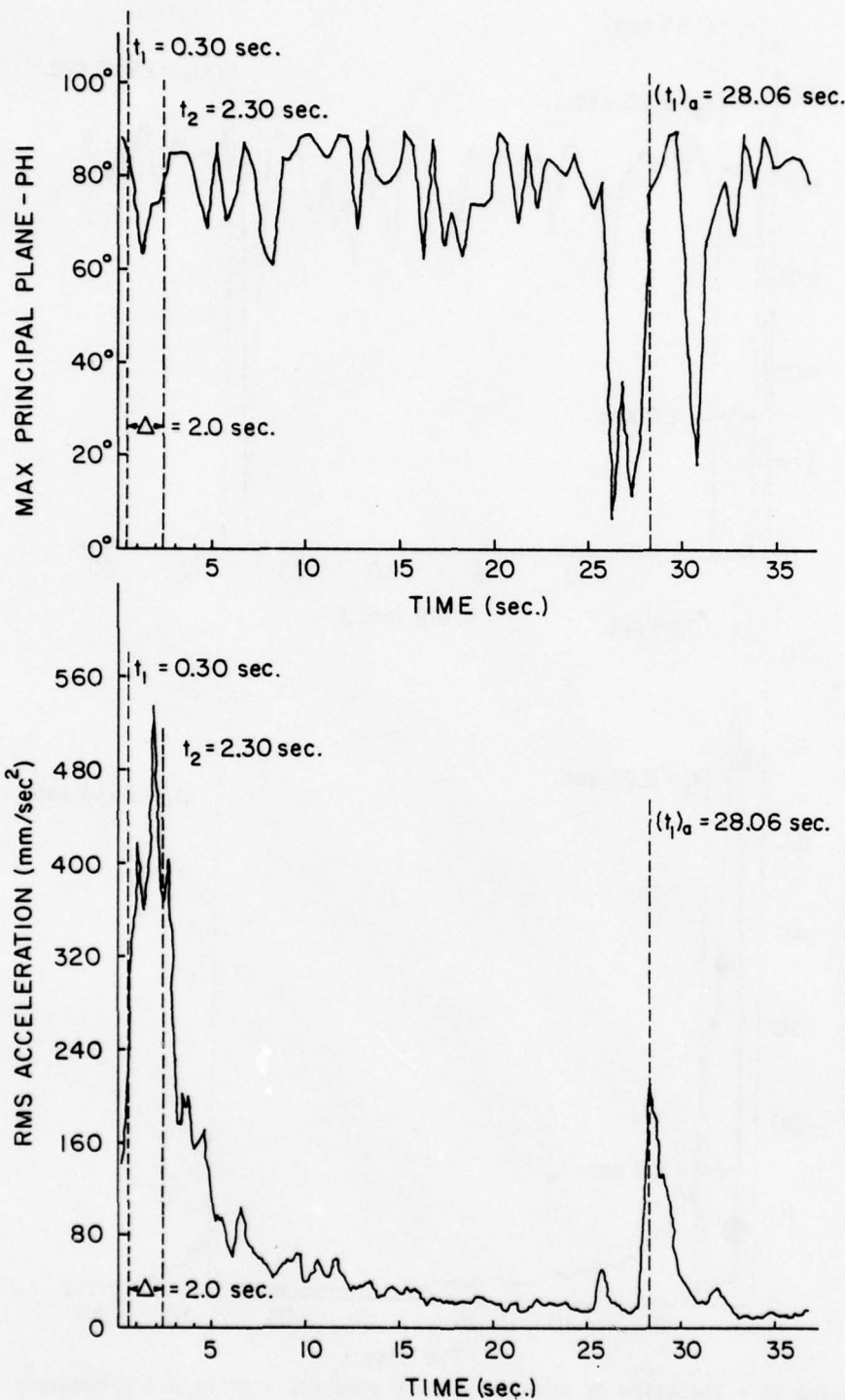


Figure 29 - VARIATION OF RMS AND ϕ_1 WITH TIME FOR RECORDED ACCELERATIONS,
STATE BUILDING, SAN FRANCISCO
(0.5 - SEC. WINDOW)

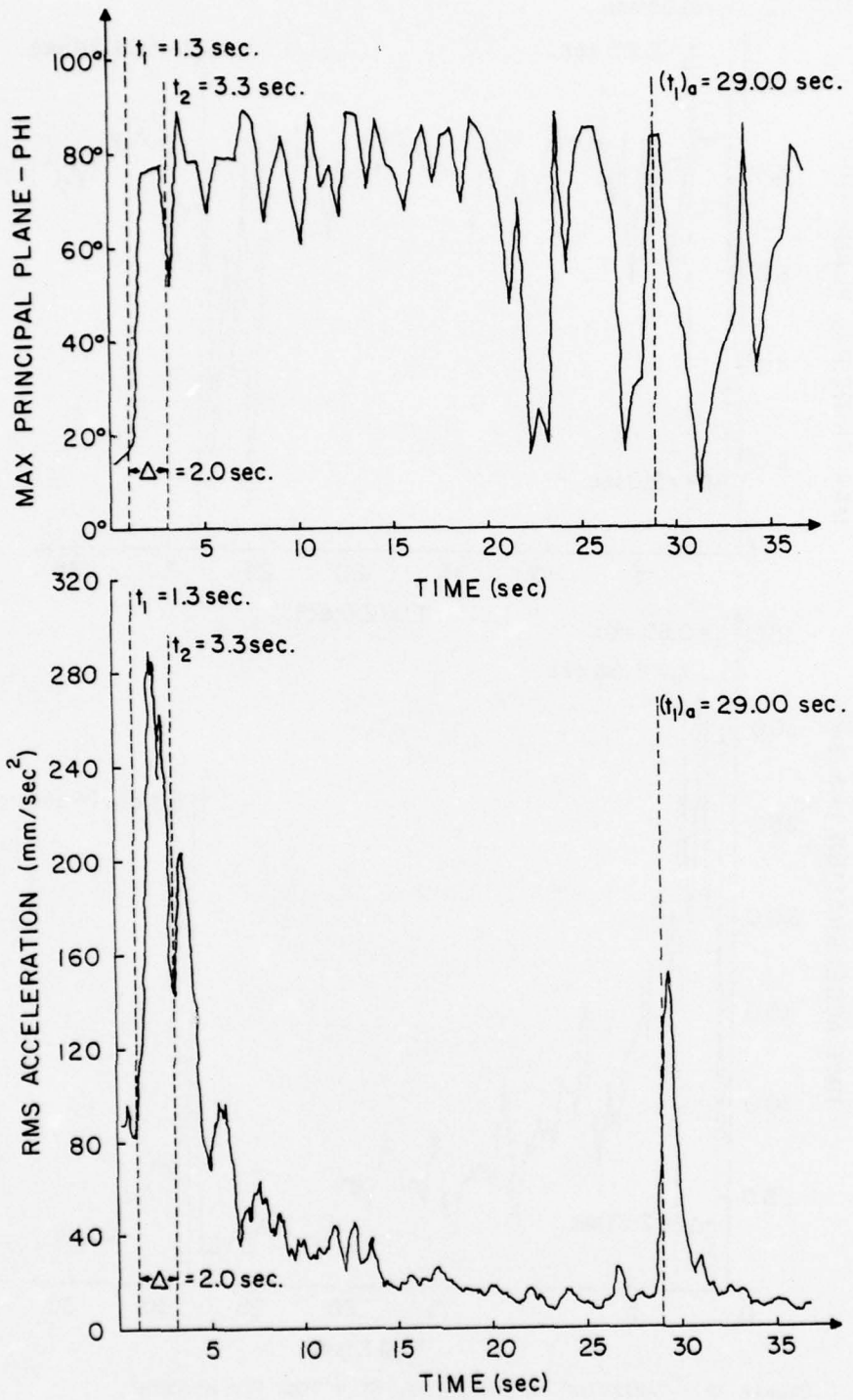


Figure 30 - VARIATION OF RMS AND ϕ_1 WITH TIME FOR RECORDED ACCELERATIONS,
ALEXANDER BUILDING, SAN FRANCISCO
(0.5 - SEC. WINDOW)

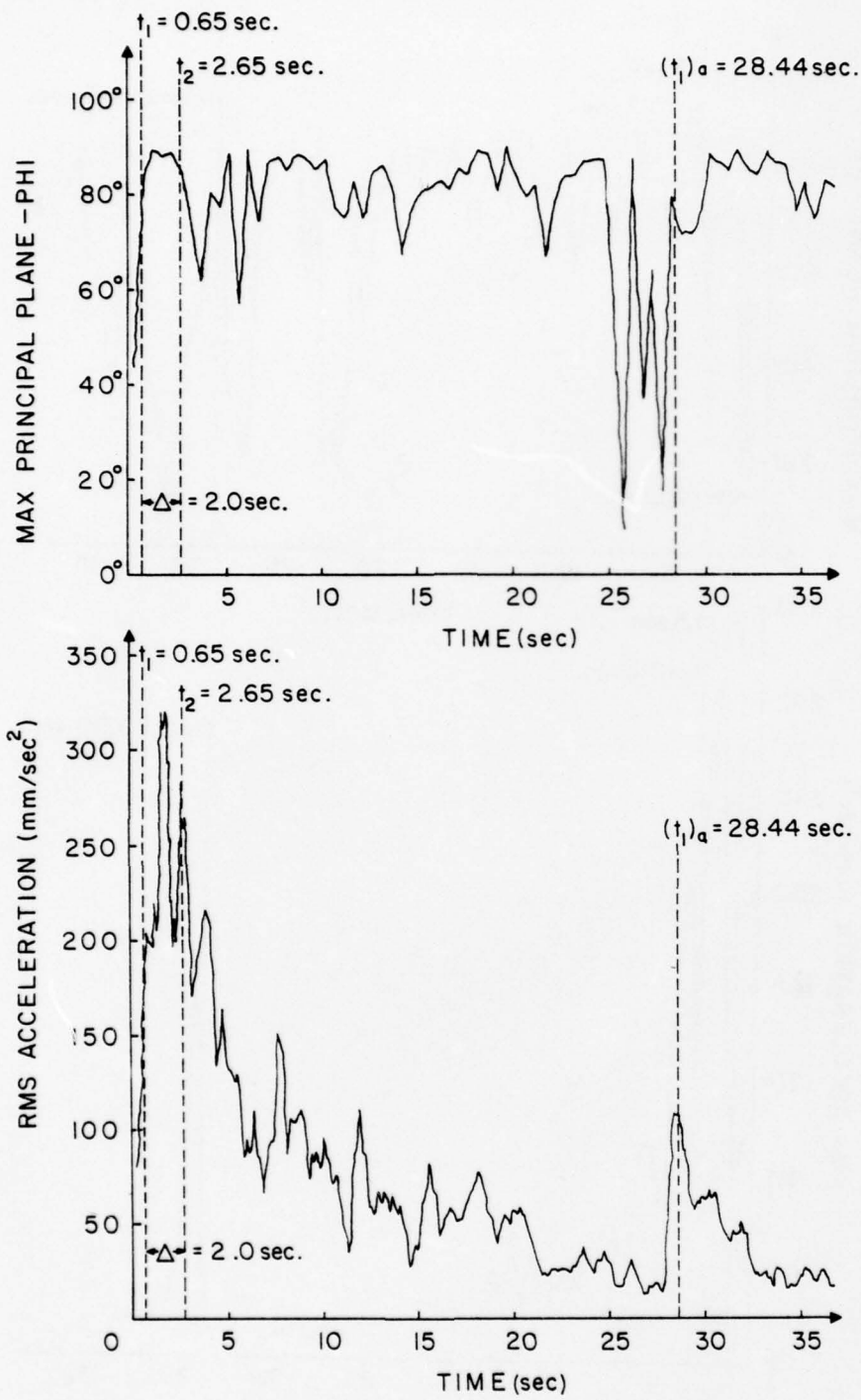


Figure 31 - VARIATION OF RMS AND ϕ_1 WITH TIME FOR RECORDED ACCELERATIONS, SOUTHERN PACIFIC BUILDING, SAN FRANCISCO

(0.5 - SEC. WINDOW)

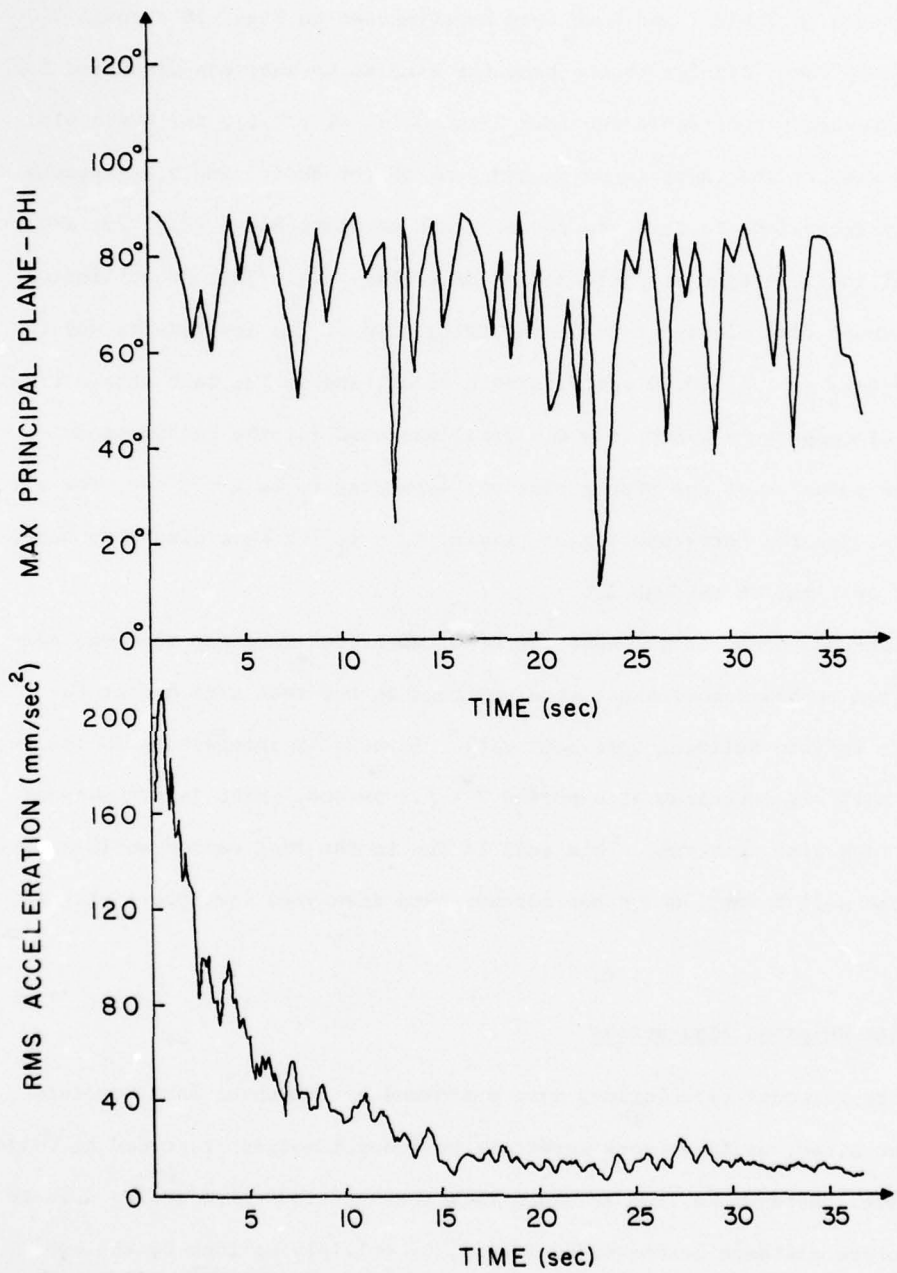


Figure 32 - VARIATION OF RMS AND ϕ_1 WITH TIME FOR RECORDED ACCELERATIONS,
OAKLAND CITY HALL, SAN FRANCISCO BAY AREA
(0.5 - SEC. WINDOW)

In particular, it was assumed that the difference $(t_1)_a - t_1$ was the same for the three downtown stations in Fig. 27. These estimated values of t_1 are included in Table 7 and have been superimposed on Figs. 26 through 31. In general, these figures show a behavior similar to what was discussed for the San Fernando records in Sections 2 and 3.1: at $t \approx t_1$, the Husid plot becomes steeper and there is an upward jump in the RMS(t) and $\phi_1(t)$ graphs. The only exceptions to this are the ϕ_1 graph at State Bldg. (Fig. 29) and both RMS and ϕ_1 graphs at Oakland City Hall (Fig. 32). This is attributed to the short time elapsed between the triggering of the instruments and the first S-wave arrival (0.30 sec.) in both cases, and to the fact that a time window of comparable width ($\delta = 0.5$ sec.) was used for the calculations.

The duration of the strong part was estimated to be $\Delta = 2$ sec. for all stations, and the corresponding end times, $t_2 = t_1 + 2$ have also been superimposed on Figs. 26 through 31.

Figure 33 presents a comparison of acceleration response spectra, computed from recorded horizontal accelerations at the rock site and at the Southern Pacific Building soft soil site. Especially interesting is the peak in the soil site spectrum at a period $T \approx 1.1$ second, which is not present in the rock site spectrum. This peak is due to the long period motions after t_2 in the soil record, which has already been discussed (see Dobry et. al., 1978a).

4.2 Site Response Simulations

Site response calculations were performed at the three San Francisco downtown sites, using as rock input the horizontal motions recorded at Golden Gate Park. Before use, the recorded rock accelerations were scaled down to incorporate distance attenuation effects, by multiplying them by the same reduction factors used by Idriss and Seed (1968), as follows:

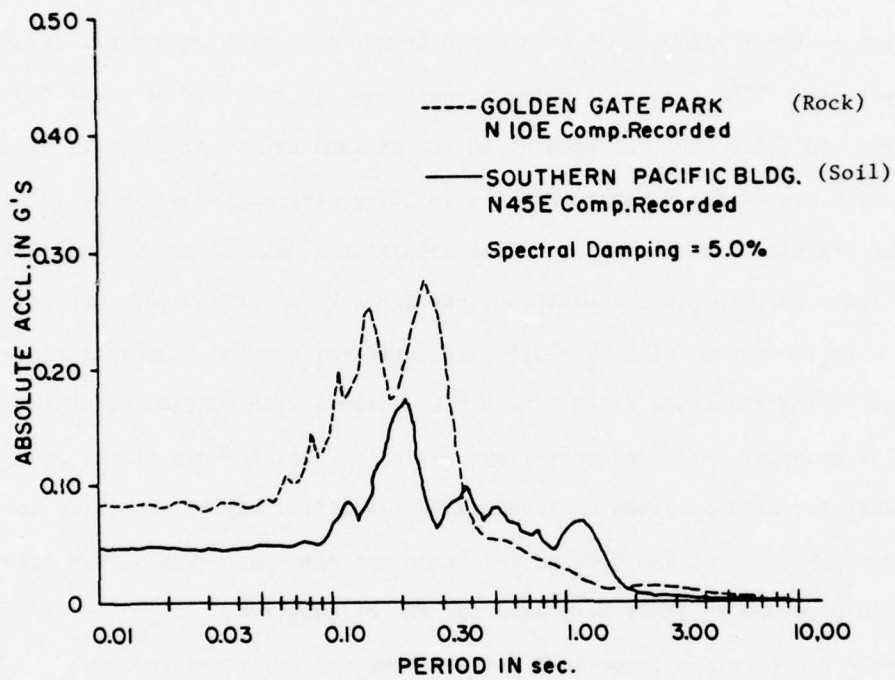


Figure 33 - COMPARISON OF RESPONSE SPECTRA FOR ACCELERATIONS RECORDED AT ROCK AND SOIL SITES, SAN FRANCISCO

<u>Site</u>	<u>Attenuation Factor</u>
State Building	0.80
Alexander Building	0.65
Southern Pacific Building	0.65

The soil profiles and geotechnical parameters used for the simulations were obtained from data by Idriss and Seed (1968), Idriss (1969) and Singh et. al. (1979). The State Building soil profile consists essentially of sand extending to the shale bedrock at a depth of 200 ft., with occasional layers of clayey sand. The Alexander Building soil profile consists of about 100 ft. of clayey and silty sand followed by 40 ft. of sand overlying bedrock. The soil conditions at the Southern Pacific Building site are shown in Fig. 34.

The program SHAKE was used for the simulations (see discussion of SHAKE in Section 3.2). In all calculations, the input rock motions were assumed to act at a rock outcrop, with $V_S = 2,500$ fps used for the San Francisco shale rock underlying the three sites. Recent experience with modulus reduction curves of granular soils and many clays indicates that the use of the standard curve for sand proposed by Seed and Idriss (1970) may be generally appropriate. Therefore, the modulus reduction and damping curves versus strain for sands provided in SHAKE were used for the calculations.

Table 8 presents a comparison between computed and simulated peak accelerations and their times of occurrence, ($t_p - t_1$).

Figure 35 presents comparisons between simulated and recorded acceleration response spectra at the soft Southern Pacific Building site. Especially interesting in Fig. 35 is the comparison at a period of about 1.1 seconds, where the recorded soil spectrum has a prominent peak. The peak in the simulated curve at this period is much less prominent or does not exist. This contradiction between recorded and simulated motions computed at this

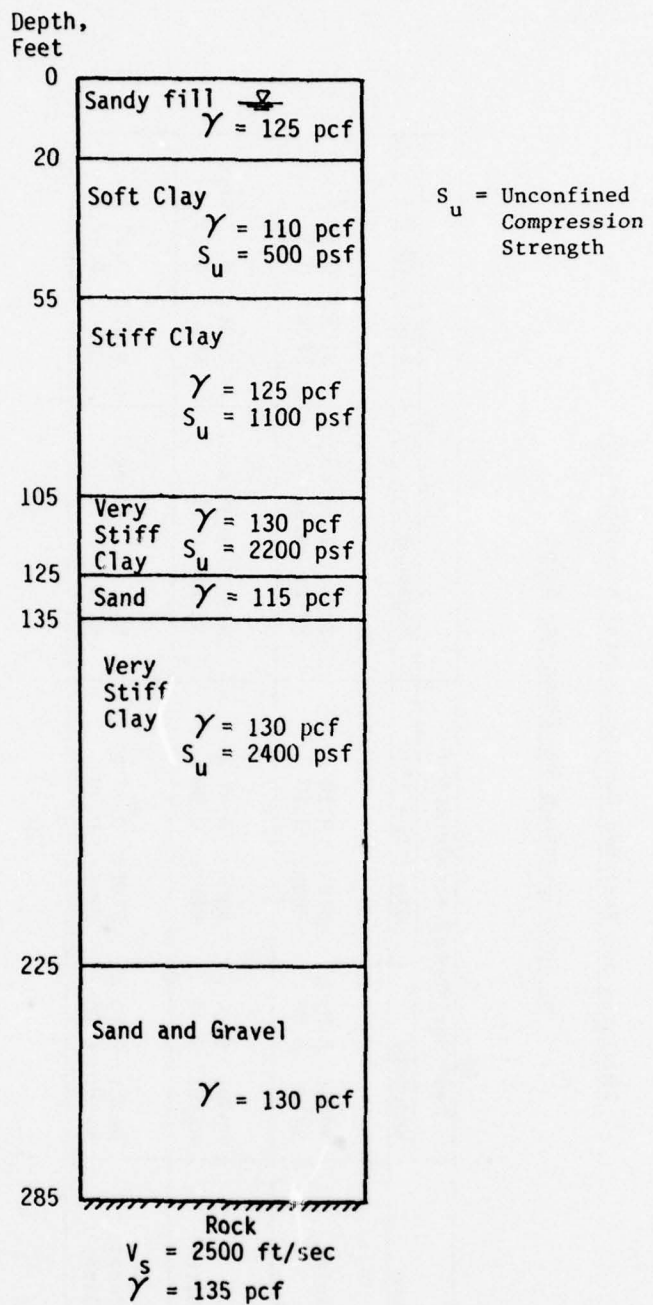


Figure 34 - SOIL PROFILE AT SOUTHERN PACIFIC BUILDING SITE USED
FOR SITE RESPONSE CALCULATIONS
(From Singh et. al., 1979)

Table 8

Simulated and Recorded Peak Horizontal Accelerations
at Three Downtown San Francisco Sites

Station Name	Peak Horizontal Acceleration			$t_p - t_1$	Simulated (*)
	Recorded	Simulated (*)	Recorded		
State Building Site	S09E: 0.09 g S81W: 0.06	N10E: 0.10 g S80E: 0.10	S09E: S81W:	1.50 sec. 1.82	N10E: 0.59 sec. S80E: 0.39
Alexander Building Site	N09W: 0.04 g N81E: 0.05	N10E: 0.07 g S80E: 0.09	N09W: N81E:	1.38 sec. 0.74	N10E: 0.43 sec. S80E: 0.95
Southern Pacific Building Site	N45E: 0.05 g N45W: 0.05	N10E: 0.06 g S80E: 0.06	N45E: N45W:	1.11 sec. 1.11	N10E: 0.68 sec. S80E: 0.90

(*) The directions of the simulated motion correspond to the N10E and S80E components of the rock input used (Golden Gate Park records).

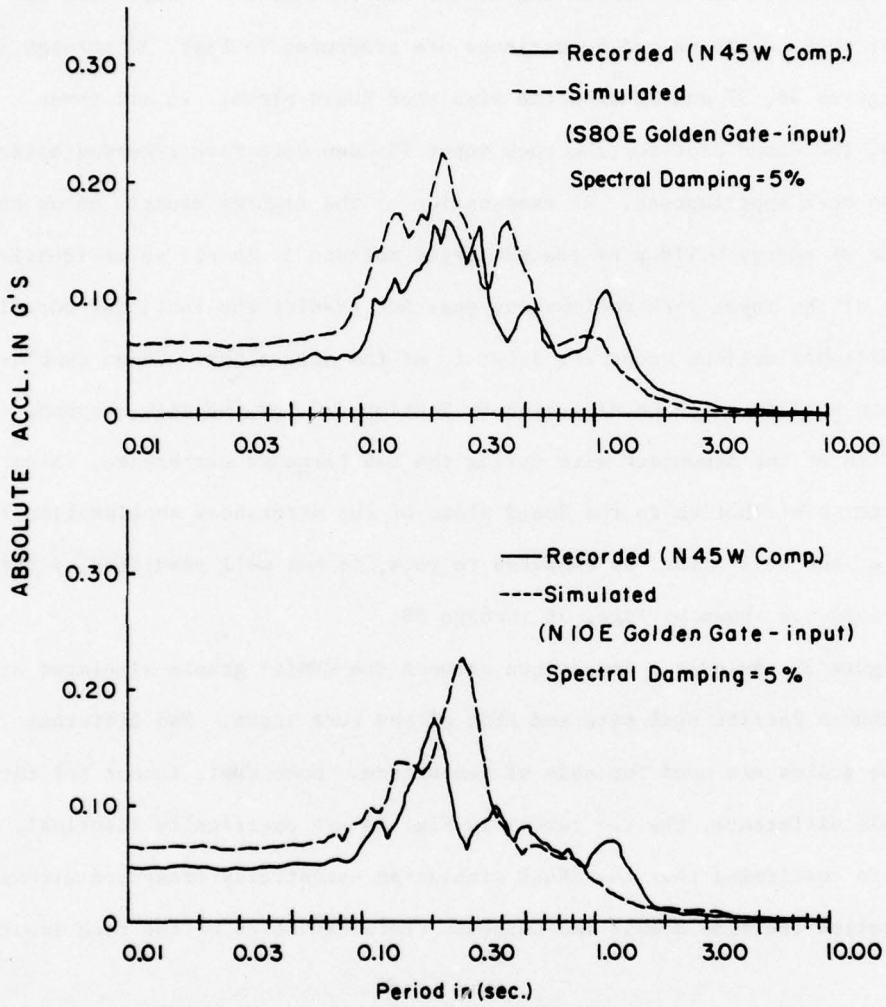


Figure 35 - COMPARISON OF RESPONSE SPECTRA FOR RECORDED AND SIMULATED ACCELERATIONS, SOUTHERN PACIFIC BUILDING SITE

site using equivalent linear techniques has also been noted by Idriss and Seed (1968) and by Singh et. al. (1979).

Time domain analyses of the simulated soil accelerograms at the three sites were performed. Normalized Husid plots and RMS(t) graphs were developed and compared with the corresponding curves recorded at the sites. The results of these analyses and comparisons are presented in Figs. 36 through 42.

Figures 36, 37 and 38 show the simulated Husid plots. In all three figures, the Husid plot for the rock input (Golden Gate Park recorded motion) has also been superimposed. An examination of the figures clearly shows that the rate of energy buildup of the simulated motions is in all cases identical to that of the input rock motions and does not predict the increased durations and additional motions occurring after t_2 at the soil sites. These conclusions are similar to those discussed in Section 3.2 for the site response simulation at the Athenaeum site during the San Fernando earthquake. Also, the larger contribution to the Husid plots of the aftershock acceleration recorded at the soil sites, as compared to rock, is not well predicted by the simulations, as shown by Figs. 36 through 38.

Figure 39 includes a comparison between the RMS(t) graphs simulated at the Southern Pacific soil site and that of the rock input. Two different ordinate scales are used for ease of comparison. Note that, except for the RMS scale difference, the two curves in Fig. 39 are practically identical, therefore confirming that the SHAKE simulation essentially preserved without modification the time domain and duration characteristics of the rock input motion.

Figures 40 through 42 include comparisons of simulated and recorded RMS(t) graphs at the three soil sites. Again, the agreement is rather poor, both in absolute RMS values and in the shapes of the curves. The simulated RMS

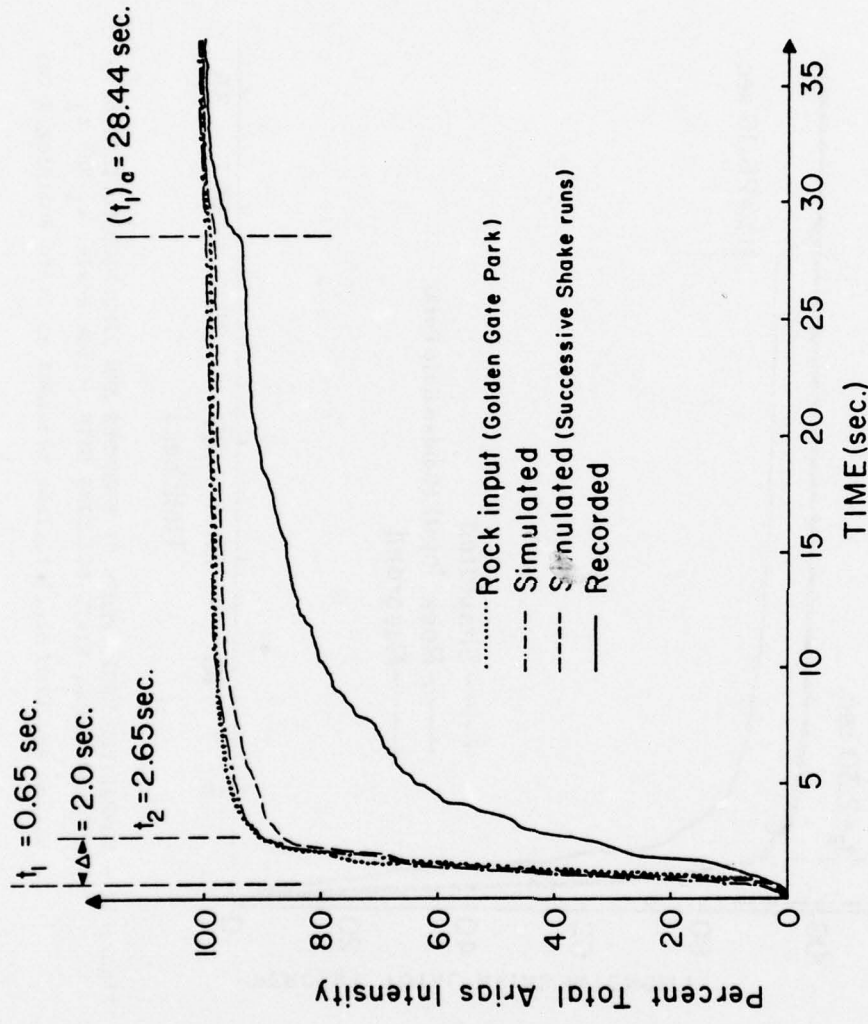


Figure 36 - NORMALIZED HUSID PLOTS OF RECORDED AND SIMULATED HORIZONTAL ACCELERATIONS, SOUTHERN PACIFIC BUILDING SITE
 (time scale, t_1 and t_2 values are from accelerograms recorded
 at Southern Pacific Building Site)

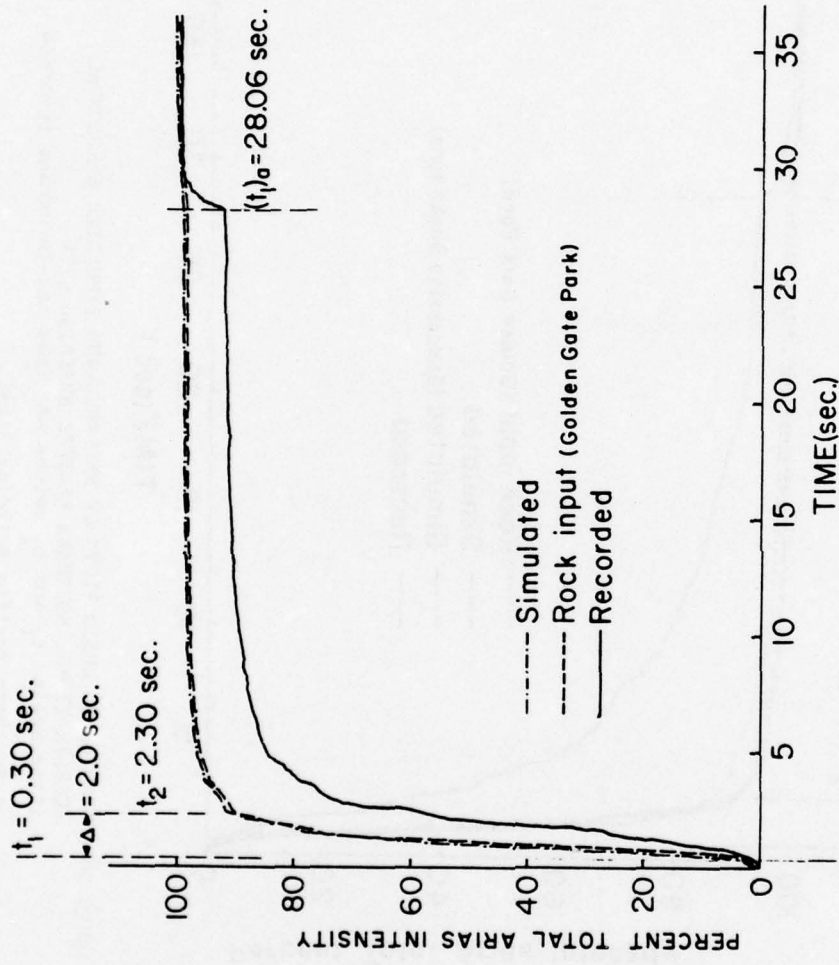


Figure 37 - NORMALIZED HUSID PLOTS OF RECORDED AND SIMULATED HORIZONTAL ACCELERATIONS, STATE BUILDING SITE (time scale, t_1 and t_2 values are from accelerograms recorded at State Building Site)

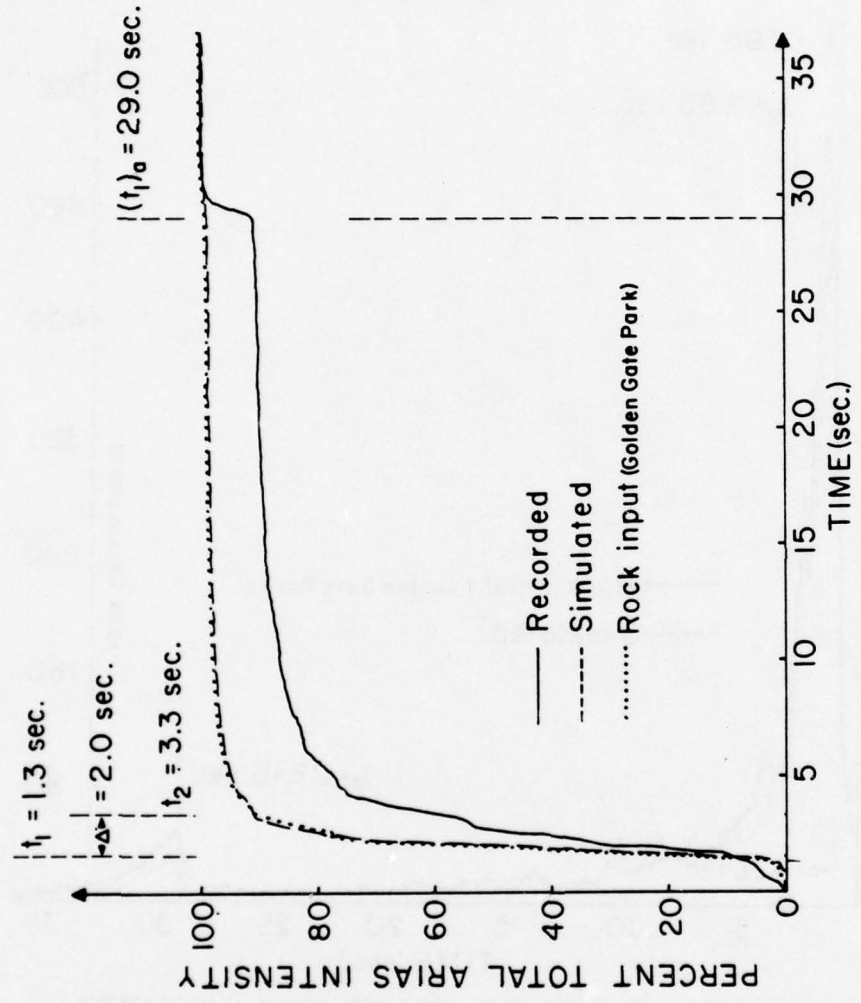


Figure 38 - NORMALIZED HUSID PLOTS OF RECORDED AND SIMULATED HORIZONTAL ACCELERATIONS, ALEXANDER BUILDING SITE (time scale, t_1 and t_2 values are from accelerograms recorded at Alexander Building Site)

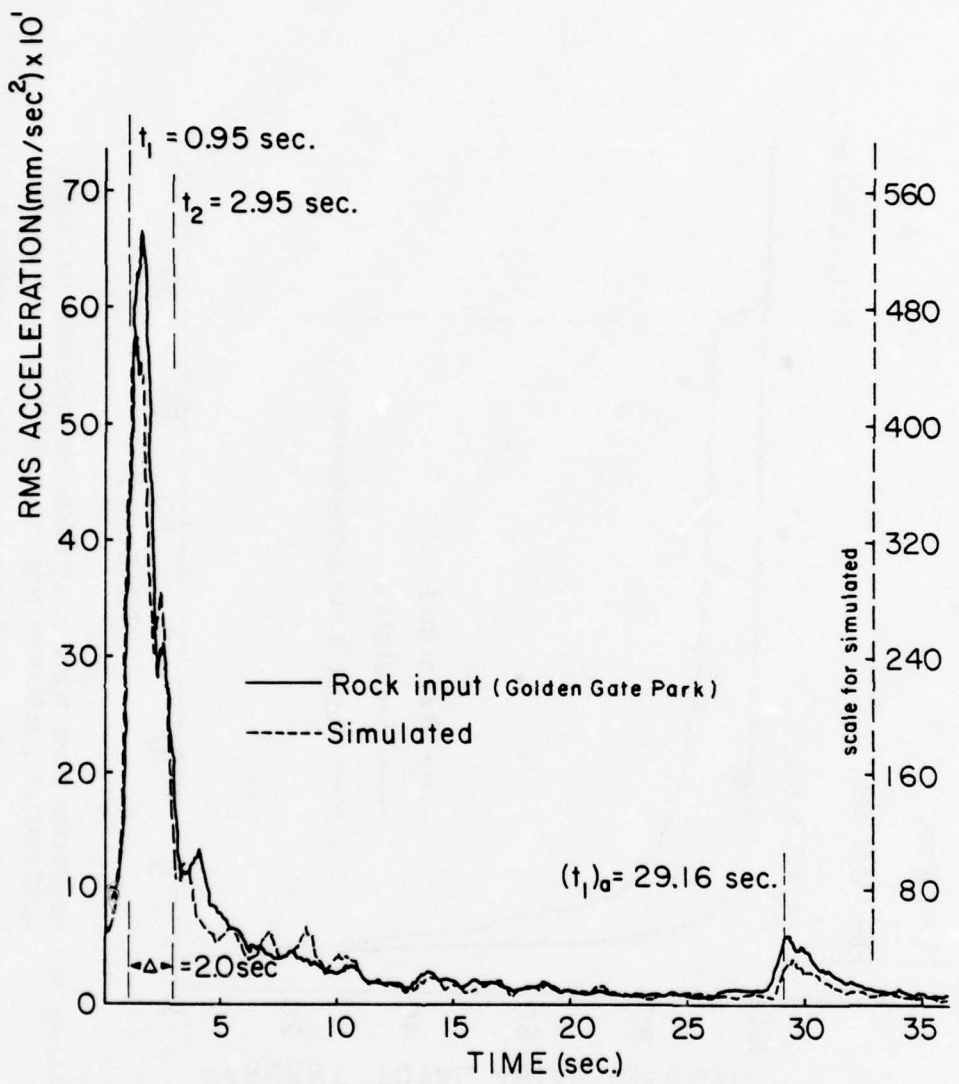


Figure 39 - COMPARISON OF RMS CURVES FOR INPUT AND OUTPUT ACCELERATIONS,
SOIL RESPONSE SIMULATION, SOUTHERN PACIFIC BUILDING SITE
(NOTICE DIFFERENCE OF SCALES FOR TWO CURVES)
(time scale, t_1 and t_2 values are from rock input)

ordinates in the strong part are in all cases significantly larger than the corresponding recorded RMS values. The difference in the RMS values could be reduced if smaller distance attenuation reduction factors for the rock input accelerations were used. However, the use of different reduction factors most probably would not change the shape of the simulated wave.

The results for the Southern Pacific Building site in Fig. 40 indicate that the relatively high intensity of shaking for $t > t_2$ is not predicted by the simulation. Also, the intensity of shaking of the aftershock recorded at the site is underpredicted. Figures 41 and 42 reveal that the aftershock motions predicted by the simulation at the other two downtown sites were also lower than the recorded motions. Idriss and Seed (1968) and Singh et. al. (1979) also found similar results when using the equivalent linear technique for site response simulations of the 1957 motions at the Southern Pacific Site. Singh et. al. have attributed this effect to the strongly nonlinear stress-strain behavior of the soil, which caused the effective damping ratio of the soil to decrease and the amplification to increase after t_2 .

A crude approximation of this nonlinear effect was attempted. In that, an additional simulation was performed at the Southern Pacific Site, in which each of the two horizontal components of the input rock motions were arbitrarily divided into two sections: from 0 to 4.65 seconds, and from 4.65 sec. to the end of the record. Each one of these input rock sections was run separately through SHAKE, therefore allowing the program to iterate to different modulus reduction and damping ratios in each section. The computed motions at the top of the soil profile were then reassembled, and their Husid and RMS graphs were calculated. The results of this simulation with successive SHAKE runs have been superimposed on Figs. 36 and 40. These figures show that the simulation with successive runs improves somewhat the agreement between simulated and

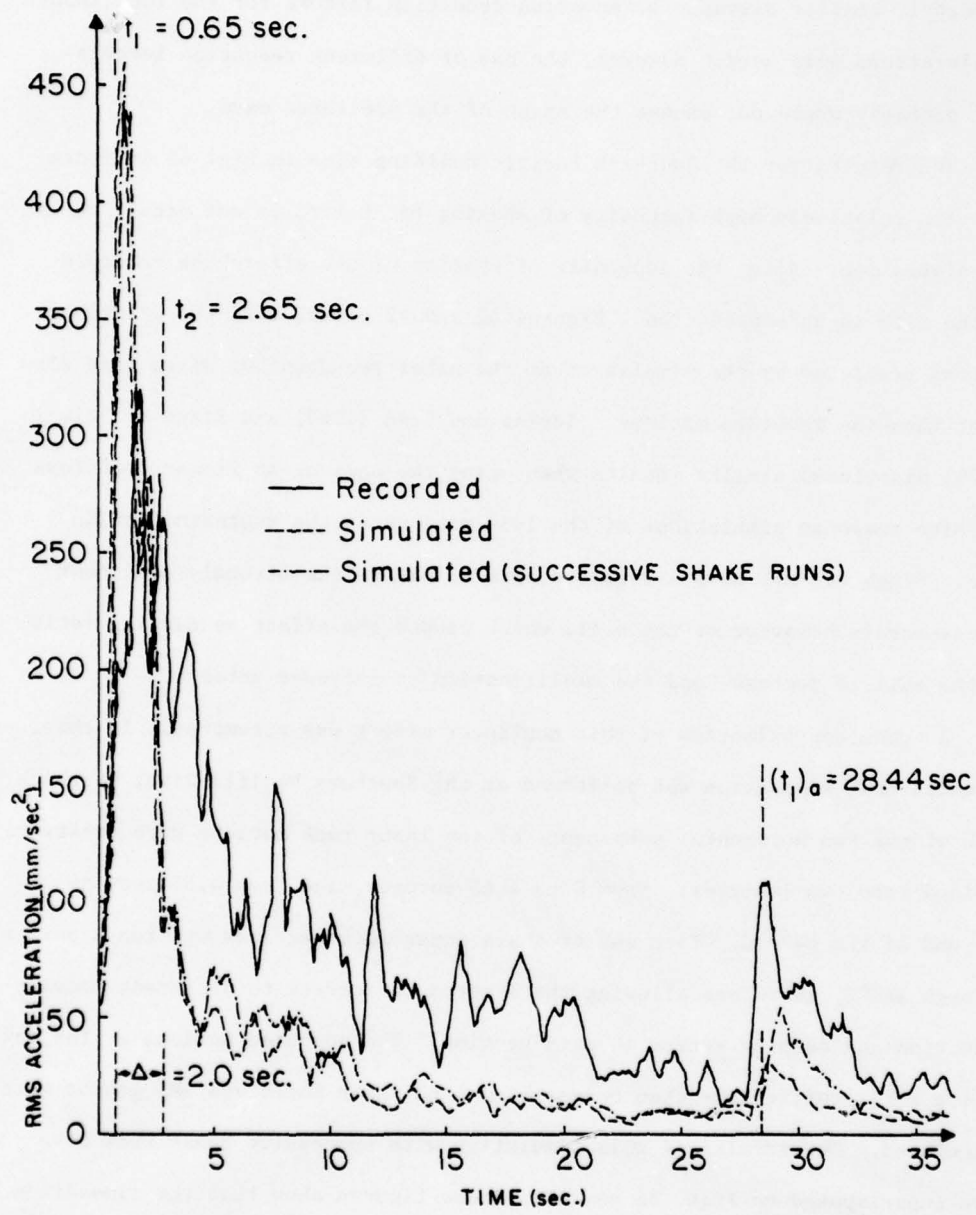


Figure 40 - COMPARISON OF RMS CURVES FOR RECORDED AND SIMULATED HORIZONTAL ACCELERATIONS, SOUTHERN PACIFIC BUILDING SITE
(time scale, t_1 and t_2 values are from recorded accelerograms)

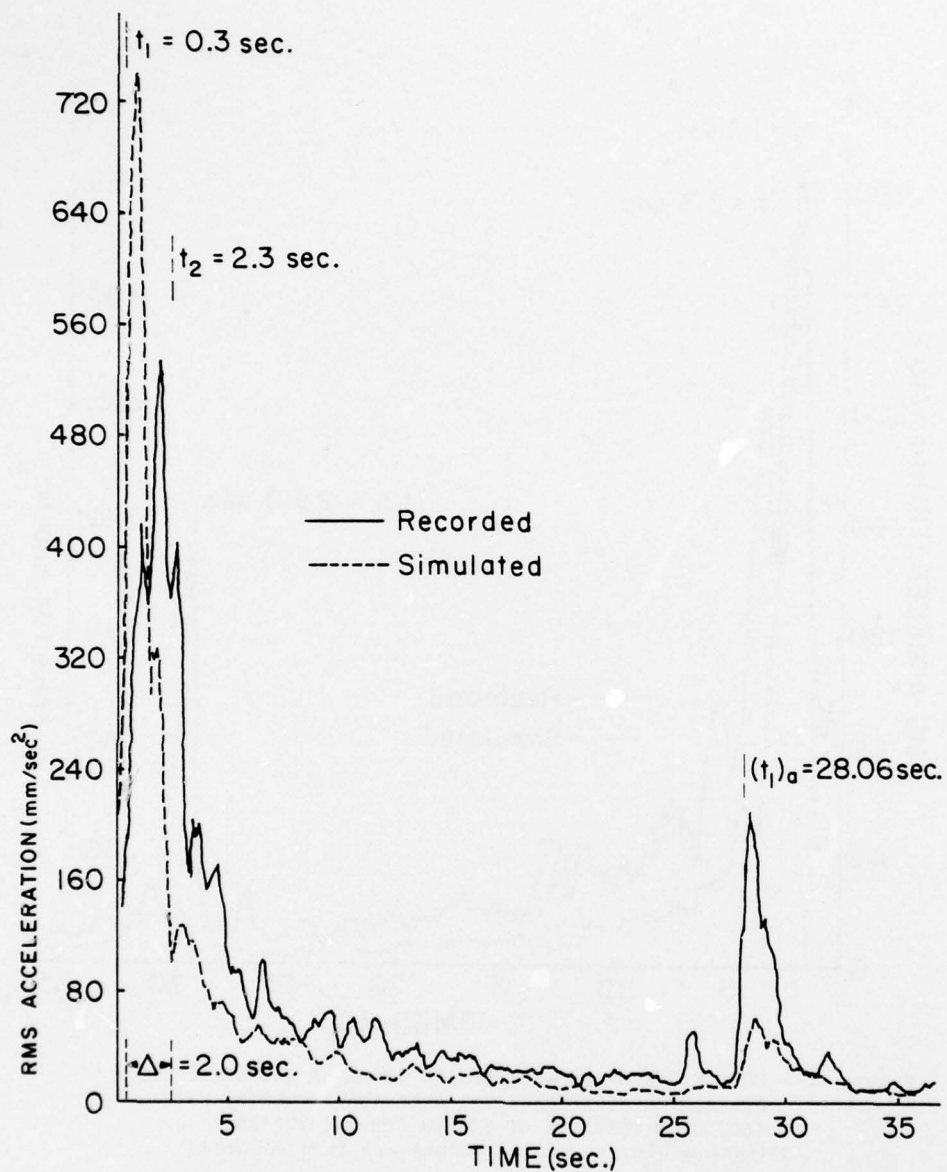


Figure 41 - COMPARISON OF RMS CURVES FOR RECORDED AND SIMULATED HORIZONTAL ACCELERATIONS, STATE BUILDING SITE
 (time scale, t_1 and t_2 values are from recorded accelerograms)

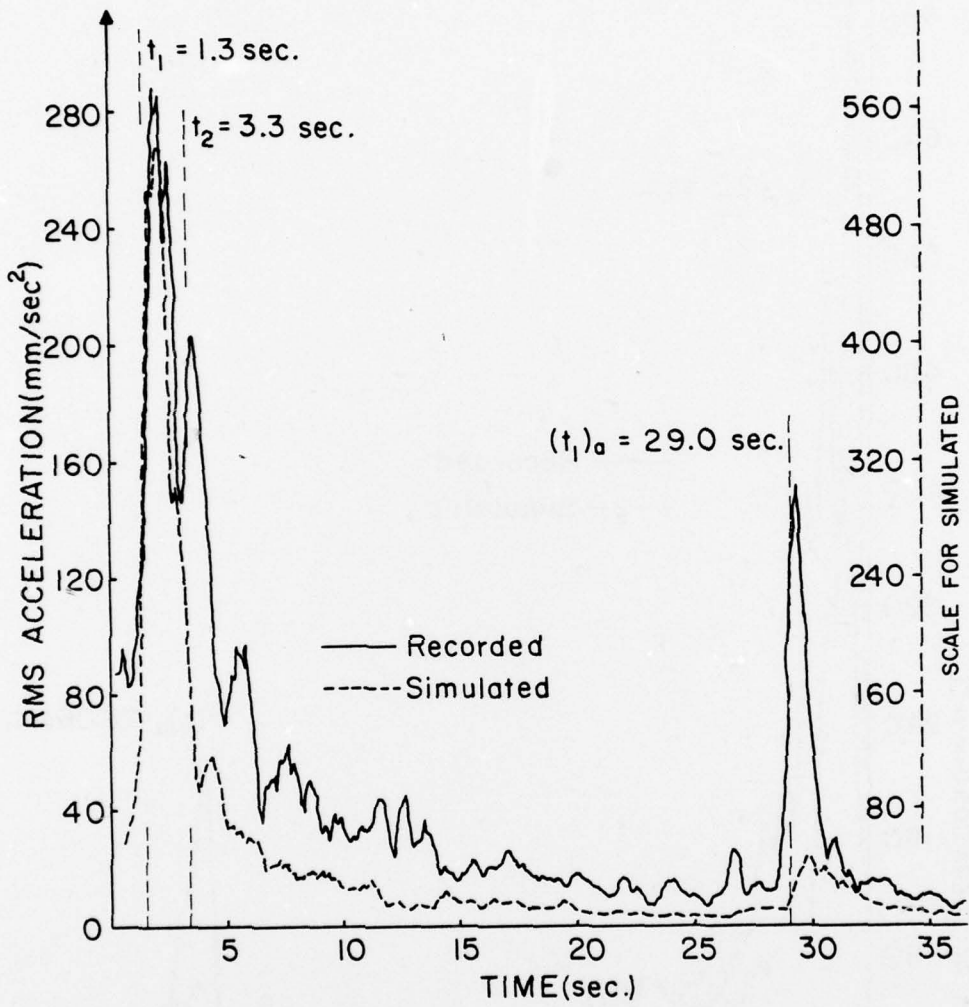


Figure 42 - COMPARISON OF RMS CURVES FOR RECORDED AND SIMULATED HORIZONTAL ACCELERATIONS, ALEXANDER BUILDING SITE
(NOTICE DIFFERENCE OF SCALES FOR TWO CURVES)
(time scale, t_1 and t_2 values are from recorded accelerograms)

recorded aftershock motions, but does not change the poor agreement between the predicted and recorded motions of the main event for $t > t_2$.

5. SUMMARY AND CONCLUSIONS

5.1 Summary

The study presents analyses of rock and soil accelerations recorded in the Pasadena and the San Francisco Bay Areas, during two earthquakes. These analyses were performed using recently developed time-domain processing techniques. A basic objective is to uncover the main time domain characteristics of strong motion accelerograms, including similarities and differences existing between rock and soil sites.

Four ground accelerograms obtained in the Pasadena area during the 1971 San Fernando earthquake were studied, including one rock site (Caltech Seismological Laboratory) and three soil sites. Also studied were five ground accelerograms obtained in the Bay Area during the 1957 San Francisco earthquake, including one station on rock (Golden Gate Park). The subsurface conditions at the soil recording stations varied between relatively stiff soils in Pasadena to a soft clay site in downtown San Francisco (Southern Pacific Building site). No deep soil sites in the sense defined by Seed et. al. (1974) were included in the study.

The results of these analyses of recorded motions are presented in Sections 3.1 and 4.1. The processing techniques used consisted basically of plotting graphs of the variation with time of: a) the buildup of energy of the vector horizontal ground acceleration (normalized Husid plot), b) the Root-Mean-Square vector horizontal ground acceleration, RMS(t) for a moving time window, $\delta = 0.5$ sec., and c) the angle between the principal direction of the vector ground acceleration and the vertical axis, $\phi_1(t)$ for the same window, $\delta = 0.5$ sec. These graphs are independent of the particular orientation of the horizontal components of the recording instruments, and do not require any prior knowledge

of the fault or epicenter location with respect to the station.

The use of these graphs in Sections 3.1 and 4.1 show that they supplement each other in providing a better understanding of the features of the motion. This includes the determination of seismic wave arrivals at each site and the consistency of these arrivals between different stations. The graphs are especially useful in determining the time of the first S-wave arrival, t_1 . At $t = t_1$, the Husid plot becomes suddenly steeper, and the $RMS(t)$ and $\phi_1(t)$ graphs jump from low to high values. This is illustrated in Figs. 10 and 15, by the graphs corresponding to the Millikan Library accelerogram recorded in Pasadena. (When the jumps do not occur, as it is the case for the Oakland City Hall station illustrated by the graphs in Fig. 32, this can be taken as a good indication that the instrument was triggered, either after t_1 by the S-wave arrivals, or very shortly (less than 0.5 second) before t_1 .) An outstanding example of this consistent behavior of the graphs at $t = t_1$ is provided by the aftershock which occurred in San Francisco about 30 sec. after the main event. The arrival of the aftershock P-waves is marked by a dip in the $\phi_1(t)$ values to $\phi_1 \approx 20^\circ$, while the first S-wave arrival coincides with a jump back to $\phi_1 \approx 80^\circ$ to 90° . This is true for the four rock and soil stations which recorded the aftershock, as shown in Figs. 28 through 31.

The strong part of earthquake motions at rock sites has been defined in other publications as having a duration $\Delta = t_2 - t_1$, with t_1 and t_2 corresponding approximately with the first and last S-wave arrivals travelling a direct path between the source and the site. The time t_2 is correlated with a flattening of the Husid plot and a decrease in values of the $RMS(t)$ graph for records on rock. This behavior at $t = t_2$ is illustrated for the two rock sites in Figs. 9 and 12 for the Seismological Laboratory station and in Figs. 26 and 28 for the Golden Gate Park station. The values $\Delta = 6$ sec. and

$\Delta = 2$ sec., respectively, used to determine t_2 are consistent with the independently estimated durations of the rupture at the generating faults during the two events.

Values of t_1 and of $t_2 = t_1 + \Delta$ were superimposed on all graphs of recorded motions, thereby cutting the record in three parts: i) the first part ($t < t_1$), ii) the strong part ($t_1 < t < t_2$) and iii) a third part ($t > t_2$). An examination of $\phi_1(t)$ graphs during the strong part shows that the accelerations were predominantly horizontal. This suggests that the direct S-wave arrivals consisted mainly of vertically (or almost vertically) propagating S-waves (SH-waves), at both rock and soil sites studied.

The separation of all records into these three parts was especially useful for determining the influence of site conditions. RMS(t) graphs and Husid plots of rock and soil records were compared after shifting the time scales so that t_1 and t_2 would coincide between stations. In the Pasadena area, these comparisons show that: a) a main wave arrival occurred at all stations at $t \approx t_1 + 3$ (see Fig. 18 and $t_p - t_1$ values in Table 4), b) the sequence of wave arrivals was almost identical between one of the soil sites (Jet Propulsion Laboratory) and the rock site, without revealing any significant difference due to site conditions (see Fig. 14), and c) some differences between the wave arrivals at another of the soil sites (Athenaeum) and the rock site are observed, including possibly some additional wave reflections in the soil at $t > t_2$ (see Fig. 18). In the downtown San Francisco area, where three soil stations were located, significant ground motions were recorded after t_2 , which were not present in the rock accelerogram. These motions, presumably also due to additional wave reflections in the soil, are especially prominent at the soft Southern Pacific Building site. These motions at the soft site have a period of about 1 second (see Figs. 27, 31 and 33).

The suggested conclusion discussed above that the wave arrivals during the strong part of the motion are predominantly SH-waves is consistent with the basic assumption made when performing one-dimensional site response analyses. Therefore, site response simulations were performed at one Pasadena soil site (Athenaeum) and at the three San Francisco downtown sites. In all cases, the recorded rock motions were used as input to the equivalent linear code SHAKE. The calculated soil accelerograms were then processed using the time domain techniques described above, and the calculated graphs were compared with the corresponding graphs obtained from: a) the recorded soil motions at the same site, and b) the rock motions used as input. These results and comparisons are shown in Sections 3.2 and 4.2.

In all cases studied, the time domain characteristics of the simulated soil motions are very similar to those of the input rock motions. The normalized Husid plots and RMS(t) graphs are about identical in shape (Figs. 10, 23 and 36 through 39). The increased motions which are present in some soil records after t_2 are not well simulated.

A possible explanation is that this is a deficiency of the equivalent linear approximation to nonlinear soil behavior, rather than a basic flaw of the one-dimensional method itself. The equivalent linear method used by SHAKE defines modulus reduction factors and damping ratios for the soil which are consistent with the level of shaking in the strong part. The use of these damping ratios for $t > t_2$, where the input rock accelerations are weaker, may produce an underestimation of the soil motion after t_2 . Therefore, a special calculation was performed for the Southern Pacific Building site, using two independent and successive SHAKE runs. It was expected that this would provide, at least in a crude way, a better representation of the nonlinear soil behavior after t_2 . However, the results, shown in Fig. 40, do not show an improved agreement between simulated and recorded soil motion after t_2 .

5.2 Conclusions

The two main objectives of this report were: a) to verify the use of the proposed time domain processing techniques for studying recorded rock and soil accelerograms, and b) to use the same techniques for evaluating the simulation of soil accelerograms provided by site response analyses.

Both objectives were accomplished. Although the proposed techniques still require some further development, their use already provides a simple and attractive way of analyzing and comparing strong motion accelerograms.

Specific conclusions for the recorded and simulated motions studied are:

- 1) Husid plots, RMS(t) and $\phi_1(t)$ graphs show clearly the beginning of the strong part ($t = t_1$) associated with the first S-wave arrival, in rock and soil sites.
- 2) Husid plots and RMS(t) graphs can be used for estimating the end of the strong part ($t = t_2$) of rock records.
- 3) The comparison of normalized Husid plots, and RMS(t) graphs between different stations, after shifting their time axes so as to make t_1 coincide, is very useful. The RMS(t) comparisons are especially fruitful, as they reveal the consistency in detail between wave arrivals at different stations during the strong part, and the additional motions present at some soil sites, after the end of the strong part. In the Pasadena area during the 1971 San Fernando earthquake, a main arrival occurred in all stations 3 seconds after the first S-wave arrival. This is shown by prominent peaks at all RMS(t) graphs at $t \approx t_1 + 3$ and also by the times of occurrence of the peak accelerations at all stations.
- 4) The site response simulations using the equivalent linear technique show that this technique computes soil accelerograms which preserve the shapes of Husid plots and RMS(t) graphs of the input rock motions. This is

reasonably consistent for the strong part, where the RMS(t) graphs of recorded rock and soil motions are generally similar. These site response simulations do not, however, predict the additional soil motions observed after t_2 . It is suggested that further investigations, including truly nonlinear site response simulations at some of the soil sites, are required for a better understanding of this effect. However, it must be noted that nonlinear site response simulations will not model other effects, which may be responsible for the motions after t_2 in some soil sites, such as surface waves, soil-structures interaction, etc.

REFERENCES

Arias, A. (1969), "A Measure of Earthquake Intensity", Seismic Design for Nuclear Power Plants, Robert Hansen, Editor, MIT Press, Cambridge, Massachusetts.

Berrill, J.B. (1975), "A Study of High-Frequency Strong Ground Motion for the San Fernando Earthquake", Ph.D. Thesis, California.

Bolt, B.A. (1973), "Duration of Strong Ground Motion", Proceedings, 5th World Conference on Earthquake Engineering, Rome, Italy.

Bond, W.E. (1979), "Engineering and Seismological Aspects of Strong-Motion Accelerations Recorded in the Western United States", Ph.D. Thesis, Rensselaer Polytechnic Institute, Troy, New York (in preparation).

Boore, D.M. and Zoback, M.D. (1974), "Two-Dimensional Kinematic Fault Modeling of the Pacoima Dam Strong-Motion Recordings of the February 9, 1971, San Fernando Earthquake", Bulletin of the Seismological Society of America, Vol. 64, No. 3, pp. 555-570, June.

Bouchon, M. and Aki, R. (1977), "Discrete Wave-Number Representation of Seismic-Source Wave Fields", Bulletin of the Seismological Society of America, Vol. 67, No. 2, pp. 259-277, April.

Campbell, K.W. and Duke, C.M. (1976), "Correlations Among Seismic Velocity, Depth and Geology in the Los Angeles Area", Research Report UCLA-ENG-7662, School of Engineering and Applied Science, University of California, Los Angeles, June.

Clough, R.W. and Penzien, J. (1975), Dynamics of Structures, McGraw-Hill, New York.

Crandall, S.H. and Mark, W.D. (1963), Random Vibration in Mechanical Systems, Academic Press, New York.

Crouse, C.B. (1973), "Engineering Studies of the San Fernando Earthquake", Ph.D. Thesis, California Institute of Technology, Pasadena.

Dobry, R., Idriss, I.M., Chang, C.Y. and Ng, E. (1977), "Influence of Magnitude, Site Conditions and Distance on Significant Duration of Earthquakes", Proceedings, 6th World Conference on Earthquake Engineering, New Delhi, India.

Dobry, R., Idriss, I.M. and Tocher, D. (1978), "Avances Recientes en la Caracterizacion de Movimientos Sismicos en Roca Y Suelo Durante Terremotos de Magnitud Moderada", Proc. Central American Conference on Earthquake Engineering, San Salvador, El Salvador, January, Vol. I, pp. 373-384.

Dobry, R., Idriss, I.M. and Ng, E. (1978a), "Duration Characteristics of Horizontal Components of Strong Motion Earthquake Records", Bulletin of the Seismological Society of America, Vol. 68, No. 5, pp. 1487-4120, October.

Dobry, R., Bond, W.E. and O'Rourke, M. (1979), "Probabilistic Model for Earthquake Accelerations", Proc. ASCE Specialty Conference on Probabilistic Models and Structural Reliability, January, Tucson, Arizona.

Eguchi, R.T., Campbell, K.W., Duke, C.M., Chow, A.W. and Patermine, J. (1976), "Shear Velocities and Near-Surface Geologies at Accelerograph Sites that Recorded the San Fernando Earthquake", Report UCLA-ENG-7653, School of Engineering and Applied Sciences, University of California, Los Angeles.

Franklin, A.G. and Chang, F.K. (1977), "Permanent Displacement of Earth Embankment by Newmark Sliding Block Analysis", Miscellaneous Paper S-71-17, Soil and Pavement Laboratory, U.S. Army Engineer Waterways Experiment Station, Vicksburg, Mississippi.

Grant, W. Paul, Arango, I. and Clayton, D.N. (1978), "Geotechnical Data At Strong Motion Accelerograph Station Sites", Proceedings, The Second International Conference on Microzonation, Vol. II, San Francisco, California.

Gutenberg, B. (1957), "Effects of Ground on Earthquake Motion", Bull. Seism. Soc. Am., 47, 221-250.

Hanks, T.C. (1975), "Strong Ground Motion of the San Fernando, California, Earthquake: Ground Displacements", Bulletin of the Seismological Society of America, Vol. 65, No. 1, pp. 193-225, February.

Hanks, T.C. (1976), "Observations and Estimation of Long-Period Strong Ground Motion in the Los Angeles Basin", Earthquake Engineering and Structural Dynamics, Vol. 4, pp. 473-488.

Hudson, D.E. and Housner, G.W. (1958), "An Analysis of Strong-motion Accelerometer Data from the San Francisco Earthquake of March 22, 1957", Bulletin of the Seismological Society of America, Vol. 48, pp. 253-268.

Hudson, D.E. and Cloud, W.D. (1967), "An Analysis of Seismoscope Data from the Parkfield Earthquake of June 27, 1966", Bull. Seism. Soc. Am. 57, pp. 1143-1159.

Hudson, D.E., Brady, A.G., Trifunac, M.D. and Vijayaraghavan, A. (1971), Strong Motion Earthquake Accelerograms - Vol. II Corrected Accelerograms and Integrated Ground Velocity on Displacement Curves. Earthquake Eng. Research Lab., Calif. Inst. of Tech., Pasadena.

Hudson, D.E. (1972), "Local Distribution of Strong Earthquake Ground Motions", Bull. Seism. Soc. Am. 62.

Husid, R. (1973), "Terremotos - Earthquakes", Editorial Andres Bello, Santiago, Chile.

Idriss, I.M. and Seed, H. Bolton (1968), "An Analysis of Ground Motions During the 1957 San Francisco Earthquake", Bulletin of the Seismological Society of America, Vol. 58, No. 6, pp. 2013-2032, December.

Idriss, I.M. (1969), "Influence of Modulus Variation With Effective Pressure on the Seismic Response of Cohesionless Deposits", Proc. Specialty Session 2 (Soil Dynamics), Seventh Int. Conf. on Soil Mech. and Foundation Eng., Mexico, August, pp. 122-124.

Jennings, P.C. (1973), "The Effect of Local Site Conditions on Recorded Strong Earthquake Motions", Proc. 42nd Annual Convention, Structural Engineers Assoc. of California, Coronado, October.

Joannon, J.G., Arias, A. and Saragoni, G.R. (1977), "The Time Variation of the Predominant Frequency of Earthquake Motion", 6th WCEE, 2-221 to 2-226.

Kameda, H. (1975), "Evolutionary Spectra of Seismogram by Multifilter", Journal of the Engineering Mechanics Division, ASCE, Vol. 101, No. EM6, December, pp. 787-801.

Kanamori, H. and Jennings, P.C. (1978), "Determination of Local Magnitude, M_L , From Strong Motion Accelerograms", Seismological Society of America Bulletin, v. 68, pp. 471-485.

Kubo, T. and Penzien, J. (1976), "Time and Frequency Domain Analysis of Three-Dimensional Ground Motions, San Fernando Earthquake", EERC 76-6, University of California, Berkeley, California.

Liu, S.C. (1970), "Synthesis of Stochastic Representations of Ground Motions", The Bell System Technical Journal, Vol. 49, No. 4, April, pp. 521-541.

Liu, S.C. (1971), "Time Varying Spectra and Linear Transformation", The Bell System Technical Journal, Vol. 50, No. 7, September, pp. 2365-2374.

Murphy, L.M., Scientific Coordinator (1973), San Fernando, California Earthquake of February 9, 1971, 3 vol., National Oceanic and Atmospheric Administration.

Oakeshott, G.B., Editor (1959), San Francisco Earthquake of March 1957, Special Report No. 57, California Division of Mines, San Francisco.

Penzien, J. and Watabe, M. (1975), "Characteristics of 3-Dimensional Earthquake Ground Motions", International Journal of Earthquake Engineering and Structural Dynamics, Vol. 3.

Perez, V. (1973), "Velocity Response Envelope Spectrum as a Function of Time, Pacoima Dam, San Fernando Earthquake, February 9, 1971", Bull. Seism. Soc. Am., 63.

Saragoni, G.R. and Hart, G.C. (1973), "Time Variation in Earthquake Frequency Content - Characterization and Relevance", 5th WCEE, Paper No. 156, 5 pages, Rome, Italy.

Schnabel, P.B., Lysmer, J. and Seed, H.B. (1972), "SHAKE - A Computer Program for Earthquake Response Analysis of Horizontally Layered Sites", Earthquake Engineering Research Center Report, No. EERC 72-12, University of California, Berkeley.

Seed, H.B. and Idriss, I.M. (1970), "Soil Moduli and Damping Factors for Dynamic Response Analyses", Earthquake Engineering Research Center Report No. EERC 70-10, University of California, Berkeley.

Seed, H.B., Ugas, C. and Lysmer, J. (1974), "Site-Dependent Spectra for Earthquake-Resistant Design", Earthquake Engineering Research Center, Report No. EERC 74-12, University of California, Berkeley.

Seed, H.B., Murarka, R., Lysmer, J. and Idriss, I.M. (1975), "Relationship between Maximum Acceleration, Maximum Velocity, Distance from Source and Local Site Conditions for Moderately Strong Earthquakes", Report No. EERC 75-17, College of Engineering, University of California, Berkeley.

Seed, H.B., Idriss, I.M., Makdisi, F. and Baneizee, N. (1975a), "Representation of Irregular Stress Time Histories by Equivalent Uniform Stress Series in Liquefaction Analyses", Report No. EERC 75-29, Earthquake Engineering Research Center, University of California, Berkeley, October.

Shannon and Wilson (1978), "Geotechnical and Strong Motion Earthquake Data from U.S. Accelerograph Stations", Report for U.S. Nuclear Regulatory Commission, NUREG-0029, Vol. 2, NRC-GA, June.

Singh, R.D. et. al. (1979), "Non-linear Seismic Response of Soft Clay Sites", Submitted for possible publication in Journal of Geotechnical Engineering, ASCE.

Steinbrugge, K.V., Bush, V.R. and Zacher, E.G. (1959), "Damage to Buildings and Other Structures During the Earthquake of March 22, 1957", included in San Francisco Earthquakes of March 1957, G.B. Oakeshott, Editor, Special Report 57, California Division of Mines, San Francisco.

Trifunac, M.D. (1971), "Response Envelope Spectrum and Interpretation of Strong Earthquake Ground Motion", BSSA, Vol. 61, No. 2, April, pp. 343-356.

Trifunac, M.D. and Brady, A.G. (1975), "A Study of the Duration of Strong Earthquake Ground Motion", Bulletin of the Seismological Society of America, Vol. 65, No. 3, pp. 581-626.

USGS (1977), "Western Hemisphere Strong-Motion Accelerograph Station List - 1976", USGS Open File Report No. 77-374, May.

Vanmarcke, E.H. and Lai, S.P. (1977), "Strong-Motion Duration of Earthquakes", Publication No. R77-16, Department of Civil Engineering, Massachusetts Institute of Technology, Cambridge, Mass.

APPENDIX 1

VARIATION OF ANGLE $\phi_3(t)$ WITH TIME
(Units of ϕ_3 are degrees)

RECORDED GROUND ACCELERograms

SAN FRANCISCO, 1957

SAN FERNANDO, 1971

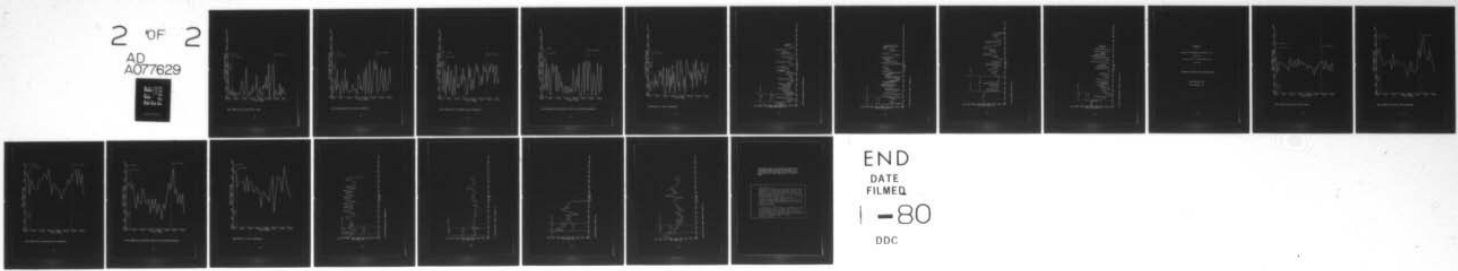
AD-A077 629 RENSSELAER POLYTECHNIC INST TROY NY DEPT OF CIVIL EN--ETC F/G 8/11
STUDY OF GROUND MOTIONS AT SOIL SITES DURING TWO CALIFORNIA EARTHQUAKES (U)
OCT 79 R DOBRY • S SINGH • W E BOND DACW37-78-M-0140

UNCLASSIFIED

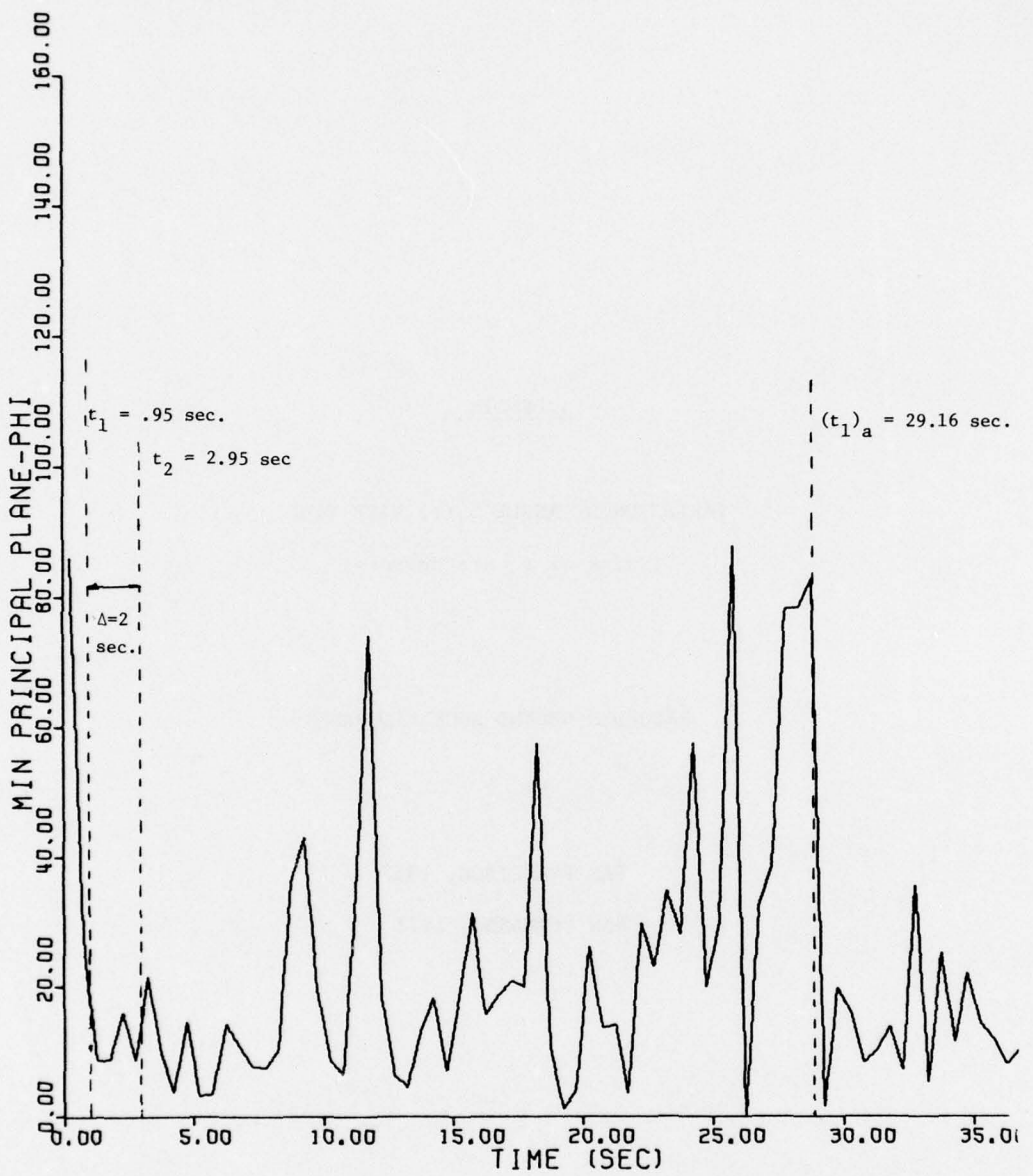
WES/BL-79-22

NL

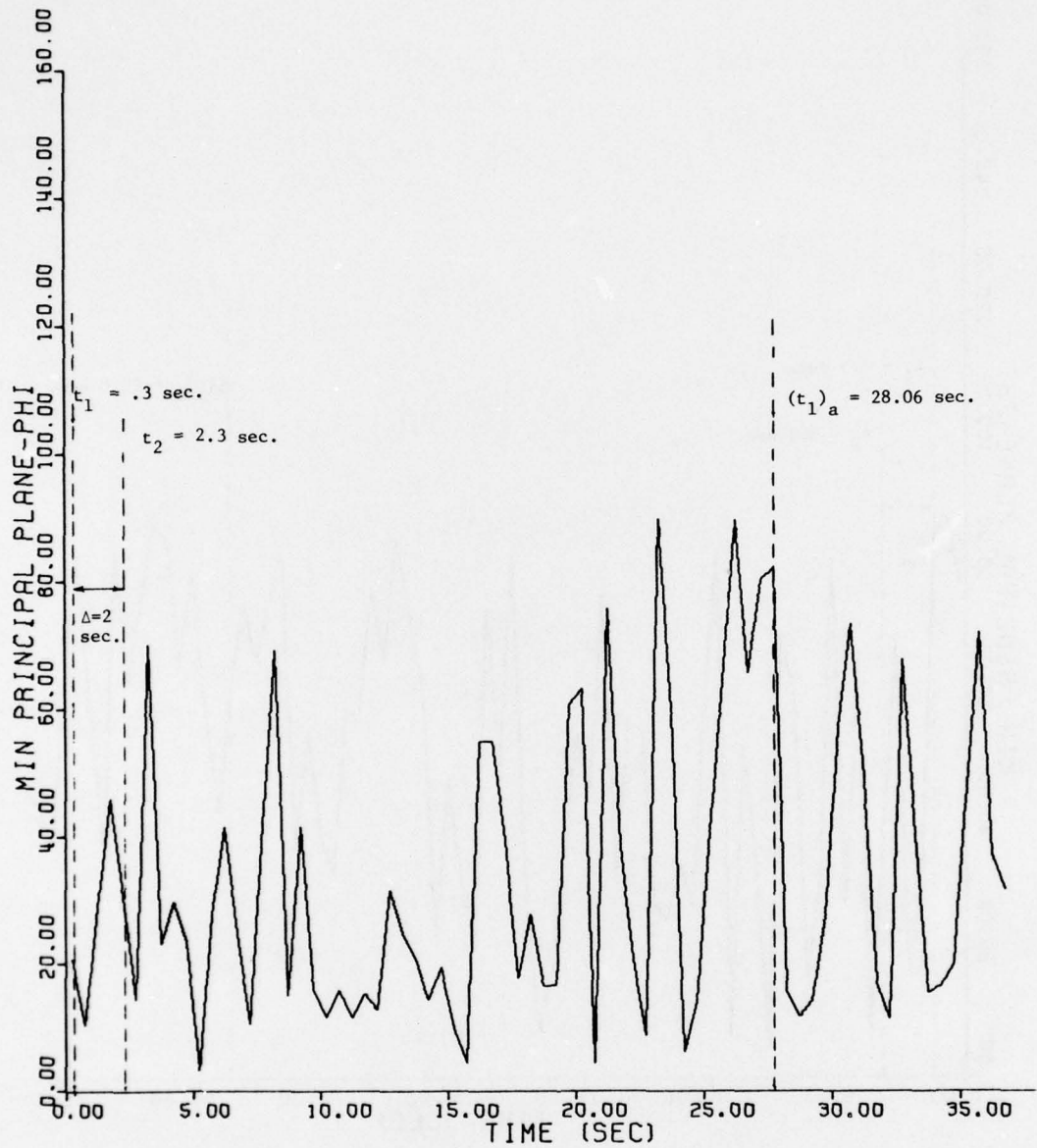
2 OF 2
AD
A077629



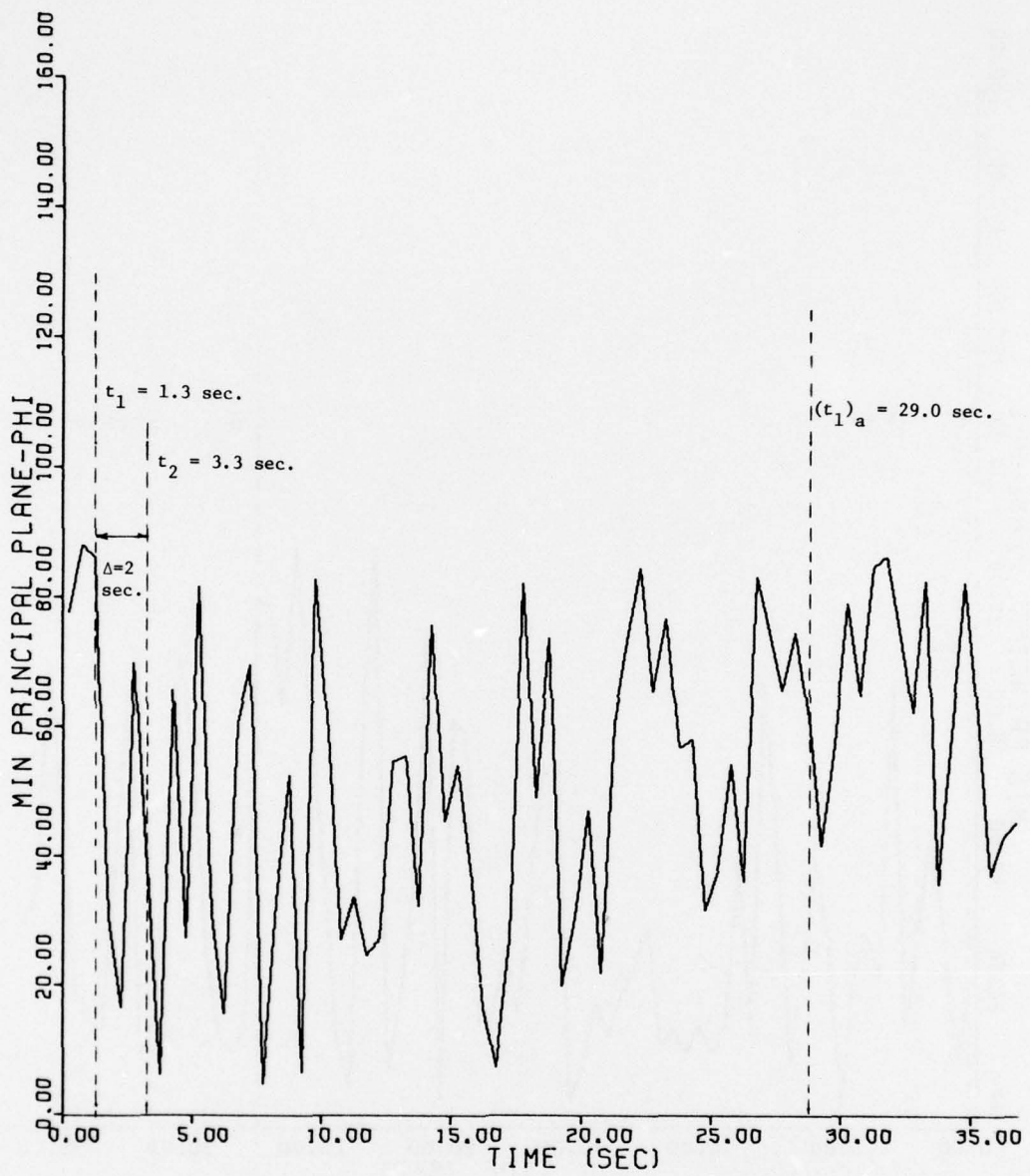
END
DATE
FILED
I - 80
DDC



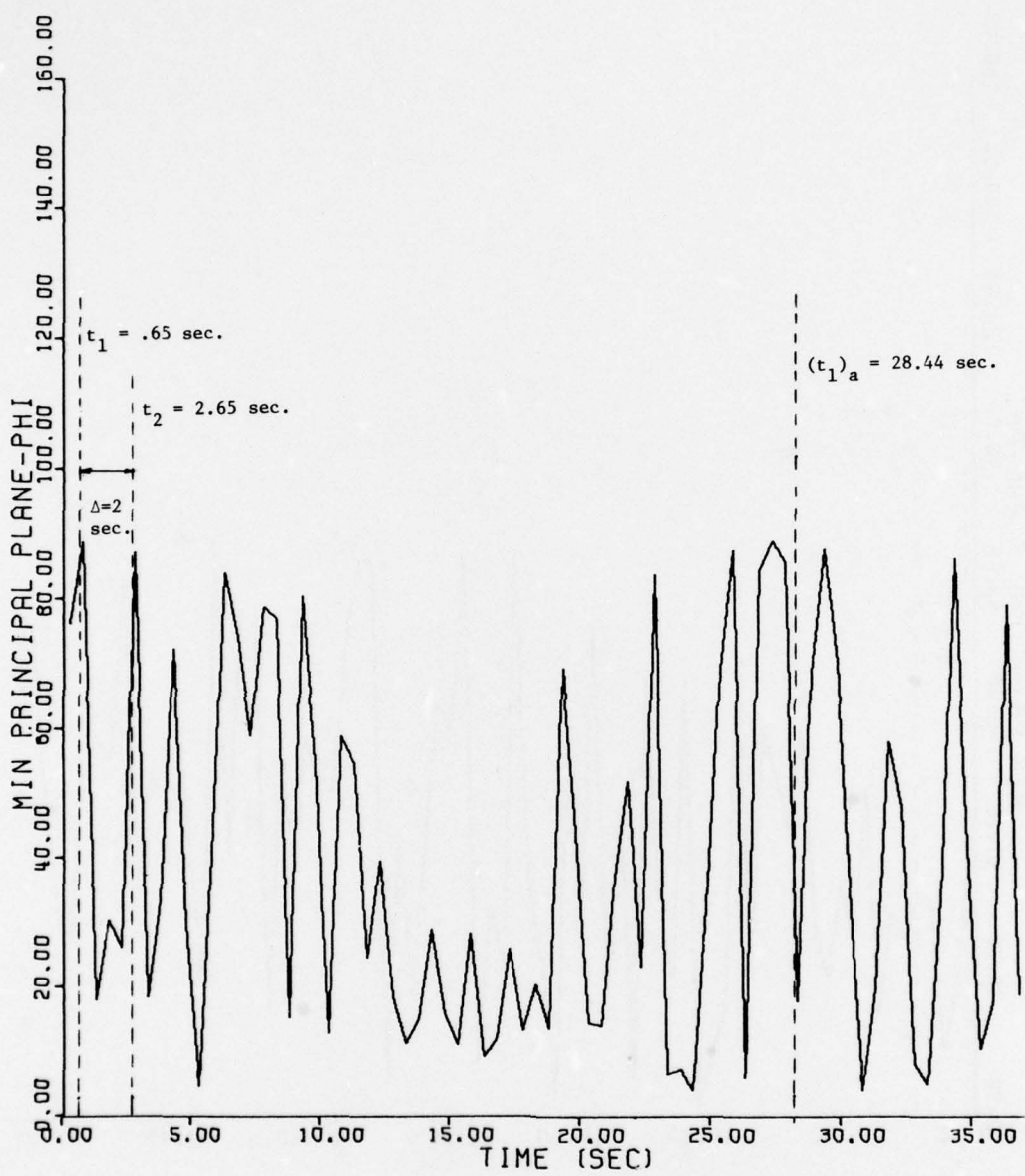
SAN FRANCISCO GOLDEN GATE PARK



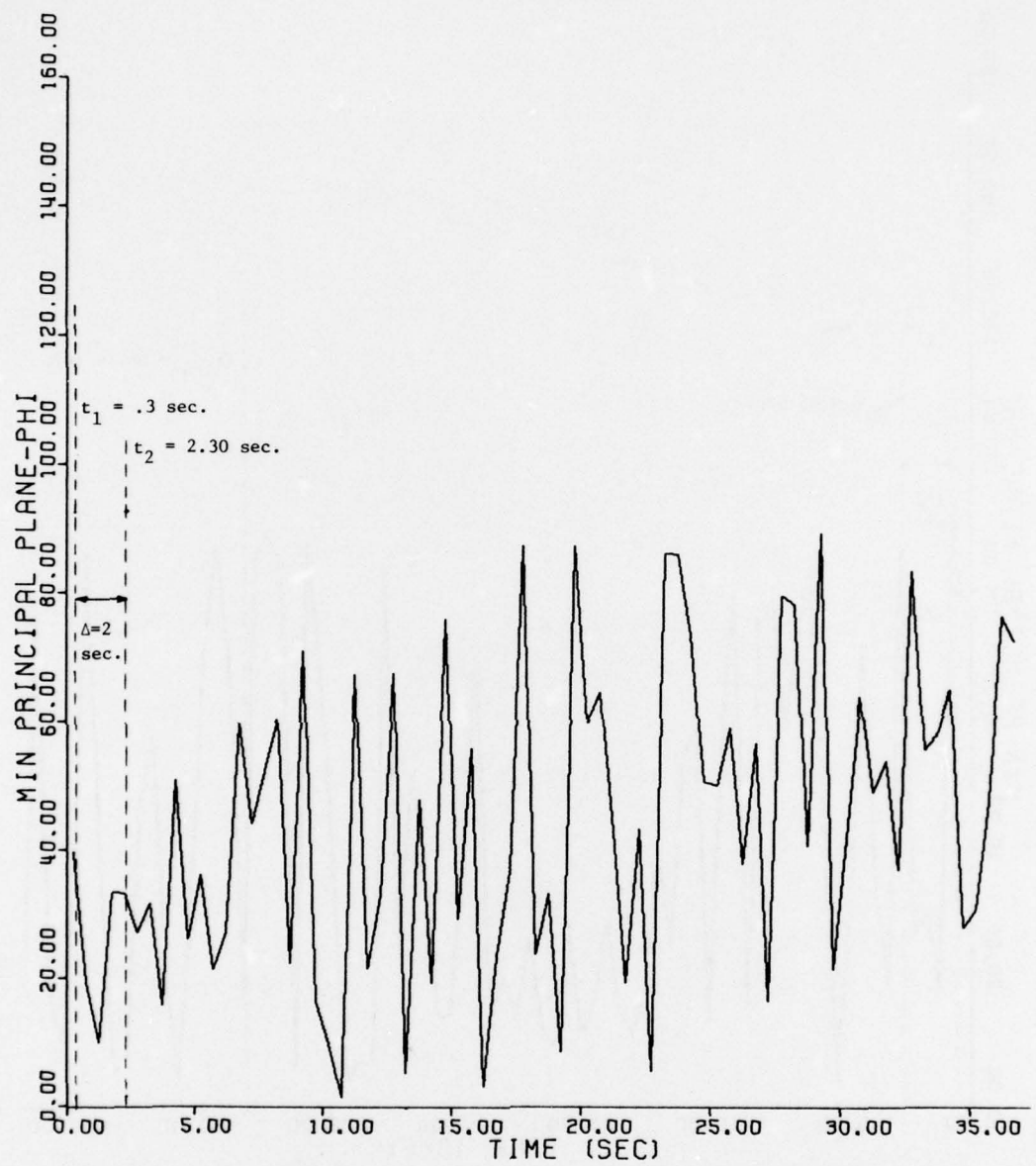
SAN FRANCISCO STATE BLDG BASEMENT



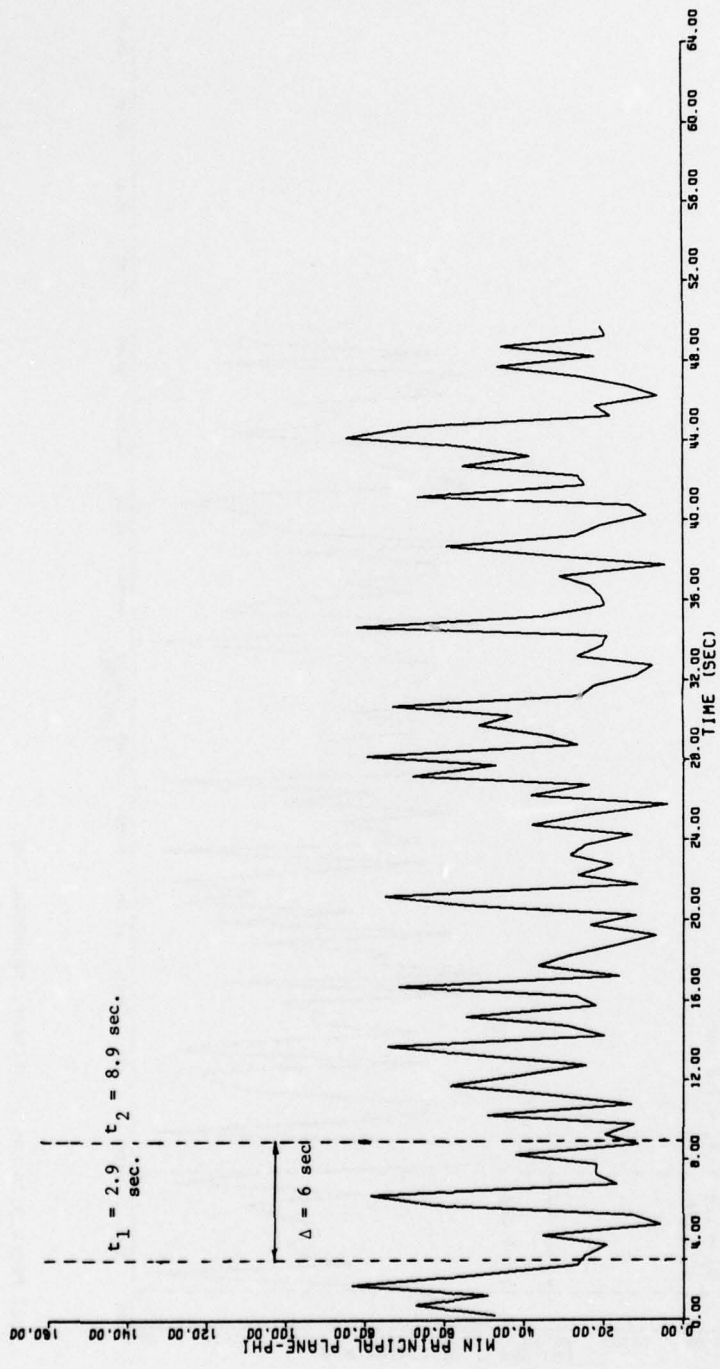
SAN FRANCISCO ALEXANDER BLOCK BASEMENT



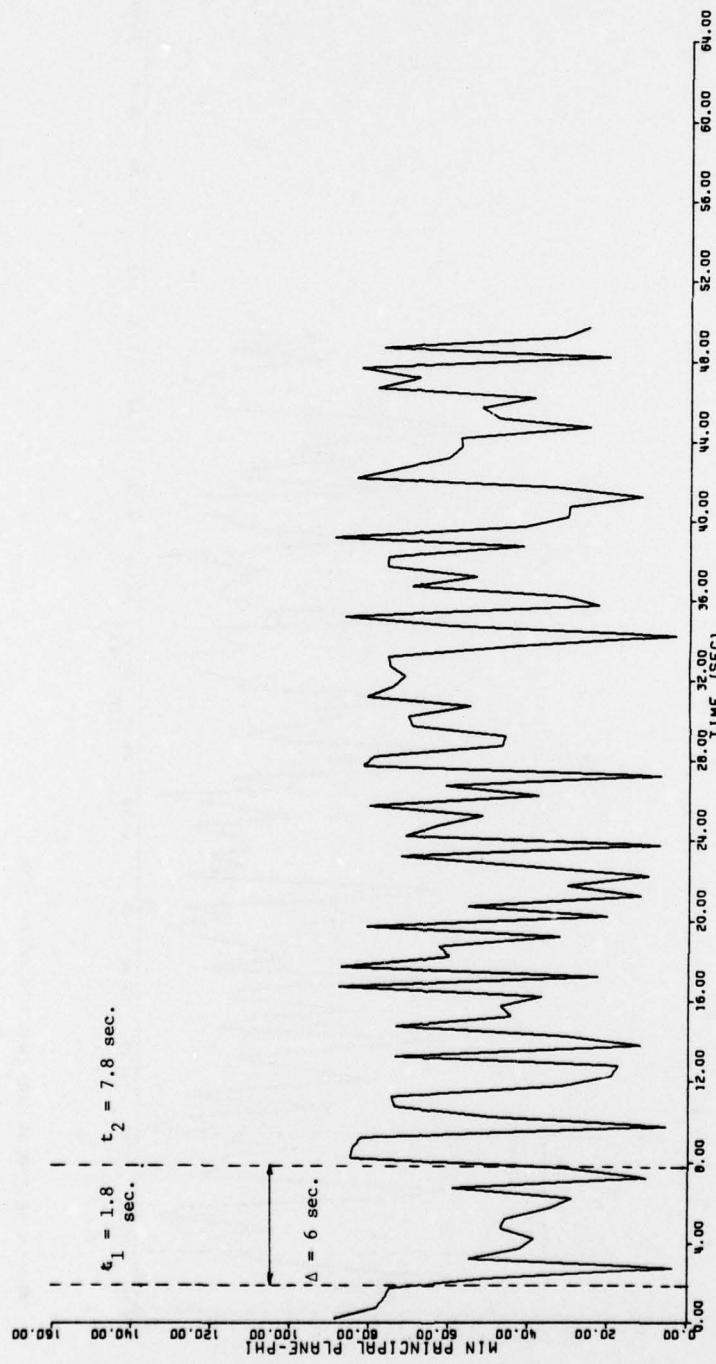
SAN FRANCISCO SOUTHERN PACIFIC BUILDING BASEMENT



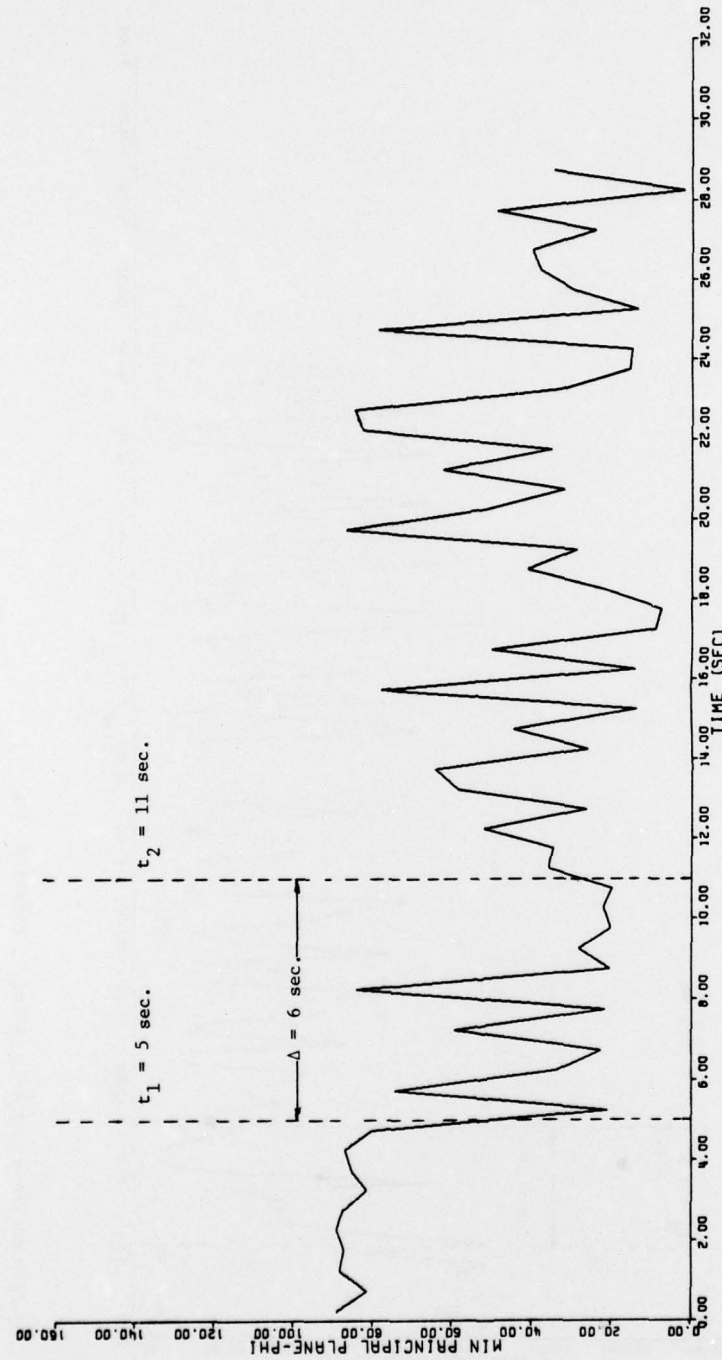
OAKLAND CITY HALL BASEMENT



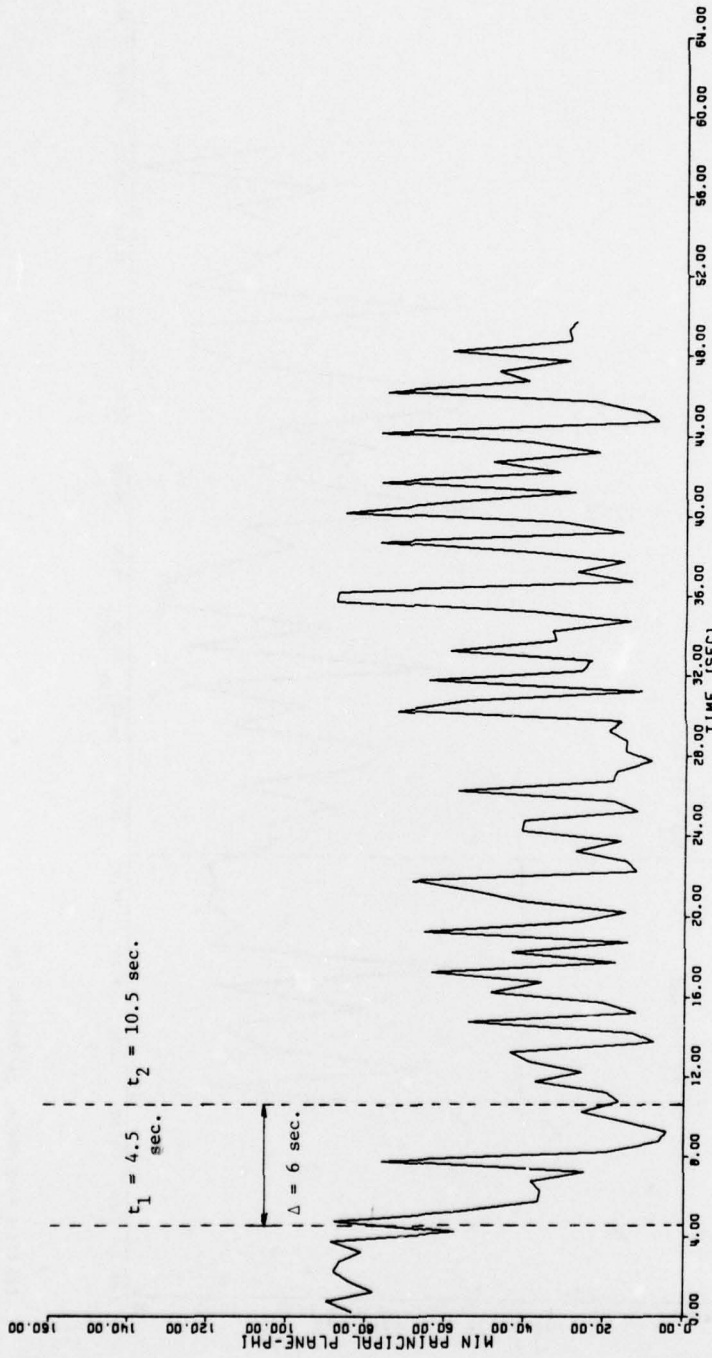
CALTECH SEISMOLOGICAL LAB., PASADENA, CAL.



JET PROPULSION LAB., BASEMENT, PASADENA, CAL.



CALTECH ATHENAEUM, PASADENA, CAL.



CALTECH MILLIKAN LIBRARY, BASEMENT, PASADENA, CAL.

APPENDIX 2

VARIATION OF PREDOMINANT FREQUENCY, $f(t)$

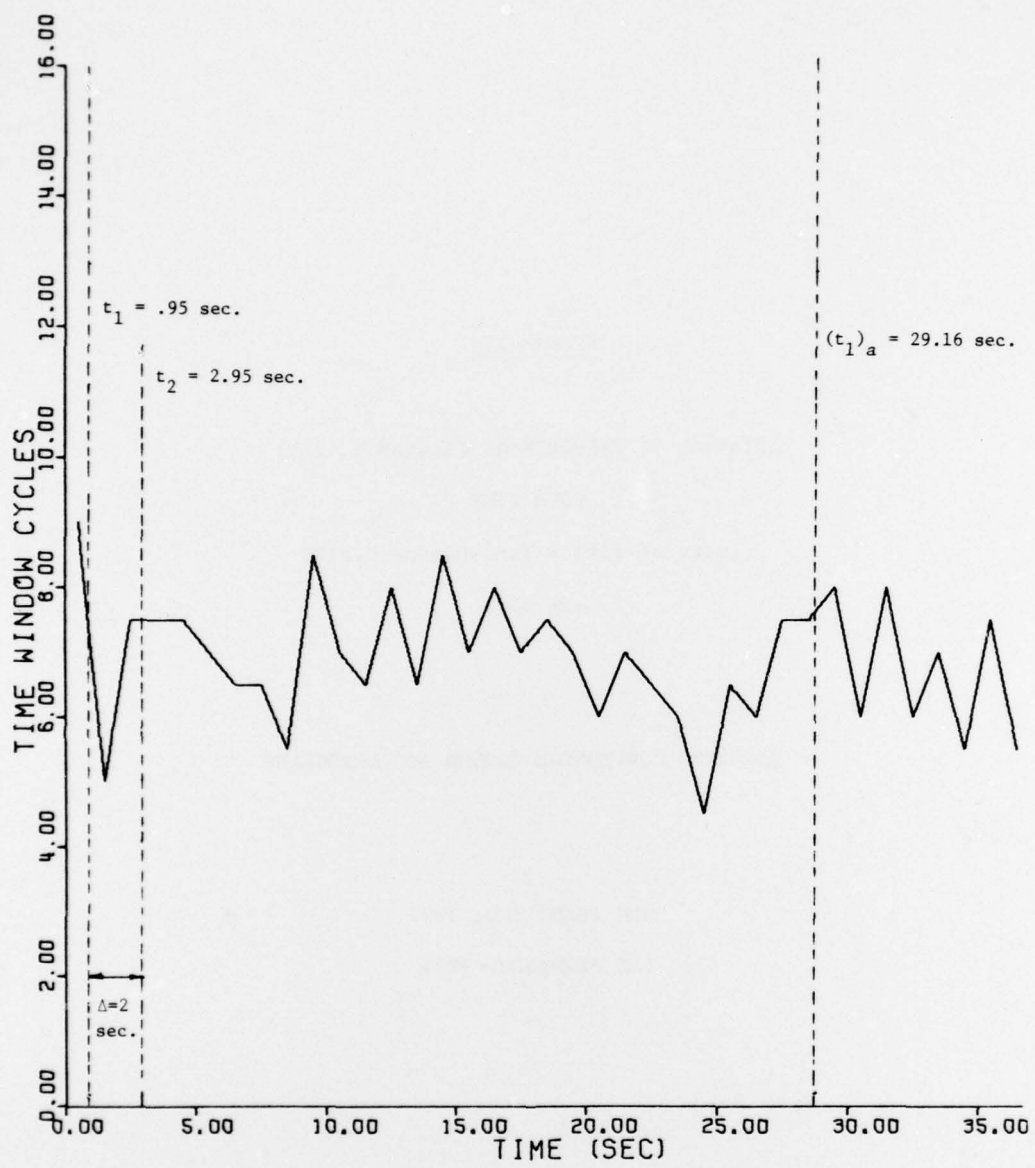
WITH TIME

(Units of $f(t)$ = Time Window Cycles
are cps).

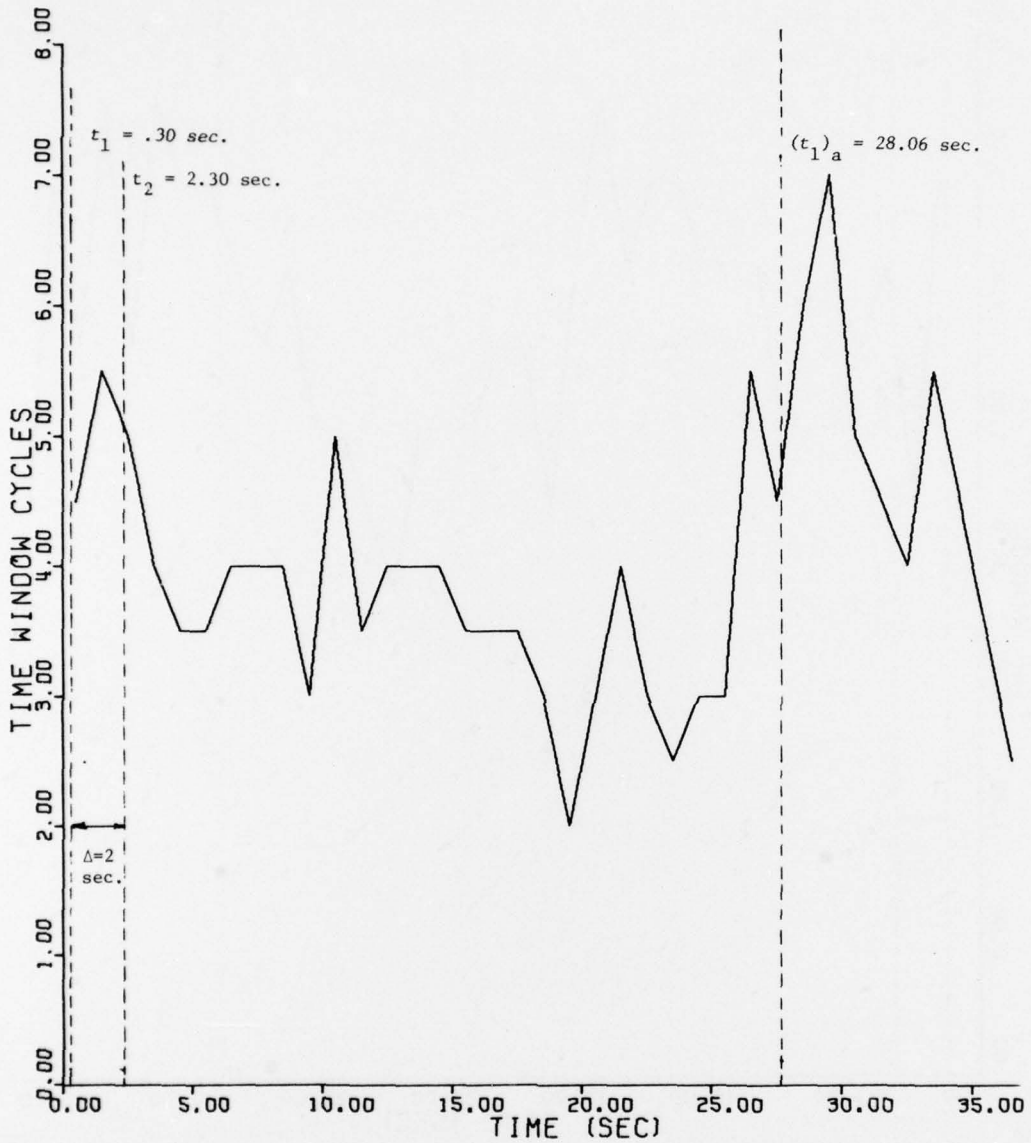
RECORDED HORIZONTAL GROUND ACCELEROGrams

SAN FRANCISCO, 1957

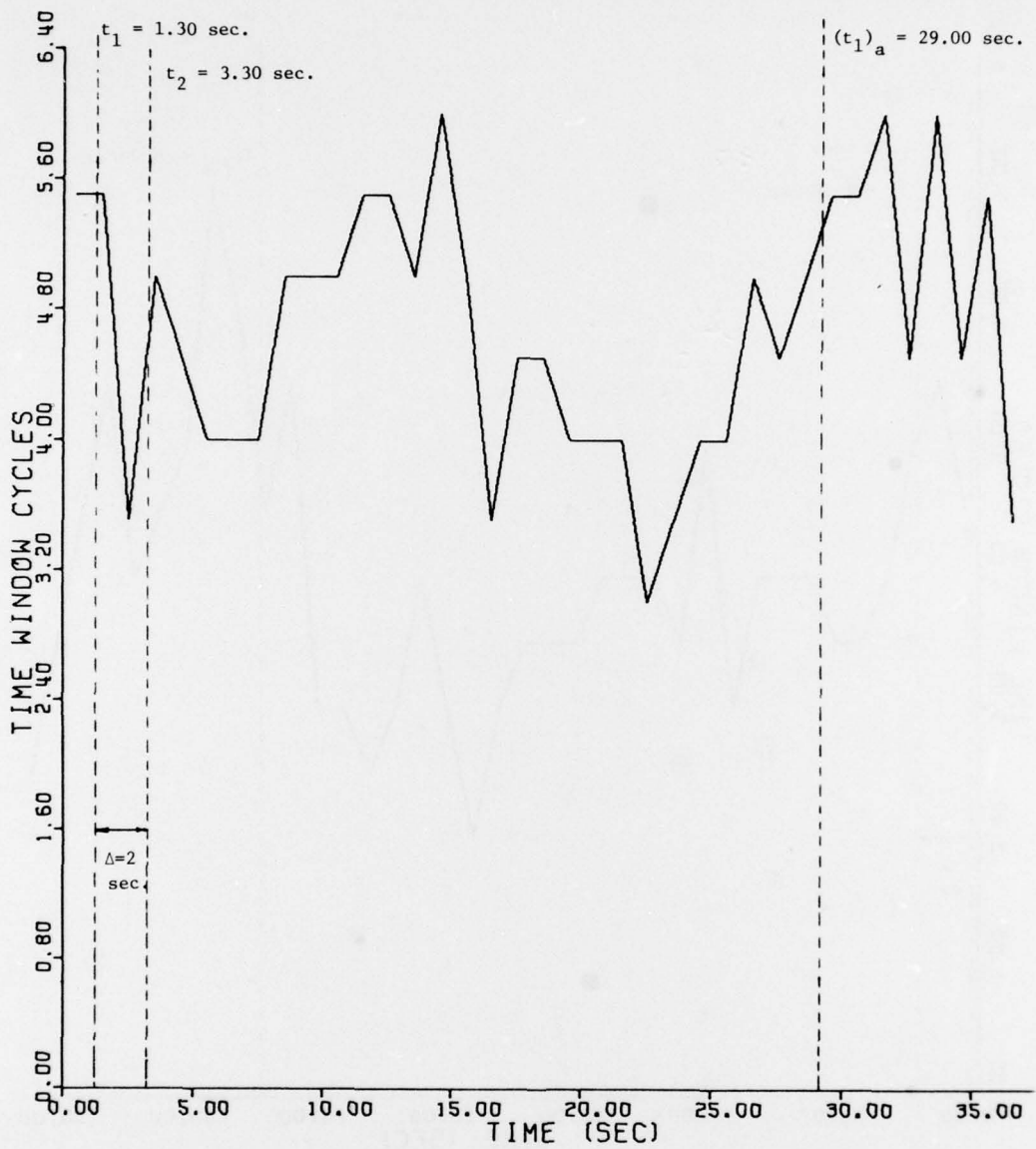
SAN FERNANDO, 1971



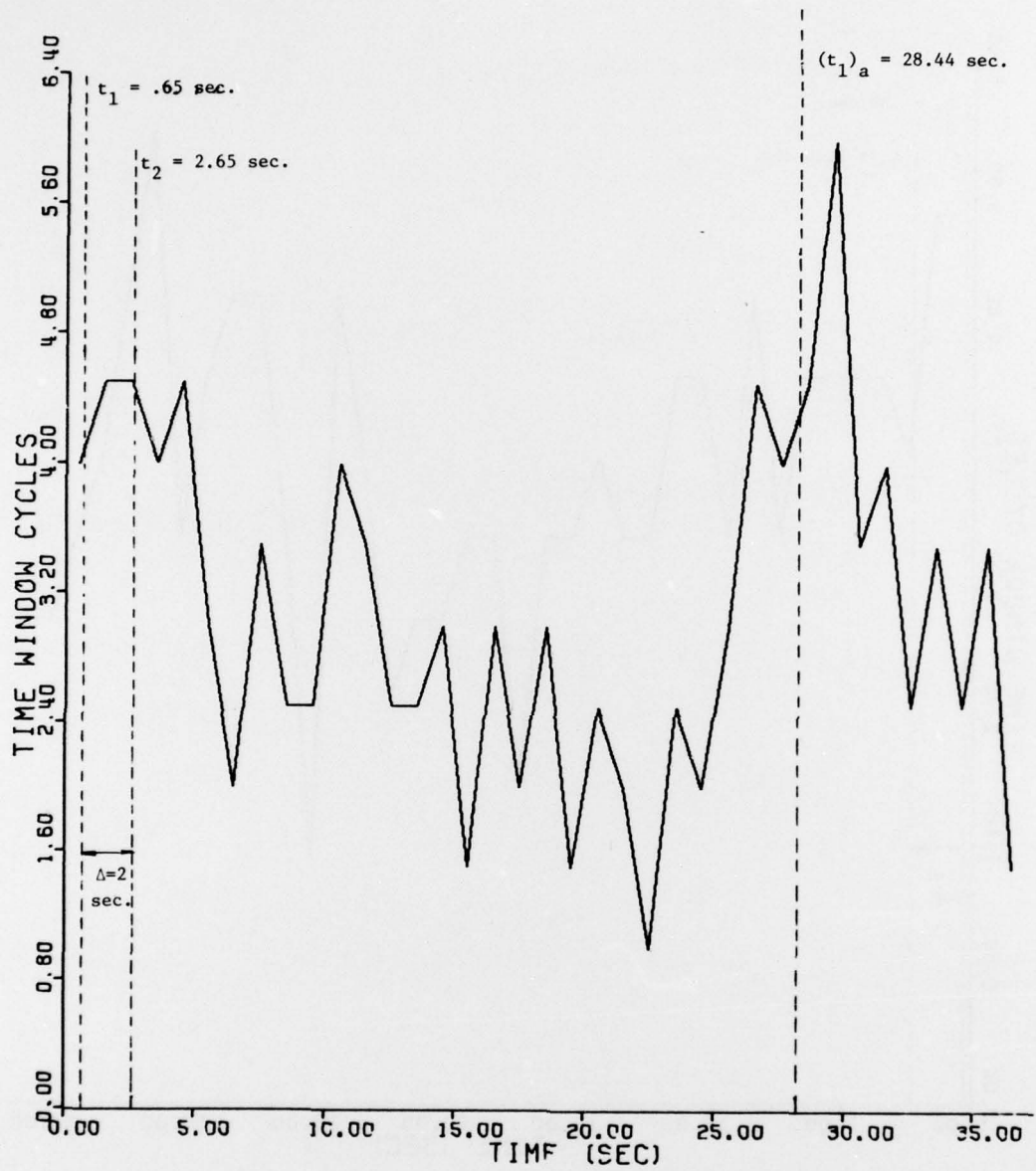
SAN FRANCISCO GOLDEN GATE PARK



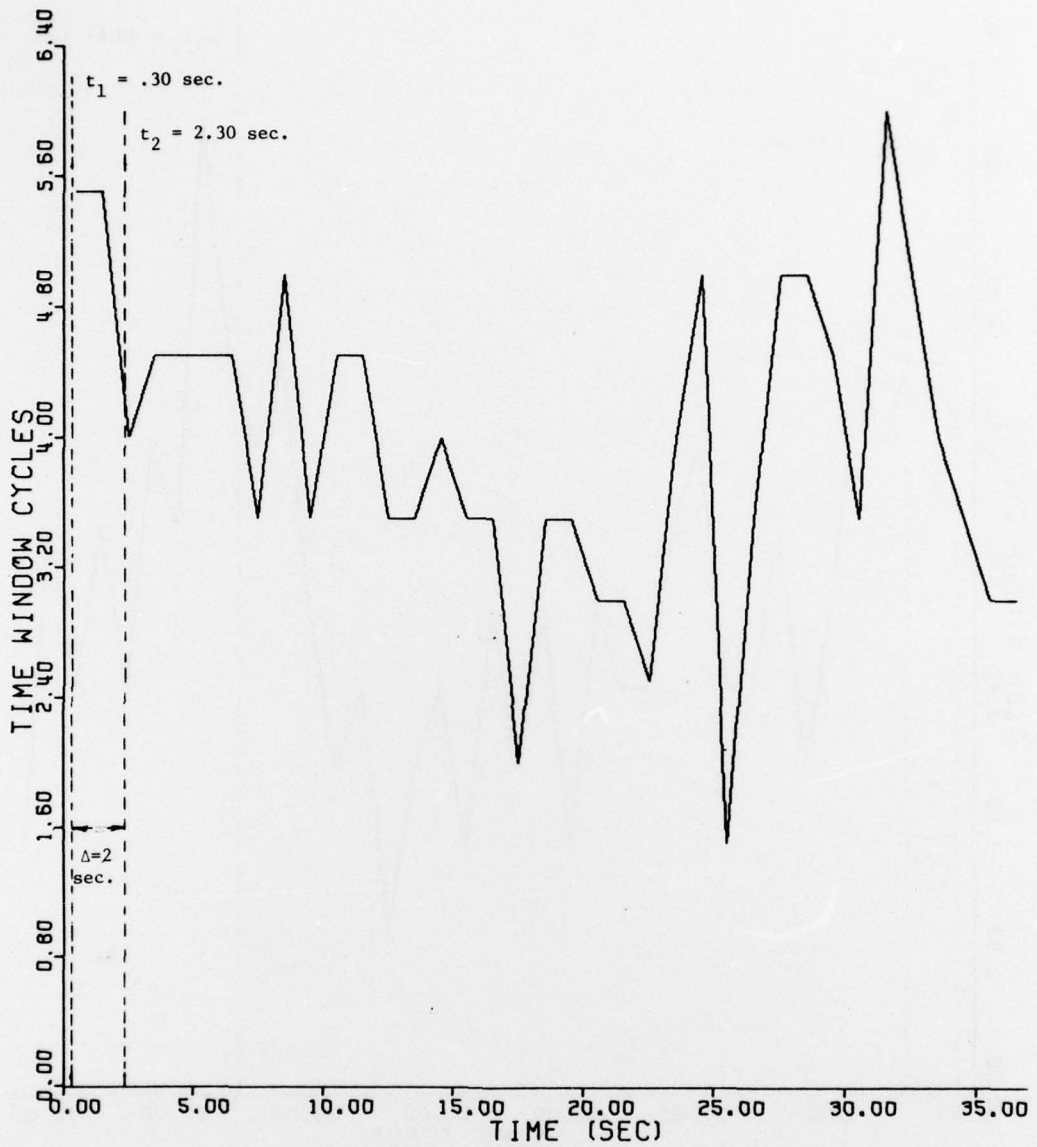
SAN FRANCISCO STATE BLDG BASEMENT



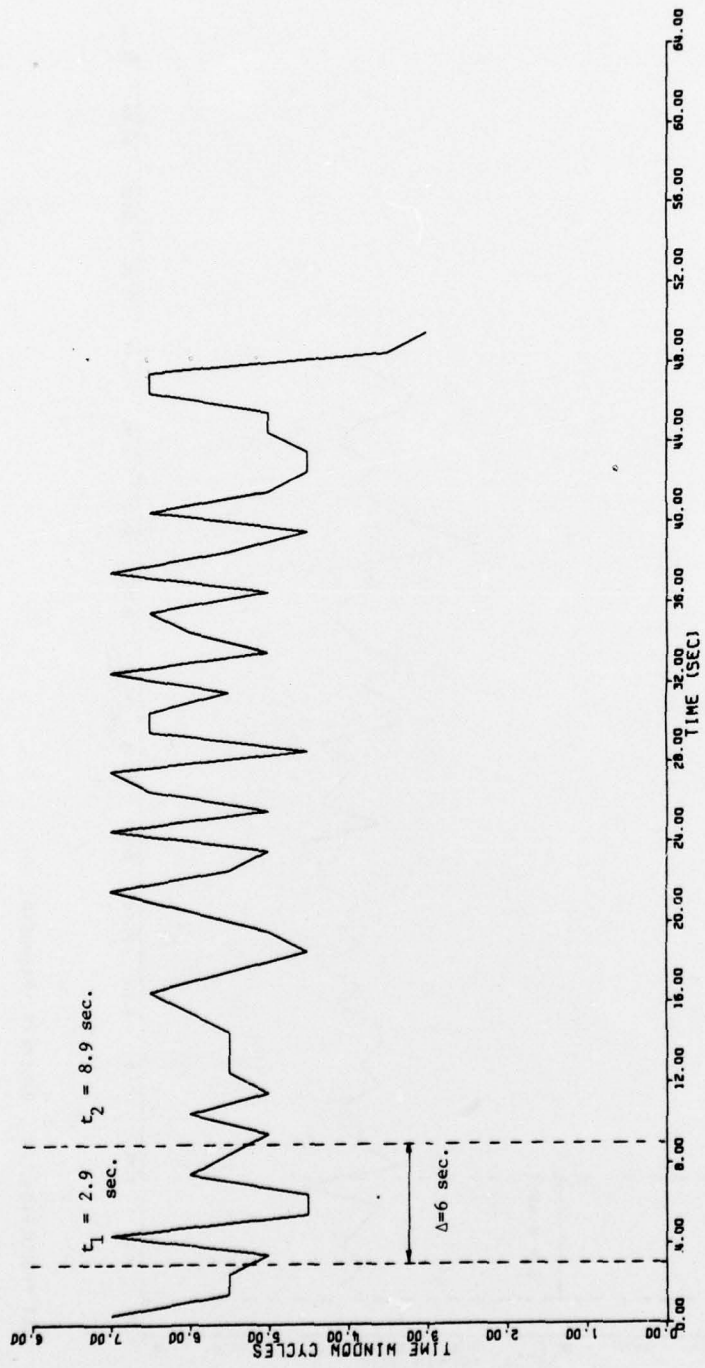
SAN FRANCISCO ALEXANDER BLDG BASEMENT



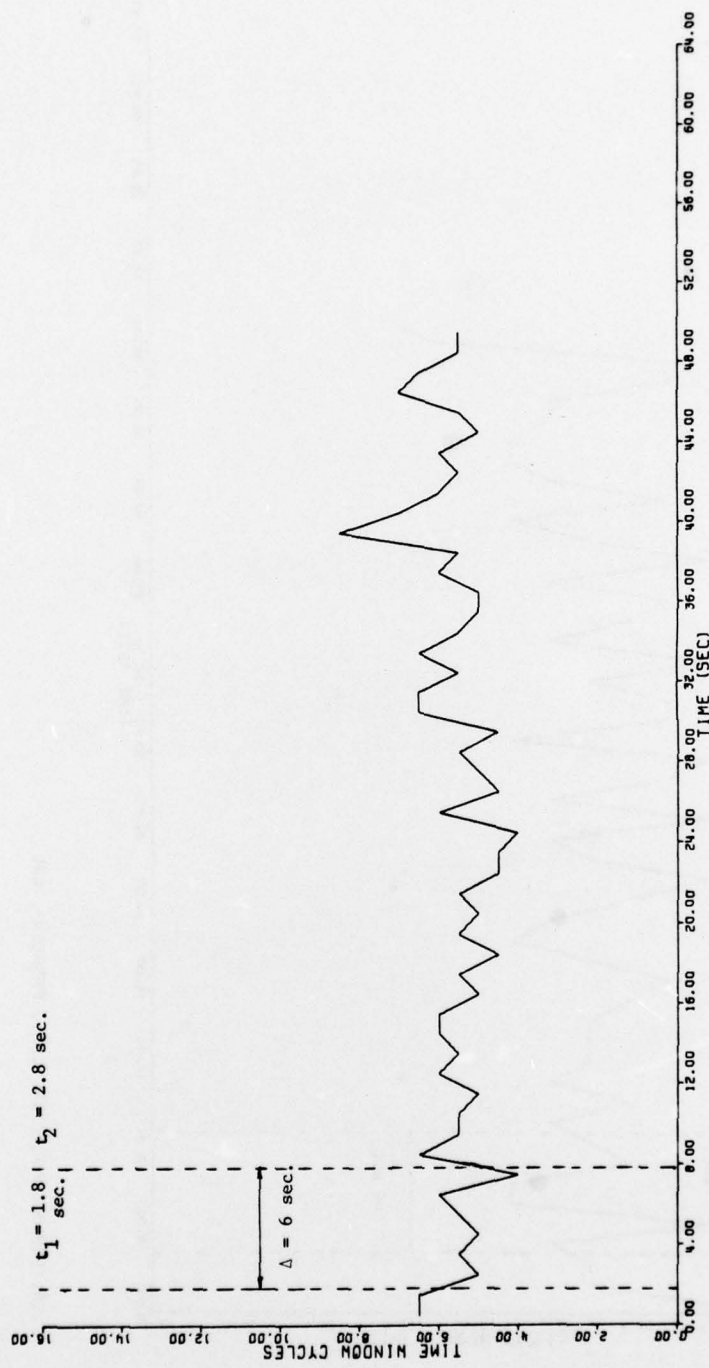
SAN FRANCISCO SOUTHERN PACIFIC BUILDING BASEMENT



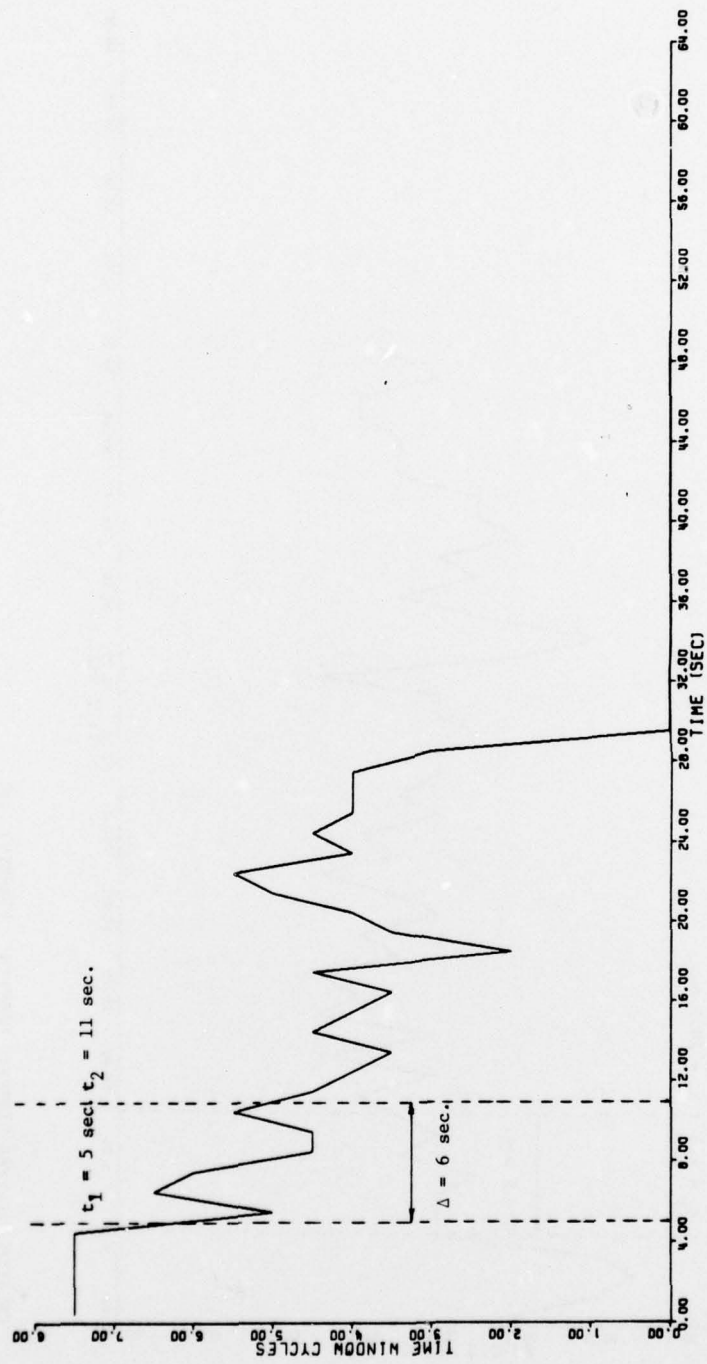
OAKLAND CITY HALL BASEMENT



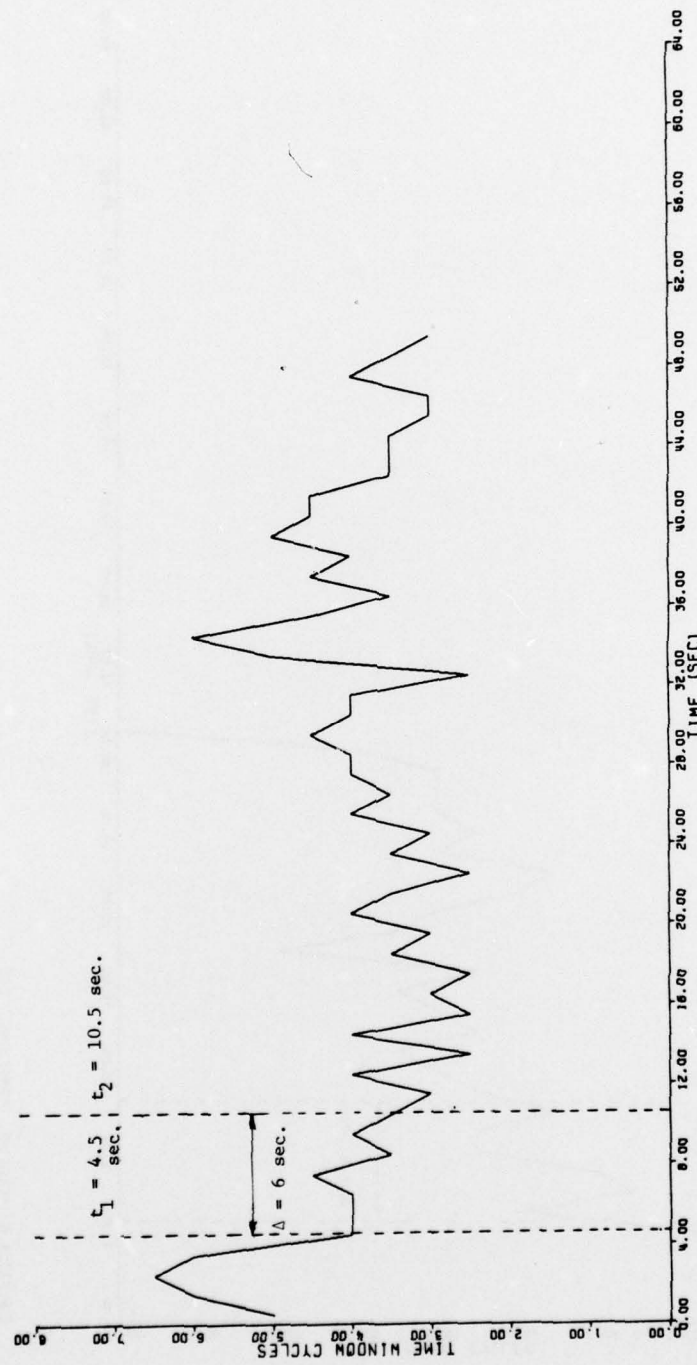
CALTECH SEISMOLOGICAL LAB., PASADENA, CAL.



JET PROPULSION LAB., BASEMENT, PASADENA, CAL.



CALTECH ATHENAEUM, PASADENA, CAL.



CALTECH MILLIKAN LIBRARY, BASEMENT, PASADENA, CAL.

In accordance with letter from DAEN-RDC, DAEN-ASI dated 22 July 1977, Subject: Facsimile Catalog Cards for Laboratory Technical Publications, a facsimile catalog card in Library of Congress MARC format is reproduced below.

Dobry, Ricardo

Study of ground motions at soil sites during two California earthquakes / by Ricardo Dobry, Sohan Singh, William E. Bond, Department of Civil Engineering, Rensselaer Polytechnic Institute, Troy, New York. Vicksburg, Miss. : U. S. Waterways Experiment Station ; Springfield, Va. : available from National Technical Information Service, 1979.

ii, 110 p. : ill. ; 27 cm. (Miscellaneous paper - U. S. Army Engineer Waterways Experiment Station ; GL-79-22)

Prepared for Office, Chief of Engineers, U. S. Army, Washington, D. C., under Purchase Order No. DACA37-78-M-0140, Work Unit No. 4A161102AT22.

References: p. 86-89.

1. Accelerograms.
2. Ground motion.
3. Earthquakes.

I. Bond, William E., joint author. II. Singh, Sohan, joint author. III. Rensselaer Polytechnic Institute, Troy, N. Y. Dept. of Civil Engineering. IV. United States. Army. Corps of Engineers. V. Series: United States. Waterways Experiment Station, Vicksburg, Miss. Miscellaneous paper ; GL-79-22.

TA7.W34m no.GL-79-22